SPATIAL VARIATBILITY OF SELECTED SOIL PROPERTIES IN AND BETWEEN MAP UNITS

by

COENRAAD HENDRIK FRAENKEL

Submitted in accordance with the requirements for the degree of
M.Sc. in Soil Science

In the faculty of Natural and Agricultural Sciences,
Department of Soil, Crop and Climate Sciences,
University of the Free State,
Bloemfontein, South Africa

Study leader: Dr. P.A.L Le Roux
Co – Study leader: Prof. L.D. Van Rensburg

November 2008

DECLARATION

I hereby declare that this dissertation hereby submitted for the Magister Scientiae degree at the University of the Free State is my own work and has not been submitted to any other University.

A also agree that the University of the Free State has the sole right to the publication of this dissertation.

Signed:

CONTENTS.....i
ABSTRACT.....ii
OPSOMMING.....iii
ACKNOWLEDGEMENTS.....iv
LIST OF TABLES.....v
LIST OF FIGURES.....vi
LIST OF SYMBOLS AND ABREVIATIONS.....vii

CHAPTER 1 16
1.1 Motivation 16
1.1.1 Spatial variation of selected soil properties in and between map units 16
1.1.2 The relationship between physical properties of selected soil forms and the root density of maize 16
1.1.3 The hydrological character of selected soil forms 17
1.2 Hypothesis and Objectives 19
1.2.1 Hypothesis 19
1.2.2 Objectives 20
2.3.1 Experimental Site 20
2.2.2 Experimental materials 20
2.2.3 Experimental design 23
2.2.4 Agronomical practices 25
2.2.4.1 Land preparation 25

CHAPTER 2 27
2.1 Introduction 27
2.2 Literature Review 29
2.2.1 Variability of soil properties 29
2.2.1.1 Statistical variation of soil properties 29
2.2.1.2 Spatial variation of soil properties. 43
2.2.1.3 Yield variation in relation to soil properties 45
2.3 Methodology 46
2.3.1 Soil Survey 46
2.2.6 Soil analysis 47
2.2.7 Statistical and spatial analysis 48
2.3 Results and Discussion 49
2.3.1 Factors of Soil Formation 49
2.3.1.1 Climate 49
2.3.1.2 Parent Material 52
2.3.1.3 Topography 53
2.3.1.4 Biology and time 53
2.3.2 Spatial variation of soils 55
2.3.2.1 Spatial distribution of soils 55
2.3.3 2 Description of the modal profiles 56
2.3.3 Spatial variation of physical and chemical properties 62
2.3.4 Spatial Variation within map units 66

2.3.5 Spatial variation between map units 69
2.4 Conclusion 70

CHAPTER 3 72
3.1 Introduction 72
3.2 Literature Review 73
3.2.3 Soil texture 76
3.2.4 Soil structure 80
3.2.4 Bulk density 85
3.2.5 Soil water content 86
3.3Methodology 89
3.3.1 Treatments 89
3.3.2 Plant Sampling 89
3.3.2.1 Above ground dry weight 89
3.3.2.2 Root sampling 89
3.3.3 Soil physical measurements 90
3.3.4 Statistical analysis 91
3.4 Results and Discussion 92
3.4.1 Interaction of soil physical properties 92
3.4.1.1 A horizon 92
3.4.1.2 B horizon 94
3.4.1.3 C horizon 96
3.4.2 Relationship between root density and soil physical properties. 100
3.4.3 Master horizons 102
3.4.4The Profile 103
3.5 Conclusion 104

CHAPTER 4 106
4.1 Introduction 106
4.2 Methodology 107
4.2.1 Experimental site 107
4.2.2 Experimental design 107
4.2.3 Experimental measurements 108
4.2.4 Calculation of K 109
4.2.5 Statistical Procedures. 109
4.3 Results and discussion 109
4.3.1 Volumetric wetness-time relationships 112
4.3.2 Matric suction – time relationships 116
4.3.3 Hydraulic head – depth relationships 116
4.3.4 Hydraulic conductivity 119
4.4 Conclusion 124

CHAPTER 5 125

REFERENCES 126

APPENDICES 132

ABSTRACT

Soils vary at all levels of observation. When describing soil physical or chemical properties we initially think in terms of homogeneous material. However, for characterizing the land use ability it is necessary to consider variability within and between soil map units as soils vary significantly over a land and within a homogeneous soil. The combinations of knowledge about soil inter relationships and the representation of the soil variability will be useful in the process of characterizing the variability of soil properties for different land use abilities, for example precision agriculture. The objectives of this study were therefore to (i) characterize the spatial variation of selected soil properties in and between map units (ii) describe the relationship between physical properties of selected soil forms and the root density of maize (iii) characterize the hydrology of the Tukulu, Sepane and Bloemdal soil forms at Paradys.

A field experiment was conducted on a 55 ha cultivated field on the experimental farm of the University of the Free State, Paradys (S -32˚35'21'', E -77˚43'6''). The experimental site was sub divided into 75 experimental plots. For objective 1 all 75 plots were analysed for pH, Ca, K, Mg, Na and 7 texture classes. For objective 2, 13 plots were selected from the 75 experimental plots to cover a range of relative dry biomass yield plots. Root samples and soil samples were taken per master horizon. They were analysed for silt + clay content, water stable aggregates, modulus of rupture, bulk density and organic carbon content. For objective 3, three modal profiles were selected and the instantaneous profile method was used to describe the volumetric wetness – time relationship, the hydraulic head – depth relationships and the hydraulic conductivity. It was clear that most of the soil physical and chemical properties had a strong relationship with clay. It was found that there was a

higher variation between map units than within map units. Despite any variation Inverse Distance Weighting (IDW) fairly accurately predicted the variation within map units varying from 97% to 99% irrespective of horizon or soil. It also accurately predicted the variation between map units varying from 91% to 94%.

It was found that the A and C horizon has varying inter relationship due to varying silt + clay contents. The B horizon is the main factor that distinguishes the three soils. The silt + clay content of the B horizon for Tukulu varied between 31% and 34%, the Sepane between 49% and 55%, and the Bloemdal between 28% and 34%. The Bloemdal had the highest root length index (RLI) followed by the Sepane and Tukulu.

It was clear that in the case of the Bloemdal and Tukulu, the C horizon controls the hydrology, while in the case of the Sepane it is the B horizon.

It may be concluded that the variation in soil properties is higher between than within map units. Soil physical properties have a close inter relationship and varying effects on the RLI. The hydrology of the Bloemdal and Tukulu is influenced by the C horizon, while the Sepane is influenced by the B horizon.

OPSOMMING

Grond varieër merkwaardig. Grond is geneigd om beskryf te word in terme van ‘n homogene liggaam. Alhoewel, as daar gekyk word na ‘n grond se vermoë vir ‘n sekere grondgebruik, moet dit beskryf word in terme van die variasie in- en tussen kaart eenhede. Die rede hiervoor is dat grond betekenisvol verskil oor ‘n landskap en in ‘n profiel. ‘n Kombinasie oor die interverwantskap tussen grond-eienskappe en die vermoë om dit ten toon te stel, is handig in die proses om grondvariasie vir sekere landelike gebruike te karakteriseer. Die doelstellings vir die studie was dus as volg: om (i) die variasie van grondeienskappe in en tussen kaarteenhede te karakteriseer (ii) die interverwantskap tussen grondfisiese eienskappe en die worteldigtheid van mielies te beskryf, en laastens (iii) om die hidrologiese eienskappe van die Bloemdal, Tukulu en Sepane op Paradys te beskryf.

‘n 55 ha Geploegde land is gebruik in ‘n veld eksperiment op die proefplaas van die Universiteit van die Vrystaat (-32˚35’21’’S,-77˚43’6’’O). Die proefterrein was onderverdeel in 75 proefpersele.

Vir doelstelling 1 was die total 75 persele geanaliseer om pH, Ca, K, Mg, Na en 7 tekstuur klasse te bepaal. Vir doelstelling 2 was 13 persele geselekteer wat gevarieer het volgens relatiewe biomassa. Op die persele is wortel- en grondmonsters geneem. Die grondmonsters is geanaliseer vir slik + klei, water stabiele aggregate, breeksterkte, brutodigtheid en organiese koolstof inhoud. Vir doelstelling 3 was die velddreineringsmetode gebruik om die volumetriese waterinhoud – tyd verhouding, die hidroliese druk – diepte verhouding en die hidroliese geleiding vermoë – diepte verhouding te karakteriseer.

Vanaf die studie was dit duidelik dat die grondfisiese en -chemise eienskappe ‘n sterk verwantskap het met die slik + klei inhoud. Daar was ‘n groter variasie tussen kaarteenhede as binne kaarteenhede. Nogtans het “Inverse Distance Weighting (IDW)” die variasie binne (97% tot 99%) en tussen kaart eenhede (91% tot 94%) redelik akkuraat voorspel ongeag die horison of grondtipe.

Die A en C horison het variërende interverwantskappe getoon. Die B horison is die hooffaktor wat tussen die drie grondtipes onderskei. Die slik + klei inhoud van die B horison het tussen 31% en 34% gevarieër, die Sepane tussen 49% en 55% en die Bloemdal tussen 28% en 34%. Die Bloemdal het die hoogste ooreenstemmende WLI gehad, gevolg deur die Sepane en Tukulu grondtipes.

Dit was duidelik dat in die geval van die Bloemdal en Tukulu, die C horison die hooffaktor is wat die vloei van water beïnvloed deur die profiel, terwyl die B horison in die geval van die Sepane die hoof faktor was.

Die variasie was groter tussen kaarteenhede as in kaarteenhede. Die grond fisiese eienskappe het ‘n sterk interverwantskap en variërende invloede op WLI getoon. Die vloei van water in die Bloemdal en Tukulu word hoofsaaklik beïnvloed deur die onderliggende C horison, terwyl die B horison in die geval van die Sepane vloei beïnvloed het.

ACKNOWLEDGEMENTS

I would like to thank the following persons and institutions:

- Dr. P.A.L. Le Roux my study leader for his valuable advice, his readiness for consultation and his much-needed support through out the project

- Prof. L.D. Van Rensburg my co study leader, who really done more than would be expected from a co supervisor. His valuable advice, readiness for consultation and mentorship will always be remembered.

- The Natural Research Foundation for funding the research project.

- Mr. C.B. Bothma for his wonderful companionship, and sharing of knowledge and memorable student life during the project.

- The Department of Soil, Crop and Climate Sciences of the University of the Free State, for offering me the research assistantship.

- The staff members in the Department of Soil, Crop and Climate Sciences, especially Mrs. R van Heerden, for the administrative and emotional assistance and Mrs. Y.M. Dessels for laboratory assistance.

- My beloved parents that gave me the opportunity to further my studies, I will be forever grateful.

- My brother and sister for their great love and kindness in a year when times were really tough.

- My wife Madré for her much needed love and support through good and difficult times.

Finally, I thank the Almighty God who I believe is the ultimate guide of this work and my life in general. I always returned to Him when I got stuck and when times where difficult.

"In every man there is something wherein I may learn of him, and in that I am his pupil."

-Ralph Waldo Emerson

LIST OF TABLES

Chapter 2 **Spatial variation of selected soil properties in and between map units**

Table 2.1 A Pearson correlation matrix (r) of soil properties on the slow forming terraces in the Andes region (n=51) (Dercon *et al.*, 2003)

Table 2.2 Percentage of soil samples in each textural class (Sobieraj *et al.*, 2003)

Table 2.3 Descriptive statistics and semi-variogram parameters of selected soil properties (Miao *et al.*, 2006)

Table 2.4 Comparison of the two representative soil profiles (Stutter *et al.*, 2002)

Table 2.5 Descriptive statistics of parameters measured in 2002 (Shahandeh *et al.*, 2005)

Table 2.6 Descriptive statistics of parameters measured in 2003 (Shahandeh *et al.*, 2005)

Table 2.7 The climate of the area (WRC report no. 1176/1/03, 2003)

Table 2.8 Correlation matrix of the soil properties for the A, B and C horizons

Table 2.9 Statistical variation of the soil properties

Chapter 3 **The relationship between physical properties of selected soil forms and the root density of maize**

Table 3.1 Primary influences of soil properties on soil requirements for optimal root elongation (Logsdon *et al.*, 1987).

Table 3.2 Root density data in relation to three soil forms with different physical properties (Data modified from Van Antwerpen, 1988 and Bennie, 1996)
Table 3.3 Root characteristics of wheat during tillering in three soils of various textures selected from Callot *et al.* (1982)
Table 3.4 Mean root length density and the standard deviation in each soil layer (Amato and Ritchie, 2002)
Table 3.5 Variation in soil physical properties for the A horizon of the Tukulu, Sepane and Bloemdal soil forms
Table 3.6 Correlation matrix for the A horizon of the Tukulu, Sepane and Bloemdal soil forms
Table 3.7 Variation in root density for the A, B and C horizon of the Bloemdal, Tukulu and Sepane soils
Table 3.8 Correlation matrix of the soil physical properties vs. root density for the A, B and C horizon irrespective of soil forms.

Chapter 4 Characterising the hydrology of the Bloemdal, Tukulu and Sepane soils at Paradys.

Table 4.1 Summary of the physical characteristics for the selected Tukulu, Bloemdal and Sepane soils
Table 4.2 Summary of the pedological characteristics for the selected Tukulu, Bloemdal and Sepane soil forms
Table 4.3 Model variables fitted to the soil water content - time data of the Bloemdal, Tukulu and Sepane soils
Table 4.4 Summary of the hydraulic conductivity and related mean volumetric water content for the soils

LIST OF FIGURES

Chapter 1 **Introduction**

Figure 1.1 Location of the experimental field site at the Paradys Experimental Farm South of Bloemfontein.

Figure 1.2 A diagrammatic layout of the IRWH-system (Hensley *et al.*, 2000).

Figure 1.3 The IRWH system prepared manually with spades and rakes at Glen Agricultural Institute, near Bloemfontein.

Figure 1.4 The contour plough preparing the dead - level contours at Paradys Experimental Farm.

Figure 1.5 The basin plough creating 10 cm deep x 1 m wide basins along the contour ridges.

Figure 1.6 Runoff water collected in the basins after a 30 mm rain event at Paradys Experimental Farm.

Figure 1.7: Schematic layout of the conventional and IRWH treatments on the 55 ha field at Paradys Experimental Farm.

Figure 1.8 Schematic layout of the IRWH structure and instrumentation used in each of the 75 experimental plots

Chapter 2 **Spatial variation of selected soil properties in and between map units**

Figure 2.1 Topsoil pH $_{(H2O)}$ as a function of elevation (Zehetner & Miller, 2006).

Figure 2.2 Kriged contour maps (a-d) of soil NO_3-N with depth in 2002 (Shahandeh *et al.*, 2005).

Figure 2.3 Kriged contour maps of (a-b) total N in 2002 and 2003, and (c) mineralized N in 2003 (Shahandeh *et al.*, 2005).

Figure 2.4 Kriged surface representation of the distribution of the sand content in the topsoil (Venter, 2003).
Figure 2.5 Kriged surface of the distribution of $pH_{(H2O)}$ in the topsoil (Venter, 2003).
Figure 2.6 Kriged surface representation of the distribution of the OC (%) in the top soil (Venter, 2003).
Figure 2.7 Kriged surface of the measured yield (Venter, 2003).
Figure 2.8 Soil cores drawn using the hydraulic core sampler.
Figure 2.9 The lower 3 position of the experimental site in the landscape.
Figure 2.10 Contour map of the 55 ha experimental site.
Figure 2.11 Soil map of the experimental site at Paradys.
Figure 2.12 Tukulu soil form
Figure 2.13 Sepane soil form
Figure 2.14 Bloemdal soil form
Figure 2.15 Distribution of the clay content for the A, B and C horizon.
Figure 2.16 Distribution of clay over the soil forms (n=75).
Figure 2.17 Map indicating the areas which was selected to be within the map units of the Tukulu, Sepane and Bloemdal soil forms.
Figure 2.18 Coefficient of variation within map units and between map units.
Figure 2.19 Accuracy of IDW predictions within map units and between map units.
Figure 2.20 Map indicating the areas that has been selected to characterize the variation between map units.

Chapter 3 The relationship between physical properties of selected soil forms and the root density of maize

Figure 3.1 Diagram showing the three basic root systems (Klepper, 1996).

Figure 3.2 Relationship between soil strength and percent of clay (Bennie & Burger, 1988).

Figure 3.3 Representation of possible paths of a root axis through a bed of aggregates (Diagram from Dexter, 1978).

Figure 3.4 Possible behaviors of seminal roots penetrating two clods separated with a crack. (Whitely and Dexter, 1984).

Figure 3.5 Change in penetrometer pressure with bulk density at various water contents (Hillel, 2004).

Figure 3.6 Relationship between the relative root length of 70-day-old maize, cotton, wheat, and groundnut plants and penetrometer resistance (Bennie, 1995).

Figure 3.7 Relation between cotton root penetration and penetrometer resistance (Taylor *et al*., 1996).

Figure 3.8 Change in penetrometer pressure with water content at different bulk densities (Bennie, 1995).

Figure 3.9 Relationship between total root length and various water applications at optimum nitrogen levels (Data processed from Van Rensburg, 1996).

Figure 3.10 Illustrating the sampling of the soil for bulk density determination (a) The core is inserted into the soil with a sliding hammer and (b) recovered without disturbing the soil inside the cylinder.

Figure 3.11 Relationship between total root length or root length index (RLI) and the soil physical quality index (SPQI) for the A-horizon (a), B-horizon (b) and C - horizon (c) over the 13 plots investigated, irrespective of soil form.

Figure 3.12 Relationship between total root length or root length index (RLI) and the soil physical quality index (SPQI) for the profiles, irrespective soil forms.

Chapter 4 **Characterising the hydrology of the Bloemdal, Tukulu and Sepane soils at Paradys**.

Figure 4.1 Experimental design for the instantaneous profile method.

Figure 4.2 Volumetric wetness-time relationship for the A, B and C horizon of the Bloemdal soil form.

Figure 4.3 Volumetric wetness-time relationship for the A, B and C horizon of the Tukulu soil form.

Figure 4.4 Volumetric wetness-time relationship for the A, B and C horizon of the Sepane soil form.

Figure 4.5 Hydraulic head profile at 30 cm, 60 cm and 90 m depths of the Bloemdal soil form over the measuring period in days after saturation (DAS).

Figure 4.6 Hydraulic head profile at 30 cm, 60 cm and 90 m depths of the Tukulu soil form over the measuring period in days after saturation (DAS).

Figure 4.7 Hydraulic head profile at 30 cm, 60 cm and 90 m depths of the Sepane soil form over the measuring period in days after saturation (DAS).

Figure 4.8 Hydraulic conductivity curves for the Bloemdal soil.

Figure 4.9 Hydraulic conductivity curves for the Tukulu soil.

Figure 4.10 Hydraulic conductivity curves for the Sepane soil.

CHAPTER 1

INTRODUCTION

1.1 Motivation

1.1.1 Spatial variation of selected soil properties in and between map units

Soils vary at all levels of observation. Typically, when describing soil physical, chemical, or biological properties we initially think in terms of homogeneous material. This is a good starting point, because it simplifies concepts and leads to results with the least number of complications. However, for characterizing soil map units it is necessary to consider variability within and between soil map units. The knowledge about soil inter-relationships and the representation of the soil variability will be useful for characterizing the variability of land suitability for example in precision agriculture. In agriculture the manipulation of variable properties increase yield, but it is uncertain which soil property limits production at a certain spot in a certain year. The modelling of spatial variation as well as the interpretation of the visual image, can effectively improve the understanding of variation in crop production.

1.1.2 The relationship between physical properties of soil form and the root density of maize

Roots are an important component in any crop production system (Klepper, 1990; Bennie, 1995 and Van Antwerpen, 1988). Various soil physical properties, individually or combined with other soil physical properties, have an influence on root development. These soil physical properties consist of soil texture, soil structure, water

content, bulk density and porosity (Klepper, 1990). Past studies on root development under South African conditions focussed heavily on the effect of irrigation practices (Bennie & Burger, 1979; Van Antwerpen, 1988 and Bennie *et al.*, 1988) and tillage practices (Bennie *et al.*, 1988; Snyman, 1987 and Van der Merwe, 1993). These tillage practices include minimum tillage, stubble mulch and no-till, which were mainly applied on sandy to sandy loam soils, with a massive apedal structure. Recent advances in tillage suggested that the Infield Rainwater Harvesting (IRWH) technique is suitable for clay and duplex soils in semi arid zones of South Africa (Hensley *et al.*, 2000; Botha *et al.*, 2004). To date none of the biophysical studies in IRWH has focussed on root development. This is seen as a serious concern as the system claims that it improves the rainwater productivity (Botha, 2006).

1.1.3 The hydrological character of selected soil forms

Soil hydrology is of crucial importance in countries such as South Africa, where the lack of water limits rain fed crop production (Hutson, 1983). The hydraulic conductivity is a challenging soil property to describe because it can change many orders of magnitude over short distances. Heterogeneity of soil properties within and between soil horizons causes some regions to be more or less favourable to flow. This flow is highly variable with extremes represented by tortuous flow between individual particles and rapid flow through large, continuous macropores.

The spatial variation in hydraulic conductivity is influenced by a lot more than topography and soil forms. The amount of water retained at relatively low values of matric suction (between 0 and 100 kPa) depends primarily upon the capillary effect and pore size distribution, and hence is strongly affected by the soil structure. To explain this phenomenon, Vanapalli *et al.* (1999) suggested that when investigating the structure of partially saturated soils, there

are two levels to be considered: macrostructure and microstructure. Macrostructure governs the soil water characteristic behaviour for the soil particularly at low suction values, while microstructure governs the behaviour of soil water characteristic at relatively high suction values. On the other hand soil texture influences the difference in pore sizes in the soil matrix. In a clayey soil, the pore size distribution is more uniform, and more of the water is adsorbed, so that increasing the matric suction causes a gradual decrease in wetness. Thus the greater the clay content in general the greater the water retention at any particular suction, and more gradual the slope of the curve (Dexter, 1978). Bulk density also has an effect on the soil water characteristics as an increase in bulk density means a decrease in total pore space in the soil and a decrease in water movement through the soil (Hillel, 2004). The organic carbon content also increases the water holding capacity and conductivity largely as a result of its influence on soil aggregation and associated pore size distribution. The organic carbon content increases the amount of water retained, especially at low suctions, but at higher suctions soil rich in organic carbon release water rapidly because of large pore spaces (Saxton & Rawls, 2006). Another problem is that of field heterogeneity that relates to the scale the hydraulic measurements are made on. Soil properties such as conductivity, porosity and pore size distribution are scale dependant and should be taken into consideration when selecting the sample size. Thus a field estimation of hydraulic character where a larger sample is taken might be more desirable (Hillel, 2004).

Further studies have to be done to identify all the factors affecting the spatial variation of the hydraulic conductivity of different soil forms, before a model to characterize the variation may be established.

1.2 Hypothesis and Objectives

1.2.1 Hypothesis

There exist many interrelations between soil properties that we have to understand before describing the variability of soil properties. Any prediction using substantial secondary information based on the knowledge of the relationship between soil properties provides better results than prediction methods not taking correlation in to consideration. After the inter relationship between soil properties are understood, a suitable interpolation technique may be used for surface representation of the distribution of certain soil properties. The combinations of knowledge about soil inter relationships and the representation of the soil variability will be useful in the process of characterizing the variability of soil suiability for different land uses for example precision agriculture and environmental sciences.

In the maize production area of South-Africa, commercial farmers are constantly debating the question on how to reduce production risk, both financial and agronomical. Individual farmers cannot do much to change the internationally based income and cost structures. Hence they are constantly searching for ideas, concepts and technologies aimed to reduce input costs per unit area without scarifying the maximum yield expectations based on the long term potential of the land. It is of utmost importance that research must provide agronomical guidance and support to farmers, helping them to stay competitive on the global landscape from a soil and water management point of view.

1.2.2 Objectives

1. Characterization of the spatial variation of selected soil properties in and between map units (Chapter 2)

2. Describing the relationship between physical properties of selected soil forms and the root density of maize (Chapter 3)

3. Characterizing the hydrology of the Tukulu, Sepane and Bloemdal soil forms at Paradys. (Chapter 4)

1.3 Methodology

1.3.1 Experimental Site

A field experiment were conducted on a 55 ha cultivated field on the experimental farm of the University of the Free State, Paradys (-32˚35'21''S,-77˚43'6''E). The experimental farm is located +/-10 km south of Bloemfontein between the N1 road to Colesberg and the N6 road to Reddersburg as indicated in Figure 1.1.

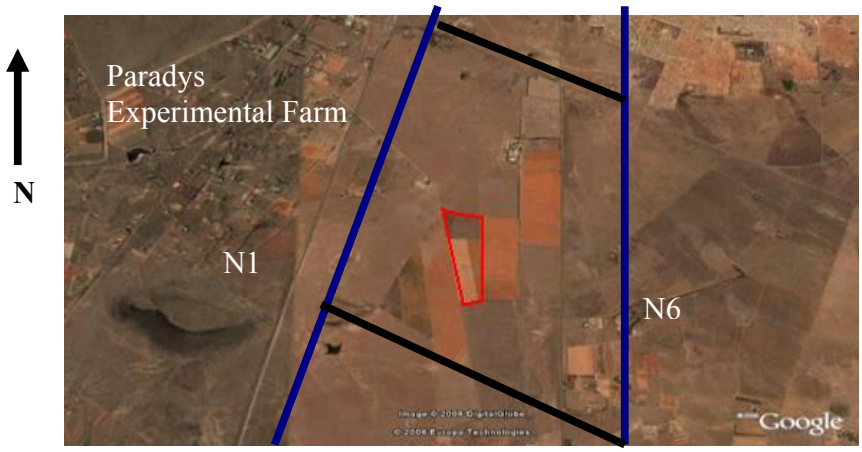

Figure 1.1: Location of the experimental field site at the Paradys Experimental Farm South of Bloemfontein

1.3.2 Experimental materials

The basic concepts of the IRWH was initiated by Hensley *et al*. (2000) and consist of a no till runoff strip sloping towards a 1 m wide basin area (Figure 1.2). The no-till strip is used

as a catchment for inducing runoff by using the natural topography of the land as well as the crusting characteristics of the soil. Runoff water is collected in the basins, a process defined as in-field runoff (Botha, 2007). Under conditions where the discharge volume from the runoff area is lower than the surface storage capacity of the basins, runoff from the land (Ex-field runoff) is assumed to be zero.

Figure 1.3 depicts the surface structure of the IRWH made manually with spades and rakes. The challenge was to obtain a similar surface structure on large scale using tractor drawn implements. This was obtained through the development of a contour plough which creates a 20 cm high contour ridge with a slope striving to be zero across the topography (Figure 1.4). The second implement, the basin plough, is presented in Figure 1.5. The basin plough creates a 10 cm deep and 1 m wide basin every 1.5 m along the ploughed contour (Figure 1.5). Figure 1.6 demonstrates the collection of in-field runoff in the basins before planting.

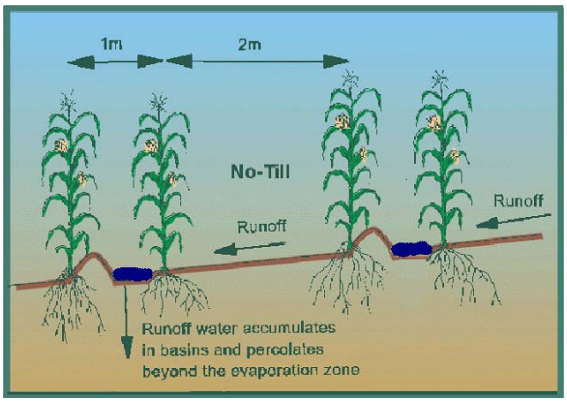

Figure 1.2 A diagrammatic layout of the IRWH-system (Hensley *et al.*, 2000).

Figure 1.3 The IRWH system prepared manually with spades and rakes at Glen agricultural institute, near Bloemfontein.

Figure 1.4 The contour plough preparing the dead - level contours at Paradys Experimental Farm.

Figure 1.5 The basin plough creating 10 cm deep x 1 m wide basins along the contour ridges.

Figure 1.6 Runoff water collected in the basins after a 30 mm rain event at Paradys Experimental Farm.

1.3.3 Experimental design

The experimental site was sub divided into 75 experimental plots (Figure 1.7). Row 3, 8 and 14 was treated as conventional plots while the rest of the rows were treated as IRWH plots. Each plot was 72 m x 72 m with rows consisting of a 2 m runoff area and a 1 m basin area. A neutron access tube was inserted in the basin area and on the runoff area. A rain gauge was inserted in the middle of the plot to capture rainfall. On the thirteen plots where root samples were taken a profile pit was made in the north western corner of the plot. The profile was morphologically described in detail. Each of the plots was separately analyzed and treated (Figure 1.8).

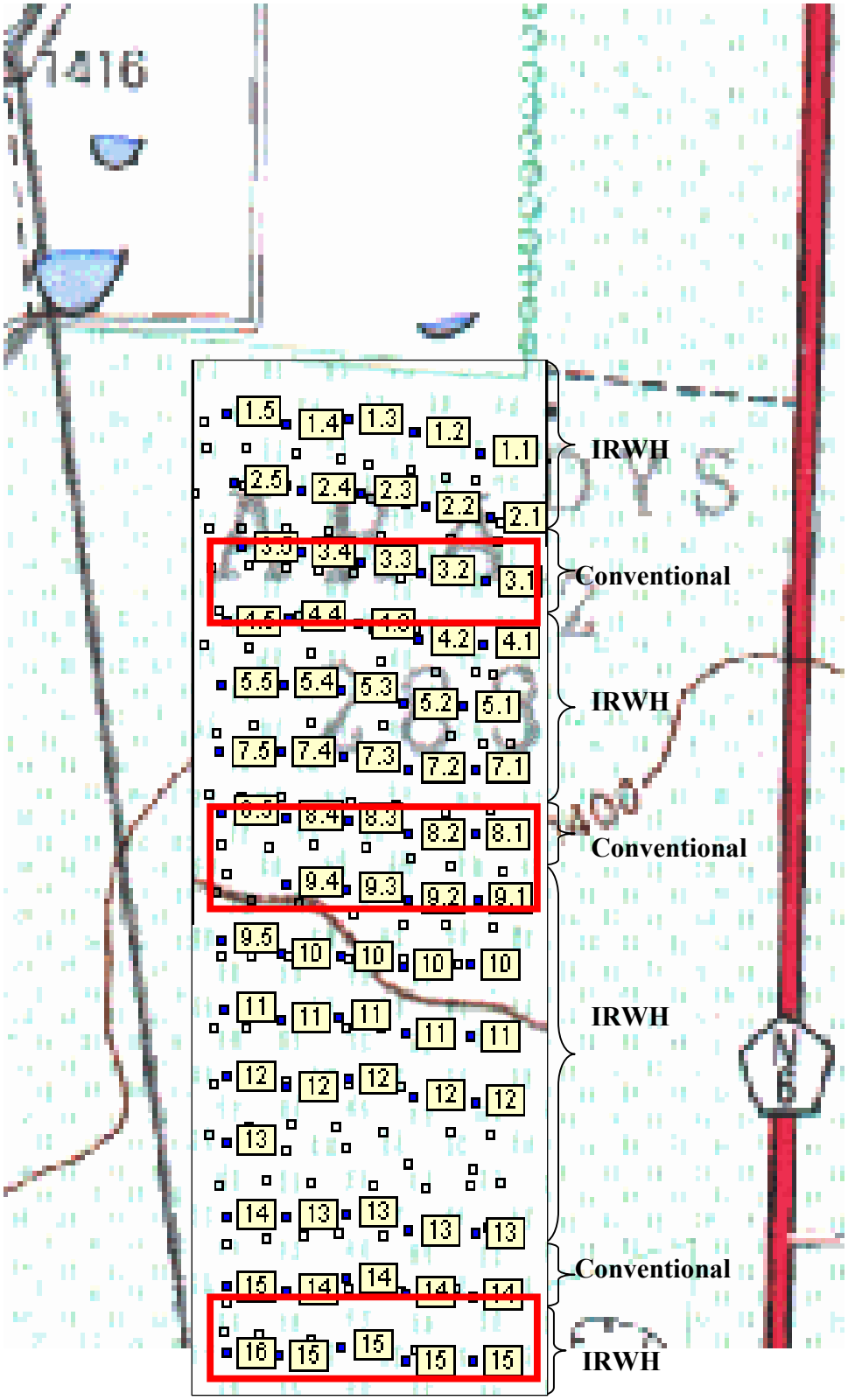

Figure 1.7: Schematic layout of the conventional and IRWH treatments on the 55 ha field at Paradys Experimental Farm.

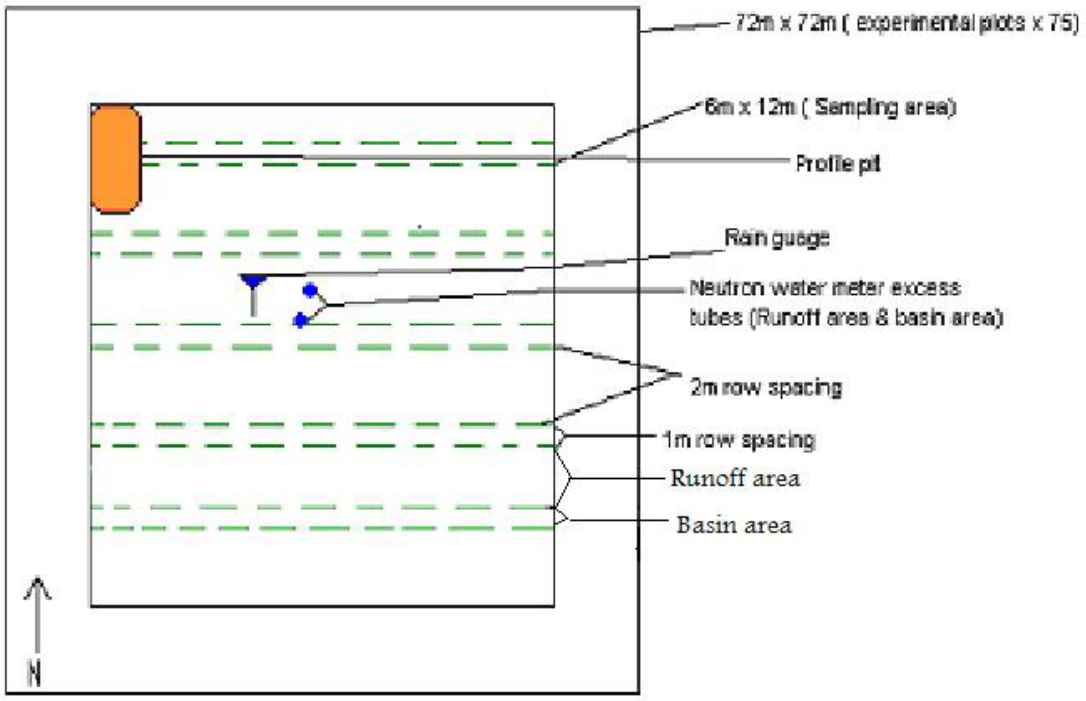

Figure 1.8 Schematic layout of the IRWH structure and instrumentation used in each of the 75 experimental plots.

1.3.4 Agronomical practices

1.3.4.1 Land preparation

Historically the 55 ha land was cultivated in a conventional manner which comprised of ploughing the land 250 mm – 300 mm deep as a primary cultivation activity. It was then disked Farrowed in most of the years to break down the clods as a secondary cultivation activity for preparing the seedbed.

Conventional: For the field trials the land was ploughed (250 mm to 300 mm deep) as a primary cultivation activity. As a secondary cultivation activity the land was disk harrowed to break down clods. During other studies that were conducted on the field profile pits were made. These profile pits indicated that compaction occurred beneath the plough layer around 300 mm deep. Just before planting the total 55 ha land was ripped 450 mm deep on the plant row to

eliminate any compaction that might have occurred. The maize was planted in tramlines on 900 mm intervals.

IRWH: A contour survey was conducted on a 0.5 m grid over the total 55 ha experimental site. The contour map was studied to divide the area into larger IRWH topographical terraces. Contour ridges (200 mm high) were made a long the contour lines to eliminate any lateral flow of water from the land. The basin plough was then implemented along the ridges to create the basins along the contour ridges. A grader was used to give the runoff area a slight slope (< 1%) towards the basin area so that in-field runoff would be increased.

The total area of the experimental site was fertilized with 3:1:0 at 150 $kg.ha^{-1}$ before planting. The maize cultivar Pan 6146 was planted at a plant population of 16 000 $plants.ha^{-1}$. The maize was planted on 10 January 2006. The total area of 55 ha was treated with Roundup and 2.4D Ester before germination.

CHAPTER 2

Spatial variation of selected soil properties in and between map units

2.1 Introduction

Research investigations have shown that the variable characteristics of soils have major effects on the fertilizer requirement and on the nutrient transport over and within a soil profile. Spatial variability causes uneven patterns in soil fertility levels and crop growth, and decreases the efficiency of fertilizers applied in the fields. The site specific management of nutrients used in precision agriculture (PA) can only be made by quantitive assessment of the spatial variability (Gupta *et al*., 1997).

Precision agriculture is an integrated information and technology based agricultural management system. The intent is to manage spatial and temporal variability associated with all aspects of agricultural production for optimum profitability, sustainability and protection of the environment. Studies have investigated within-field variability of soil properties and evaluated the impact of site specific management on crop production and other land use purposes (Miao *et al*, 2006).

However for many applications of what it is necessary to consider the variability of the soil. In agriculture the manipulation of these variable properties of what will increase yield, but it is uncertain which soil property limits production at a certain spot in a certain year. Through advanced interpolation techniques the variation in soil properties may be visually characterized, so that the effect of the variation on yield may be correlated. Different sampling methods and interpolation techniques as well as the understanding of surfaces for

the use in interpolation is of great importance, as it is clear that soil properties will be characterized according to circumstances using the appropriate sampling method and interpolation technique that suits the circumstances the best (Hillel, 2004).

The modelling of spatial variation as well as the interpretation of the visual image to affectively determine the reason why areas does not give the suspected yield, is a tool that may be used by precision agriculture. This process reduces inputs and causes an increase in production. The precise amount of fertilizer application for example may be determined for each part of the land, rather than treating the whole land uniformly in the fertilizer application process. Thus, the correct model and interpolation technique may assist the farmer in its decision making.

The objectives of this chapter therefore are to (i) do a thorough literature study on statistical and spatial variation of soil properties, (ii) describe the morphology of the soil forms found at the experimental site, (iii) describe the chemical and physical characteristics of the soil forms found at the experimental site and (iv) justify that a soil map is in fact a useful spatial representation by indicating that there is a higher spatial variation between map units than within map units and that by using the correct interpolation processes one will be able to characterize this spatial and variation effectively.

2.2 Literature Review

2.2.1 Variability of soil properties

2.2.1.1 Statistical variation of soil properties

Physical properties

Texture: In an experiment done on the spatial variability in soil properties on slow-forming terraces in the Andes region of Ecuador, Dercon *et al*. (2003) sampled the soil in bands following the contour. They were located every 1 m beginning at the highest point of elevation and including the lowest point on the terrace. The soil depth for all samples was 0 – 15 cm. Texture fractions of sand, silt and clay were analyzed. The Shapiro-Wilk W-test was used to test for normality and the Pearson correlation was calculated to examine the relationship between pairs of variables. (Cody & Smith, 1997).. Statistical significance was tested at 0.01 and 0.05 level. Stepwise multiple regression analysis was used to test the hypothesis on each experimental site at a significance level of 0.01.

Through the study it was found (Table 2.1), that clay content was significantly ($P \leq 0.01$) positively correlated with characteristics such as phosphate (P) ($R^2 = 0.84$), pH ($R^2 = 0.88$) and aluminium (Al) ($R^2 = 0.54$), but negatively correlated with organic carbon (OC) ($R^2 = -0.73$). Soil fertility is normally positively correlated with clay content (Scholes *et al*., 1994). However, in the higher and humid regions of the Andes region increasing clay content is often associated with the presence of old volcanic tuff having high Al toxicity and high P fixation. Silt and clay were significantly related to relative distance in five to six terraces.

Table 2.1 A Pearson correlation matrix (r) of soil properties on the slow forming terraces in the Andes region (n=51) (Dercon *et al.*, 2003)

	$pH_{(H2O)}$	Corg	N total	C/N	NO^{3-}	P	K	$pH_{(NaF)}$	Al_{ex}	P_{ret}	K_{ex}	Ca_{ex}	Mg_{ex}	BS	CEC	Silt	Clay	Sand	Distance
$pH_{(H2O)}$	-																		
Corg	-0.09	-																	
N total	-0.19	0.67	-																
C/N	0.14	0.26	-0.49	-															
NO^{3-}	-0.46	0.33	0.27	0.07	-														
P	-0.47	0.19	0.08	0.14	0.71	-													
K	0.29	0.22	0.09	0.22	0.32	0.26	-												
$pH_{(NaF)}$	-0.20	-0.51	-0.63	0.30	0.26	0.44	0.02	-											
Al_{ex}	-0.30	-0.60	-0.50	-0.11	-0.28	-0.09	-0.59	0.41	-										
P_{ret}	-0.26	-0.51	-0.54	0.20	0.17	0.35	0.05	0.81	0.43	-									
K_{ex}	0.26	0.64	0.60	-0.10	-0.04	-0.18	0.42	-0.72	-0.61	-0.59	-								
Ca_{ex}	0.19	0.63	0.69	-0.26	-0.20	-0.37	0.03	-0.90	-0.44	-0.75	0.86	-							
Mg_{ex}	0.28	0.55	0.63	-0.26	-0.31	-0.44	0.04	-0.92	-0.46	-0.78	0.84	0.97	-						
BS	0.21	0.55	0.63	-0.28	-0.29	0.43	0.01	-0.92	-0.44	-0.77	0.82	0.96	0.99						
CEC	-0.01	0.08	-0.08	0.21	0.41	0.32	0.29	0.35	0.04	0.28	-0.09	-0.25	-0.38	-0.14		-			
Silt	0.10	0.66	0.64	-0.10	0.26	0.05	0.29	-0.64	-0.71	-0.69	0.55	0.59	0.61	0.29	0.63		-		
Clay	-0.19	-0.73	-0.71	0.17	0.02	0.27	0.04	0.88	0.54	0.84	-0.75	-0.91	-0.89	-0.18	-0.88	0.20		-	
Sand	0.20	0.63	0.62	-0.18	-0.17	-0.40	-0.11	-0.84	-0.34	-0.76	0.72	0.92	0.88	0.08	0.85	-0.16	0.50		-
Distance	-0.27	0.29	0.36	-0.18	0.45	0.46	0.37	-0.19	-0.35	0.05	0.34	0.17	0.13	-0.15	0.16	0.01	0.39	-0.16	

In another study conducted on the spatial variability of soil properties and their relationship with soybean yield, Cox *et al*. (2003) found that the variability of sand, clay and silt fractions were dependant on the topography. The spatial variability expressed as the coefficient of variation (CV) of the properties was as follows: sand 25%, clay content 28%, which is an indication of the relatively stability of these two properties. The silt fraction had a low spatial CV of 11%. It is thus clear that textural fractions tend to have a low spatial variation over topographic landscapes that tend to be more level, while it will tend to vary more spatially with a topographic landscape that varies in elevation, aspect and slope.

Low correlation between relative distance and other soil properties may be explained in several ways: (i) that soil properties did not show a logical pattern of spatial variability or a gradient in the direction of the terraces, (ii) the gradient was highly site dependent and (iii) the gradient was not linear. Correlation were significant when considering each slow-forming terrace separately, indicating that spatial variability is site dependent.

Hydraulic properties:

Saturated hydraulic conductivity (Ks): This is a challenging soil hydraulic property to describe because it can change many orders of magnitude over short distances. Heterogeneity of soil properties within and between soil horizons causes some regions to be more or less favorable to flow. The flow of water is highly variable with extremes represented by tortuous flow between individual particles and rapid flow through large, continuous macro pores.

Sobieraj *et al.* (2003) found that spatial patterns were clearly evident for topography and soil textural components, as reflected in scatter plots. Scatter plots however, showed considerable noise and little to no spatial structure at the coarsest sampling scales of 25 m and 10 m. These contrasting results suggest no link between Ks and these physical properties at coarse sampling scales. Which was remarkable was that these spatial patterns of Ks corresponded perfectly with the textural and topographic data of transect 6 that was studied. Why did this hydraulic boundary occur for one topographic/texture step and not the other? A correlation was found only in the locations where the concentration of sand $\geq$ 80% and clay $\leq$ 20%, suggesting that very coarse textures (loamy sand and sand) are influential in controlling Ks (Table 2.7).

Table 2.7 Percentage of soil samples in each textural class (Sobieraj *et al.*, 2003)

Transect	Depth (cm)	Sandy clay (%)	Sandy clay loam (%)	Clay loam (%)	Sandy loam (%)	Loamy sand (%)	Sand (%)
2	0 - 12.5	4.3	53.2	0	22.6	15.5	4.3
	40 -50	31.7	56.1	2.4	7.3	2.4	0
4	0 - 12.5	0	100	0	0	0	0
	40 - 50	14.3	85.7	0	0	0	0
	90 - 100	64.6	35.4	0	0	0	0
6	0 - 12.5	0	0	0	41.2	43.1	15.7
	40 - 50	0	58.8	0	17.6	23.6	0
	90 - 100	33.3	56.9	0	9.8	0	0

Thus through terminology of Ringrose & Voase (1991) the spatial variability of Ks is similar to that of soil texture only when the sand component is greater than 80%, suggesting that the textural macroporosity is more significant than bioporosity for extremely coarse textures.

In another study on the spatial variability of soil hydraulic conductivity along a tropical rainforest catena (Sobieraj *et al.*, 2003), K_{sat} was measured along an transect at depths of 20, 30, 50

and 90 cm with a compact, constant - head permeameter. K_{sat} was found to not be significantly different between these soil forms at any depth except for 90 cm. Calculations of the mean indicate a relatively constant value for K_{sat} at depths of 20, 30 and 50 cm.

Had there been a soilform controlled spatial structure of K_{sat} they would have expected a stronger correlation between measurements on the same soil form than between measurements on two different soil forms. They concluded that the strong topography dependence of soil forms along a transect is not reflected in a similar dependence of K_{sat} and tentatively attributed this lack of dependence to the overriding influence of bioturbation - controlled macroporosity. Thus through both studies it may be concluded that the spatial variation of saturated hydraulic conductivity is influenced by a lot more than topography and soil forms. Bioturbation controlled macroporosity and soil texture with a sand fraction of more than 80% for example have a definite affect on the spatial variation in K_{sat} as well. Further studies have to be done to identify all the factors affecting the spatial variation of the saturated hydraulic conductivity, before a model to characterize the variation may be established

Chemical properties

Calcium and Magnesium: Burt & Park (1999) previously described variability in exchangeable Ca and Mg across a granitic hill slope in Southwest England. They attributed minimal variation of Ca and Mg in surface soils to similarities in behavior as nutrient cations, with tight cycling in vegetation and uniform atmospheric and litter fall inputs. Data from a study on the spatial variability in soil ion exchange chemistry in a granitic upland catchment suggested the contrasting behavior of Ca and Mg, and a variation of Ca between plots that arise due to the

nature of organic material as a result of varying litter decomposition rates and vegetation types (Stutter *et al.*, 2002). In this experiment high CV values are comparable with those reported for agricultural situations where high variability is attributed to differences in management practices.

Gupta *et al.* (1997) modelled the spatial variability of soil chemical parameters for site-specific farming using stochastic methods. They found that Ca varied from 576 to 816 mg L^{-1} and the CV value was 11% in the x-direction and 9% in the y-direction. Mg varied between 107 and 124 mg L^{-1} and the CV value was 13% in the x-direction and 11% in the y –direction, which are both stable coefficients of variation. The non-significant differences in the x- and y- direction indicated the presence of similar soil form, crop residue, soil moisture and field topography in both directions at the study site.

Dercon *et al.* (2003) indicated in Table 2.1 that Ca and Mg is 97% correlated, which shows that the degree of variation for both these parameters tend to be identical. In the same experiment comparisons where made between predicted and measured data and it was found that the differences between the two was less than 10% for Ca & Mg, which is a clear indication that if certain parameters such as litter decomposition and vegetation types are known that a good prediction of the variation in Ca & Mg may be made.

Potassium: Gupta *et al.* (1997) found in their experiment that potassium concentration values exhibited a greater degree of variation compared to Ca and Mg parameters (Table 2.1). The CV value for K was 19% in the x- direction and 15% in the y-direction in relation to the Ca and Mg concentration values that varied between 9% and 13% respectively. In the same

experiments models indicated that the difference in measured and predicted values are between 16% and 26% which is a lot higher than the differences for Ca and Mg. This is an indication that K has a tendency to have a higher degree of variation. Miao *et al.* (2006) conducted a study on the magnitude of variability in soil properties and found that K had a large variation within the field, ranging from 65 to 282 mg kg^{-1} at site 1 and from 67 to 192 mg kg^{-1} at site 2 (Table 2.3).

Table 2.3 Descriptive statistics and semi-variogram parameters of selected soil properties (Miao *et al.*, 2006)

Soil Variables	Field	Mean	Min	Max	CV (%)
OM (g kg^{-1})	1	39	10	76	36.5
	2	28	15	42	24.8
CEC (cmol kg^{-1})	1	16.5	9.1	25.1	23.6
	2	11.1	6.9	17.2	26.9
pH	1	6.3	5.3	7.6	6.3
	2	6.3	4.7	7.6	9.5
pH (mg kg^{-1})	1	35.5	14	81	45.3
	2	31.4	16	107	56.8
K (mg kg^{-1})	1	147	65	282	26.6
	2	124	67	192	28.1
S (mg kg^{-1})	1	9.2	7	12	10.7
	2	9.3	7	19	25.1
Zn (mg kg^{-1})	1	1.9	1.4	2.5	13.6
	2	4.2	2.6	12	48

Stutter *et al.* (2002) compared two profiles namely the Typic Placaquod and the Typic Humaquept (Table 2.4). In both soil horizons (organic and mineral) of the Humaquept the order of abundance for the base forming cations was Mg > Ca > K > Na. Although the same order of abundance was observed for the Placaquod organic horizon, the sequence of the mineral subsoil differed as follows: K > Mg > Na > Ca, respectively. Previous analysis of bulk soil mineralogy for the Pacaquod plot showed a dominance of quartz (51%), with 26% K-feldspar, 15% Na-Ca feldspar albite, and 3.8% of dioctahedral phyllosilicates, that

probably comprises kaolinite, mica and illite. Such mineral compositions are most likely to contribute K and Na through weathering, accounting for the increased prevalence of K with depth in the Placaquod. Through this study it may be a clear indication that the distribution of cations down the profile and spatially, may be a result of the exchange material.

pH: Soil pH ($_{H2O\ \&\ KCl}$) has been recognized by many experiments to have a low spatial variation. Miao *et al*. (2006) found that the CV for pH varied between 6.3% and 9.5%, which is significantly lower than the rest of the parameters found in Table 2.3. Zehetner & Miller (2006) found that soil acidity decreased with increase in elevation (Figure 2.1).

This is likely caused by higher acidity inputs due to higher rainfall, by greater leaching of basic cations, and by greater activity of acidic humic substances as a result of slowed organic matter decomposition at higher elevations.

Cox *et al*. (2003) stated that pH was the one soil property that did not have a high spatial variation that changed yearly. In both their years of study (1998 & 1999), pH had the lowest variability of 11% and 12%, respectively. From the figures it is thus clear that pH is a soil property that has the tendency to have a low spatial variation over years if the cultivation practices stay unchanged.

Table 2.4 Comparison of the two representative soil profiles (Stutter *et al.*, 2002)

Typic Placaquod		
Parent Material	Coarse granitic drift	
Slope	3-5 degrees uniform	
Altitude (m)	405	
Aspect	E	
Surface form	Hummocky	
Dominant vegetation	Calluna vulgaris	
Horizon	**Depth(cm)**	**Description**
Oi	0>1	Thin litter Calluna fragments
Oa	1>12	Abundant roots, some quartz
		fragments present at base
AE	12>19	5YR5/1, Loam
Bh(s)1	19>60	5YR3/3, sandy clay loam, stoney layer (25cm),
		increased OM and root mat over thin placic horizon
		(approximately 58-60cm)
Bs2	60+	5YR5/8, weakly indurated, horizon
Typic Humaquept		
Parent Material	Coarse granitic drift	
Slope	3-5 degrees concave	
Altitude (m)	385	
Aspect	WNW	
Surface form	Level	
Dominant vegetation	Calluna vulgaris	
Horizon	**Depth(cm)**	**Description**
Oi/Oe	0>2	Some litter, mainly partly decomposed, spong material
Oa	2>20	Fewer Roots, dense, seeping at base
Ah	20>25	7.5YR3/3, sandy loam, abundant stones, wet, high humic content
Bw1	25>40	7.5YR4/3, sandy clay loam grading to
		7.5YR5/4 silty clay loam, wet, some OM at base
Bw(s)2	40+	7.5YR5/6, gritty clay loam, some iron staining

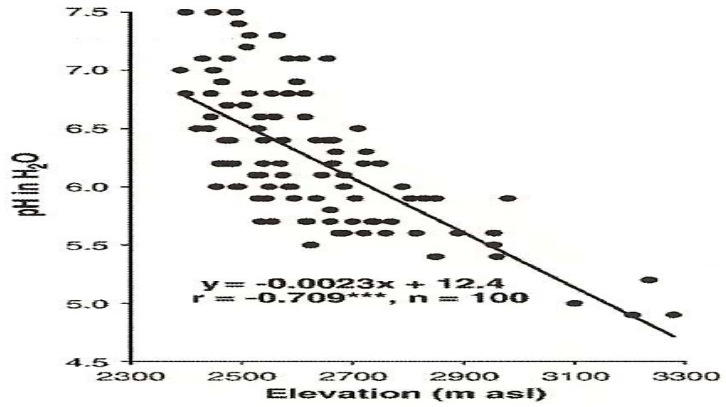

Figure 2.1 Topsoil pH $_{(H2O)}$ as a function of elevation (Zehetner & Miller, 2006).

Nitrogen: Nitrogen fertilization has historically been an important crop input from production, economic, and environmental standpoints. Currently it receives more scrutiny because of the increased cost of N fertilizer and concerns about environmental degradation, and demands for mandatory nutrient planning (Dinnes *et al.*, 2002). To implement variable - rate fertilization or site - specific nutrient management practices, databases that provide spatial distributions of soil properties are needed. Geostatistical techniques have been used to explore the structure of spatial variation in agricultural soil by mapping areas of environmental concern and developing site-specific fertilizer application maps (Cambardella & Karlen, 1999).

Shahandeh *et al.* (2005) used the coefficient of variation to describe the variability of nitrogen. The parameters measured varied spatially and temporarily. Among the N parameters, N_{min} values tended to be the most variable, with CV values of 27% and 46% in 2002 and 2003, respectively (Table 2.5 & 2.6). The range in N_{min} for the 63 samples collected across the field in 2002 was from 6 to 35 mg kg^{-1}, with a mean value of 20 mg kg^{-1} and from 1 to 33 mg kg^{-1}, with a mean value of 16 mg kg^{-1} in 2003. The N_{min}

variability observed in the experiment was similar to CV values of 24% and 36.4%. The results in Table 2.5 and 2.6 showed that soil N measurements tended to become more normally distributed in years following N application. Total N and N_{min} in 2003 remained the same, with moderate and strong spatial dependence, respectively. Nitrate N became weak or random in 2003, indicating spatial independence. Other parameters, such as initial soil NH_4-N and NO_3-N concentrations and soil C mineralized, were weakly or not spatially correlated in either 2002 or 2003 (Shahandeh *et al.*, 2005).

Table 2.5 Descriptive statistics of parameters measured in 2002 (Shahandeh *et al.*, 2005)

Parameter	Mean	Max	Min	CV
Grain Yield (kg ha^{-1})	6430	8685	4528	14
Total N (mg kg^{-1})	966	1230	727	12
Organic N (mg kg^{-1})	963	1221	725	12
NH_4-N (initial) (mg kg^{-1})	4	9	2	31
NO_3-N (initial) (mg kg^{-1})	12	21	8	24
Inorganic N (initial) (mg kg^{-1})	16	26	11	22
NH_4-N @ 24d (mg kg^{-1})	5	8	2	25
NO_3-N @ 24d (mg kg^{-1})	31	44	17	19
Inorganic N @ 24d (mg kg^{-1})	36	52	19	18
N mineralised @ 24d (mg kg^{-1})	20	35	6	27
NO_3-N 15 cm (mg kg^{-1})	29	50	18	22
NO_3-N 30 cm(mg kg^{-1})	53	88	36	19
NO_3-N 60 cm (mg kg^{-1})	93	148	62	18
NO_3-N 90 cm (mg kg^{-1})	120	193	84	18
CO_2-C @ 24d (mg kg^{-1})	246	431	78	22
SOC (mg $C.g^{-1}$)	9	13	2	18
Clay (%)	54	64	42	10

Table 2.6 Descriptive statistics of parameters measured in 2003 (Shahandeh *et al.*, 2005)

Parameter	Mean	Max	Min	CV
Grain Yield (kg.ha^{-1})	4298	5141	2554	13
Total N (mg.kg^{-1})	767	1085	552	16
Organic N (mg.kg^{-1})	760	1082	544	16
NH_4-N (initial) (mg kg^{-1})	8	26	3	51
NO_3-N (initial) (mg.kg^{-1})	4	7	2	18
Inorganic N (initial) (mg.kg^{-1})	12	31	7	34
NH_4-N @ 24d (mg.kg^{-1})	7	10	4	18
NO_3-N @ 24d (mg.kg^{-1})	21	35	7	32
Inorganic N @ 24d (mg.kg^{-1})	28	42	13	25
N mineralised @ 24d (mg.kg^{-1})	16	33	1	46
NO_3-N 15 cm (mg.kg^{-1})	16	21	12	13
NO_3-N 30 cm(mg.kg^{-1})	31	40	22	12
NO_3-N 60 cm (mg.kg^{-1})	58	71	41	11
NO_3-N 90 cm (mg.kg^{-1})	84	105	62	11
CO_2-C @ 24d (mg.kg^{-1})	271	370	202	16
SOC (mg.C g^{-1})	10	26	7	38

Nitrate N and clay content were significantly related to yield and seemed to be responsible for variation in high- and low-yield plots, respectively. Residual NO_3 - N was positively related with yield in both high- and low-yield environments, while clay content exhibited a negative relationship with grain yield in low-yielding plots. Total N in low-yielding plots was positively related to NO_3 - N and $N_{min,}$ while clay content and N_{min} were negatively related (Figures 2.2 and 2.3).

(a) 15 cm (b) 30cm

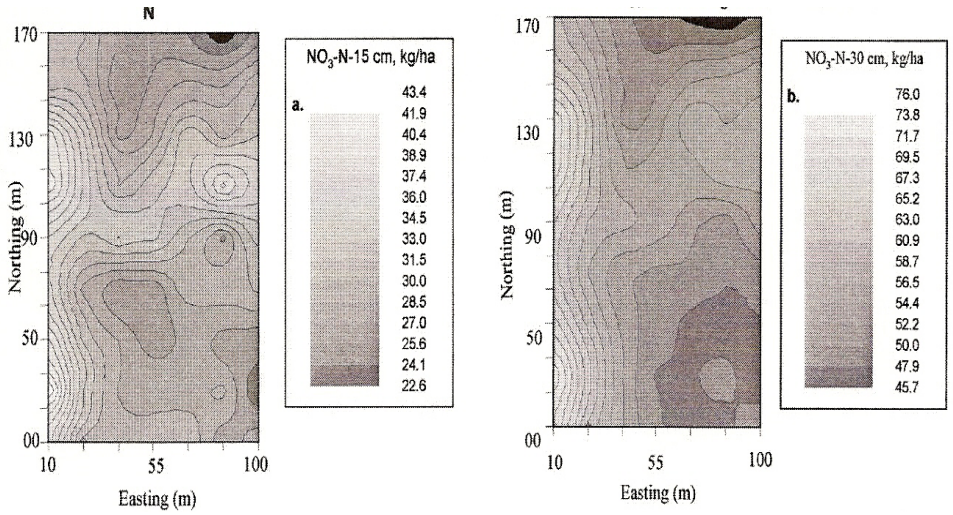

(c) 60cm (d) 90cm

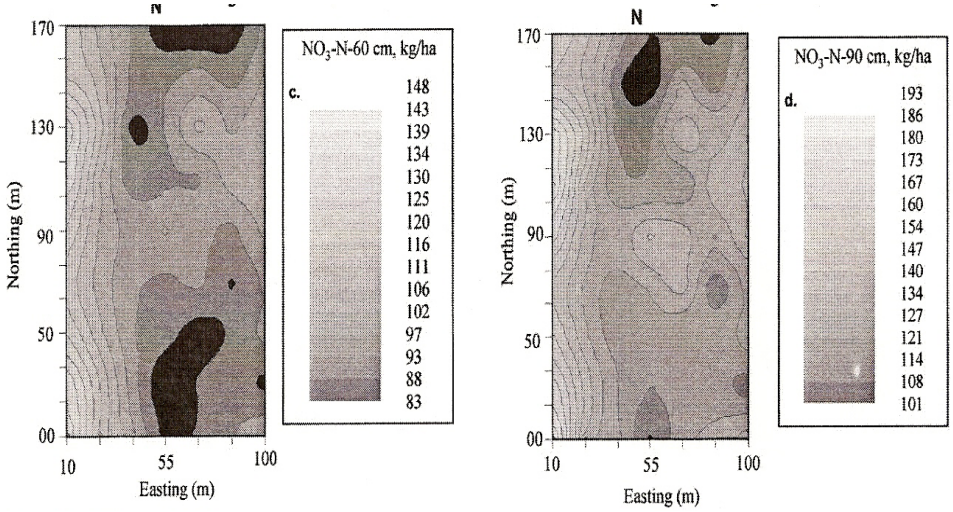

Figure 2.2 Kriged contour maps of (a-d) soil NO_3-N with depth in 2002 (Shahandeh *et al.*, 2005).

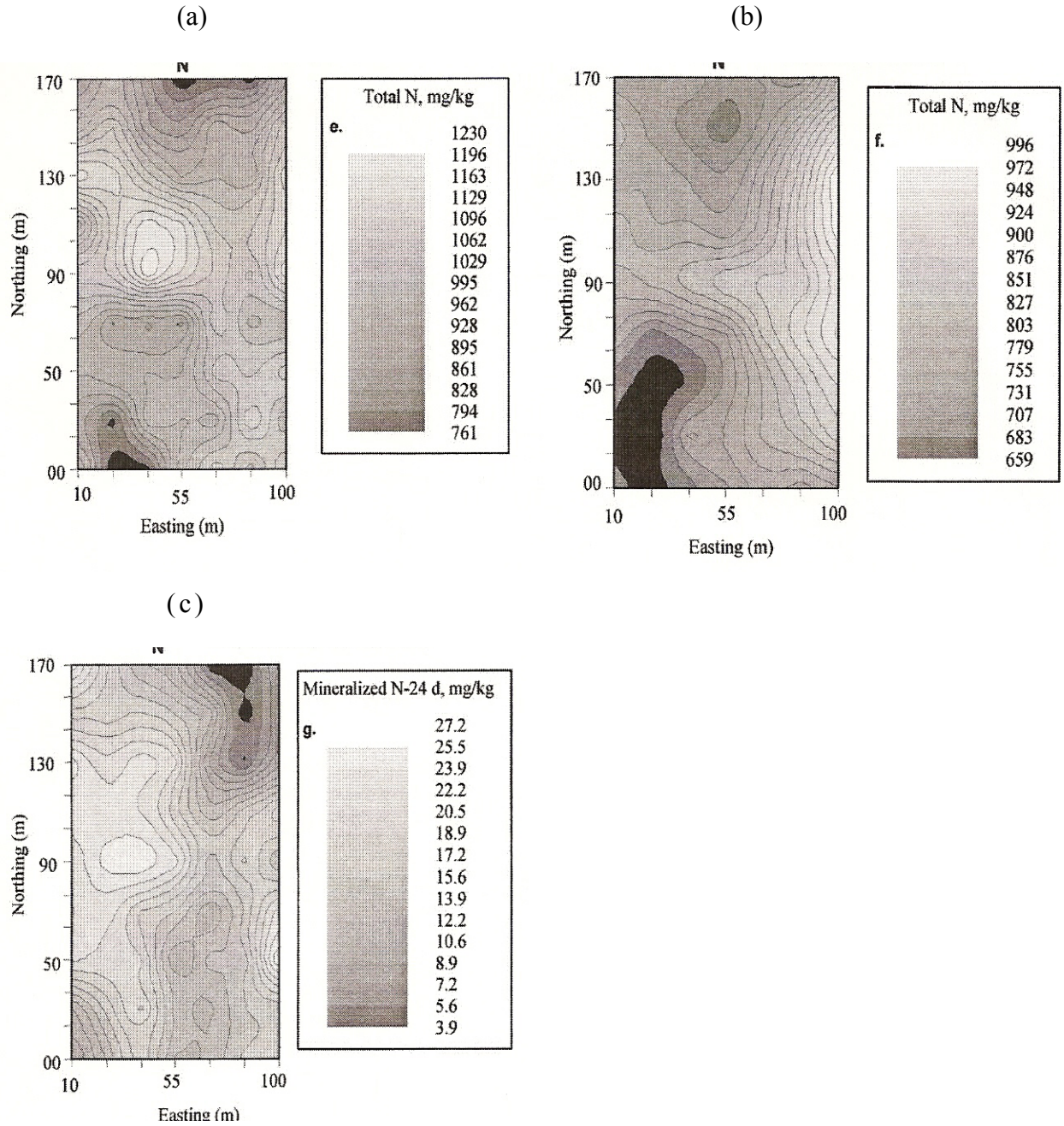

Figure 2.3 Kriged contour maps of (a-b) total N in 2002 and 2003, and (c) mineralized N in 2003 (Shahandeh *et al.*, 2005).

2.2.1.2 Spatial variation of soil properties.

Kriging is used to generate spatial presentations of the variation in soil properties. The spatial structure of the soil properties is described by a semi – variogram. It is estimated as the average of the squared differences between all observations separated by a lag distance. From the variogram generated for the soil properties, Kriging may be used to generate a surface that illustrates the distribution of various soil properties (De Clerq *et al.,* 2001). Surface representation of soil property variation has been modelled through Kriging for an 18 ha lucerne stand in the Brits district in the North West Province of South Africa (Venter, 2003).Through this presentation, together with knowledge of the interrelationship between soil properties a better result may be generated

Physical Properties

Sand content: The sand content increases from the western corner across the land to the eastern corner (Figure 2.4). Sand content is an inherent soil property and cannot be manipulated by management practices. The sand content has inverse correlation towards soil pH as a sandy soil looses its base forming cations through leaching, resulting in a decrease in pH. From the surface representation of the sand content it is clear that in the areas for example the eastern corner where the sand content is high a low pH will result (Figure 2.3). The water retention of the soil also has an inverse correlation to the sand content. An increase in sand content causes the soil to be more freely drained resulting in a decrease in water retention. The base forming cations also decreases as the sand content of the soil increases. This due to the fact that a sandy soil looses is base forming cations through the process of leaching (Venter, 2003).

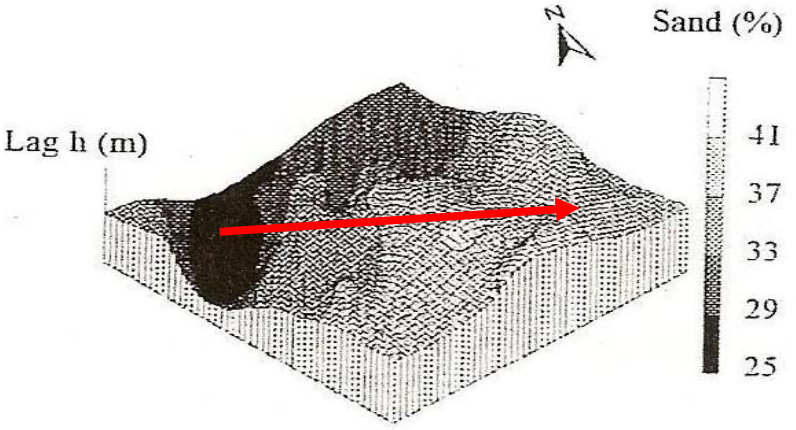

Figure 2.4 Kriged surface representation of the distribution of the sand content in the top soil (Venter, 2003).

Chemical Properties

pH: The pH $_{(H2O)}$ is the lowest in the south - easterly corner of the land and increases gradually to the northern part (Figure 2.5).

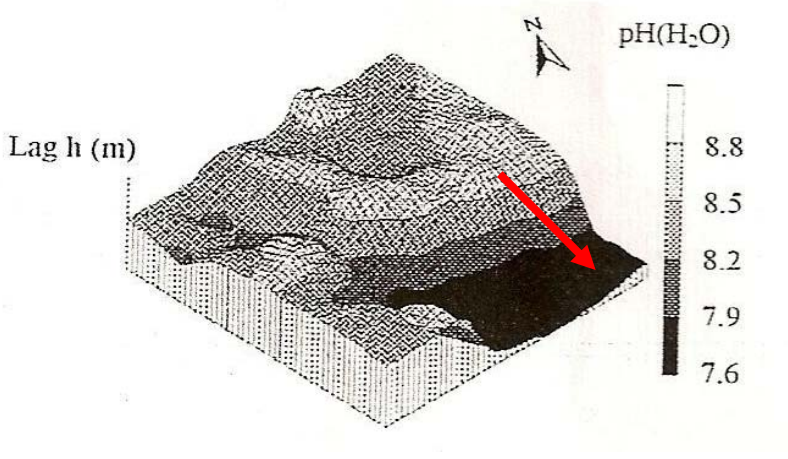

Figure 2.5 Kriged surface of the distribution of pH$_{(H2O)}$ in the top soil (Venter, 2003).

Organic carbon content: The distribution of OC in the soil is spatially relatively uniform (Figure 2.6). Though there seems to be an area in the north easterly corner of the land that gradually decreases to the eastern corner. This correlates with the same transect in the pH surface representation. The reason may be due

to the increase in organic carbon, resulting in higher mineralization and a decrease in pH.

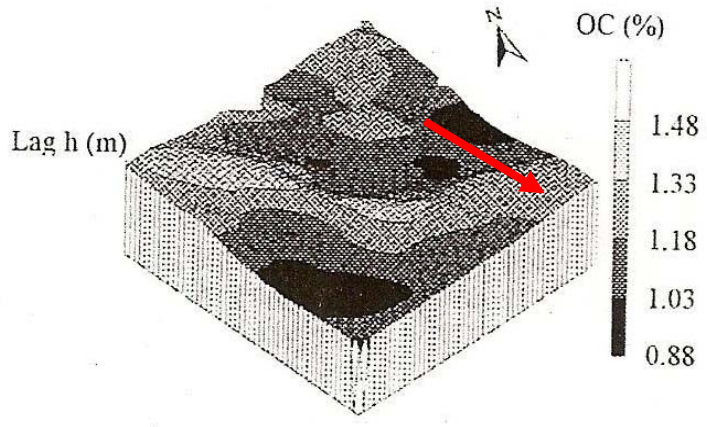

Figure 2.6 Kriged surface representation of the distribution of the OC (%) in the top soil (Venter, 2003).

2.2.1.3 Yield variation in relation to soil properties

Measured Yield: The map generated for the measured yield indicated that values were generally larger in the south - eastern corner of the land (Figure 2.7). There is a clear resemblance between measured yield and best correlated soil properties, soil pH and OC. This makes it clear that yield may be fairly accurately predicted from soil properties such as pH ($_{H2O}$), OC (%) and sand content (%) of the soil.

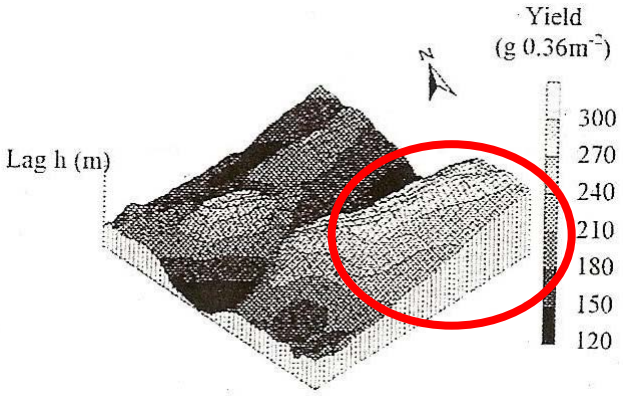

Figure 2.7 Kriged surface of the measured yield (Venter, 2003).

2.3 Methodology

2.3.1 Soil Survey

A hydraulic soil auger was used to draw soil cores on a 50 m grid (Figure 2.8) as it is more economical than digging 75 profile pits over the 55 ha. Using the core sampler is also more effective than using the commonly used Thomson or Edelman hand augers as the core sampler preserves for example strucure, peds and other morphological features. This is essential in the classification and description of the soil forms. A profile pit was made on each of the thirteen plots that were selected in Chapter 3. All the observations (cores and pits) were classified according to the Soil Classification Working Group, 1991, but only the thirteen profile pits were morphologically described in detail (Appendix Q, R and S). The core samples were described according to soil form, depth and field estimates of texture.

Figure 2.8 Soil cores drawn using the hydraulic core sampler.

2.2.6 Soil analysis

Each of the 75 experimental plots was chemically & physically analyzed for Ca, Mg, Na, K, pH ($_{H20}$), pH ($_{KCl}$) & particle size distribution (seven class) according to the Non-Affiliated Soil Analysis Work Committee, 1990.

2.2.7 Statistical and spatial analysis

Maps were drawn of the different physical and chemical parameters using WISH (Lukas, 1992). A thorough literature study was conducted on various interpolation techniques (Appendix U). Inverse distance weighting (IDW) was selected as the most suitable interpolation technique for the specific analysis. It was used to predict parameter values in areas where data was deleted to calculate the degree of accurate prediction in a certain area which could then be an indicator of the amount of spatial variation in a certain area. The coefficient of variation and the 25% and 75% quartile was calculated using NCSS, 2000 (Hintze, 2000) and was used as an indication of the spatial variation within and between map units.

2.3 Results and Discussion

2.3.1 Factors of Soil Formation

The soil forms (Tukulu, Sepane and Bloemdal) occurring at the experimental site differs from the Ca22 Land type data seen in Appendix T. All three soil forms do not make part of the land type data. Tukulu and Sepane soils were only included in the updated version of the South African soil classification system. The following soil forming factors may though have an influence on the occurrence of these three soil forms at the experimental site.

2.3.1.1 Climate

Rainfall: The Free State is a summer rainfall area with the highest and most reliable rainfall occurring in February and March. During November, December and January the rainfall is erratic with much of it in the form of high intensity rainfall events. The high evaporation demand and relatively low rainfall make this a semi - arid climate. The long term mean rainfall is 542.7 mm per annum (Table 2.7). The rainfall together with the topography may cause the movement of clay downwards in the landscape. This may result in the occurrence of pedocutanic B horizons down slope and the occurrence of red apedal B horizon higher up in the landscape.

Temperature: Low temperatures below freezing point coupled with very little rainfall are experienced during the winter (Table 2.7). While high temperatures around 30˚C coupled with less than frequent rainfall events occur during summer. During the summer months the evaporative demand is very high dropping during autumn.

Aridity index: The high temperature, low humidity and low to moderate strong winds drives a very high evapotranspiration demand of between 250 mm and 300 mm per month during the summer months, dropping to around 100 mm per month during winter months (Table 2.7). The aridity index peaks at 0.45 during March resulting in excess of water in the soil profile draining to the subsoil. This water causes signs of wetness in the underlying material where impermeable materials occur. The distribution of soils on this area by implication is influenced by an underlying impermeable layer. This causes the hydrology of these soils to be influenced by a transient water table due to excess water in the profile and interflow from higher lying soil bodies. In this climate there is no shortage of radiation or temperature in the summer months.

Leaching during March can play a role to remove free salts and move clay in the profile. Although cation distributions in the profiles indicate some leaching of free salts, the increase in clay with depth is rather due to mixing processes like bioturbation, pedoturbation as well as from windblown and colluvial deposits (Le Roux, 1996).

Table 2.7 The climate of the area (WRC report no. 1176/1/03, 2003).

Parameter	Jul	Aug	Sept	Oct	Nov	Dec	Jan	Feb	Mar	Apr	May	Jun	Long term total
Rain (mm)	8.1	11.6	19.3	49	68.2	66.6	83.4	77.6	80.7	49.3	19.9	9	542.7
Evap (mm)	93.5	140	197	239	256	291	276	207	177	126	110	81.9	2198.2
Max Temp.	17.8	20.6	24.4	25.4	28.3	30.2	30.8	29.5	27.4	23.9	20.5	17.9	24.8
Min Temp.	-1.6	0.9	5.2	9.2	12	14	15.3	14.8	12.6	7.8	2.8	-1.1	7.5
Ave Temp.	8.1	10.7	14.8	17.5	20.1	22	23	22.1	19.9	15.8	11.6	8.2	16.2
AI	0.08	0.08	0.09	0.2	0.26	0.22	0.3	0.37	0.45	0.39	0.18	0.11	0.232

2.3.1.2 Parent Material

Three main types of parent materials occur in this area, namely Dolerite, Beaufort Sandstone and Shale.

Dolerite: These are examples of basic igneous rocks. It has no free quartz and weathers to silicate clays. It contains high amounts of swelling clays and gives rise to clay contents of between 30% and 40%.

Beaufort Sandstone: These parent materials are examples of 2:1 clay minerals high in clay content (40% - 45%). They weather and give rise to Pedocutanic B horizons which is highly active in the swelling and shrinking process.

Shale: The influence of this parent material to soil form is very similar to the sandstone but may result in slightly higher clay contents. The parent materials give rise to clay contents of 40%. Wind blown sands have a major influence on soil form occurrence. The influence is the highest in the occurrence of the Bloemdal soil form and declines to the Tukulu and the Sepane soil form.

The influence of these silicate clays swelling ability is reduced by the mix up of windblown sands as well as the colluvial influence of Mudstone and Schale. The increase in clay content downwards in the profile can be explained by a combination of addition by the different parent materials and pedoturbation. Because the weathering of clay forming parent materials gives rise to higher clay contents in the bottom of the profile and windblown sand give rise to higher sand contents in top soils, it results in an increase in clay downwards in the profile. Pedoturbation (bioturbation and argillo-pedoturbation) may be responsible for the mixing.

2.3.1.3 Topography

The experimental site is situated on the lower 3 position in the landscape (Figure 2.9) and is sloped 0.3% in an easterly direction. The slope shape is linear convex (Figure 2.10). The distribution of soil forms can not be explained by topography using available topographical data. A more detailed analysis is needed of the micro topography. The Bloemdal with a larger contribution from wind deposits is expected to cover the convex/convex positions, while the Sepane covers the areas where water will accumulate. Absence of major topographically features is emphasised by the presence of materials with signs of wetness in the bottom of all these soil forms. The topography aids in interflow of water from higher lying soil bodies down slope.

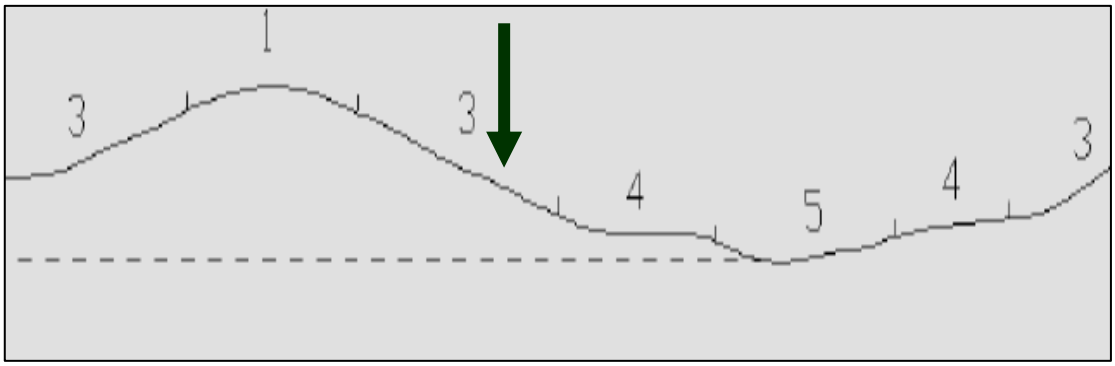

Figure 2.9 The lower 3 position of the experimental site in the landscape.

2.3.1.4 Biology and time

Time and biological factors does not distinguish between the soils in the experimental field. These soils are very old and the influence of time is visible in the well developed horizonization.

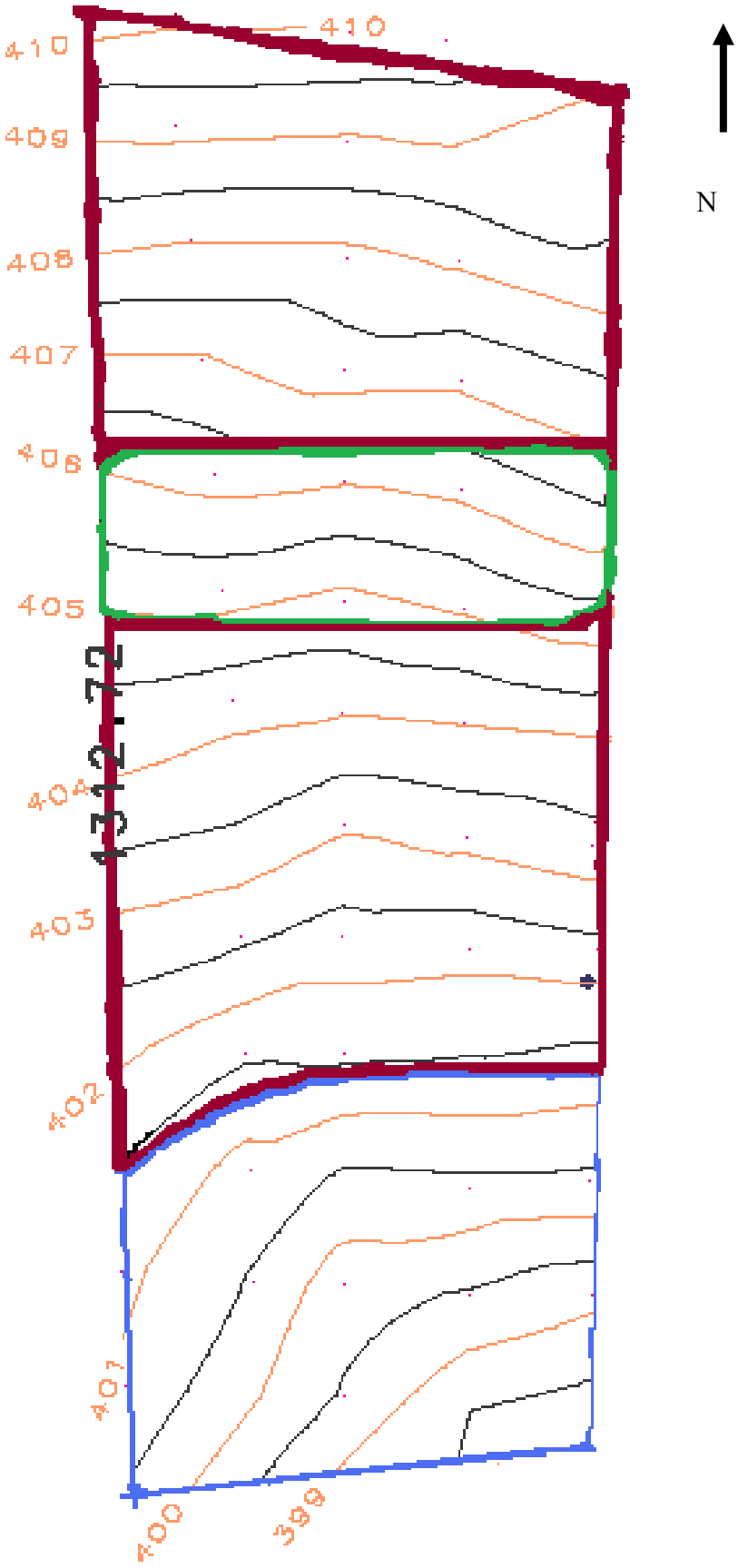

Figure 2.10 Contour map of the 55 ha experimental site.

2.3.2 Spatial variation of soils

2.3.2.1 Spatial distribution of soils

A soil map was drawn of the 55 ha (Figure 2.11). The Tukulu soil form dominates the area covering 75% of the total area (55ha), followed by the Sepane soil form 15% and the Bloemdal soil form 10% of the 55 ha experimental site. The circled areas in Figure 2.11 indicate the experimental plots that were morphologically described in detail from a profile. The squares indicate the modal profile for the Tukulu (profile nr 1.1, 1.5, 5.1, 7.1 and 12.2) Sepane (profile nr 12.1, 13.1, 14.2, 15.1 and 15.2) and Bloemdal (profile nr 8.1, 10.5, 11.1 and 11.3) which were morphologically described in detail (Figure 2.12, 2.13 and 2.14).

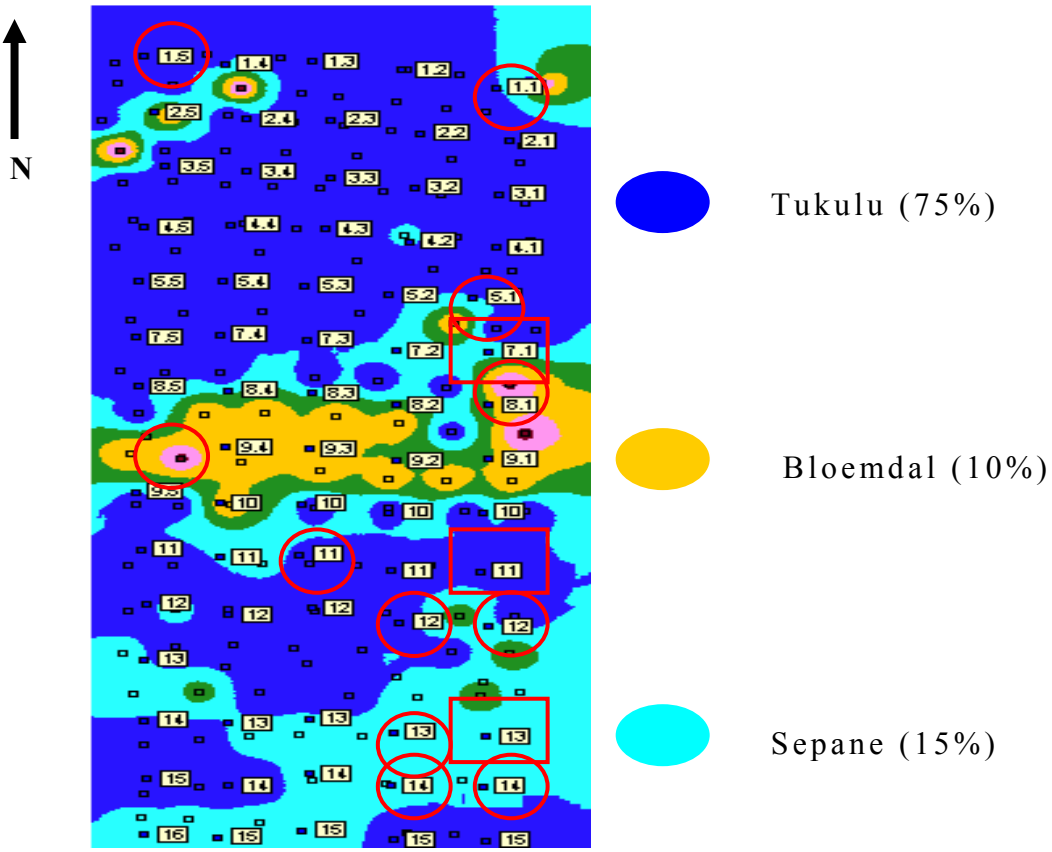

Figure 2.11 Soil map of the experimental site at Paradys.

2.3.2 2 Description of the modal profiles

From the soil survey the three following modal profiles were identified and morphologically described. Thorough profile descriptions may be found in Appendix Q, R and S.

Tukulu: The soil is of the Tukulu Dikeni (1220) family The thickness of the A, B and C horizons over the 13 profiles varied with 10 mm in the A horizon, 210 mm in the B horizon and 300 mm in the C horizon. The CV values for horizon thickness were 0% for the A horizon, 23% for the B horizon and 14% for the C horizon. The A horizon is a sandy clay loam comprising of 18% clay, while the B and C horizon is a sandy clay of 28% and 48% clay respectively. The variation in clay content within the selected range varied between CV values of 1% for the A horizon, 0% for the B horizon and 3% for the C horizon. The parent material is chemically weathered colluvial Dolerite and Mudstone over the 5 selected Tukulu profiles. The structure of the A horizon is massive apedal, with the B horizon having a weak developed sub angular blocky structure of medium size (10 mm – 25 mm). The structure of the C horizon varies between a medium and strong developed prismatic structure (5 mm – 15 mm). An abundance of red, yellow, grey and black mottles occur in the C horizon. The transition between the horizons in all cases is clear between the A horizon and B horizon and abrupt between the B horizon and C horizon. Lime occurred in the B horizon of only two of the Tukulu profiles

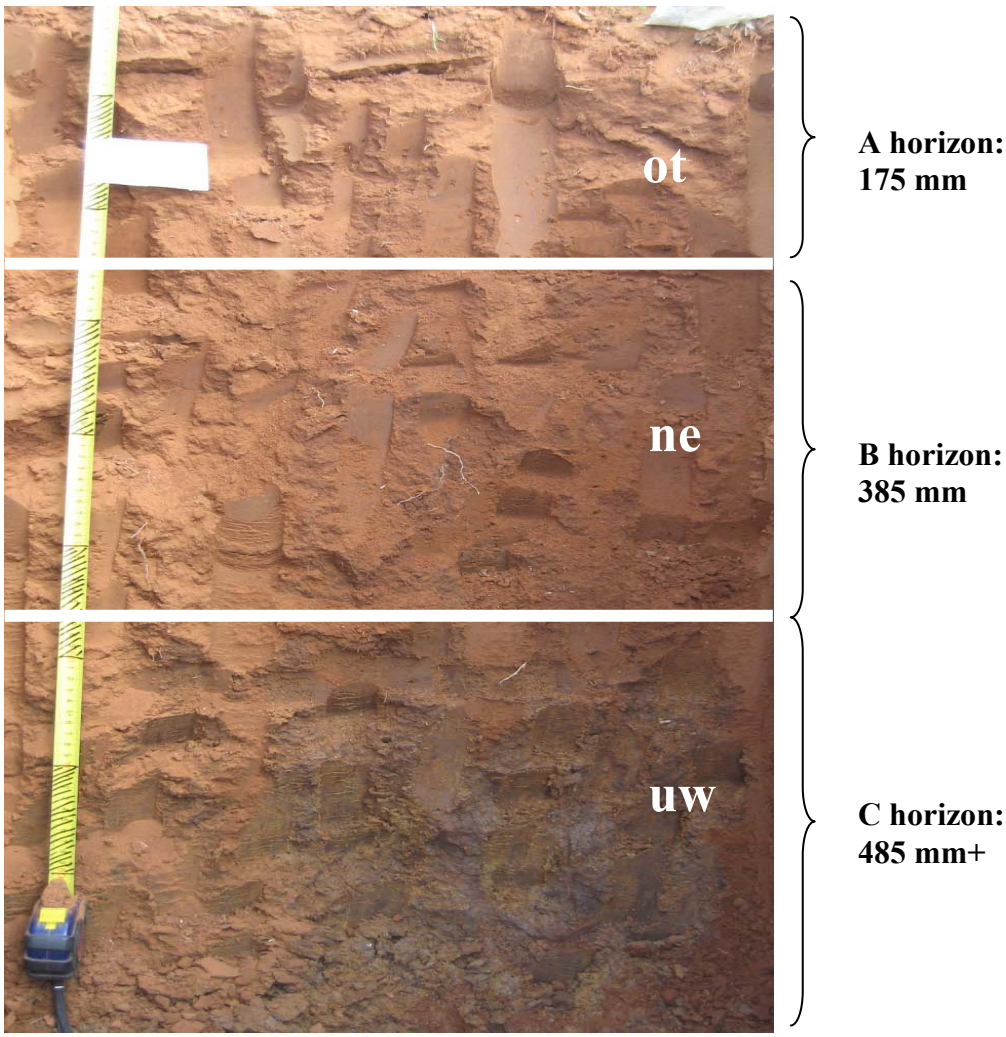

Figure 2.12 Tukulu soil form.

Sepane: The soil is of the Sepane Katdoorn (1210) family. The thickness of the A, B and C horizons over the 5 selected profiles varied from 40 mm in the A horizon to 200 mm in the B horizon and 150 mm in the C horizon. The CV values for depth being 8% for the A horizon, 23% for the B horizon and 46% for the C horizon. The A horizon of the modal profile is a sandy clay loam comprising of 19% clay, while the B and C horizon is a sandy clay of 35% and 45% clay respectively. The CV values over the 5 selected profiles vary between 6% in the A and B horizon to 4% in the C horizon. The parent material is chemically weathered Shale over the 5 selected Sepane profiles. The structure of the A horizon is massive apedal, with the B horizon having a medium developed blocky structure of medium size (10 mm – 25 mm). The structure of the C horizon is of a well developed medium size prismatic structure (10 mm – 25 mm). An abundance of red, yellow, grey and black mottles occur in the C horizon. The transition between the A, B and C horizons in all cases is abrupt. No lime occurred in any of the horizons.

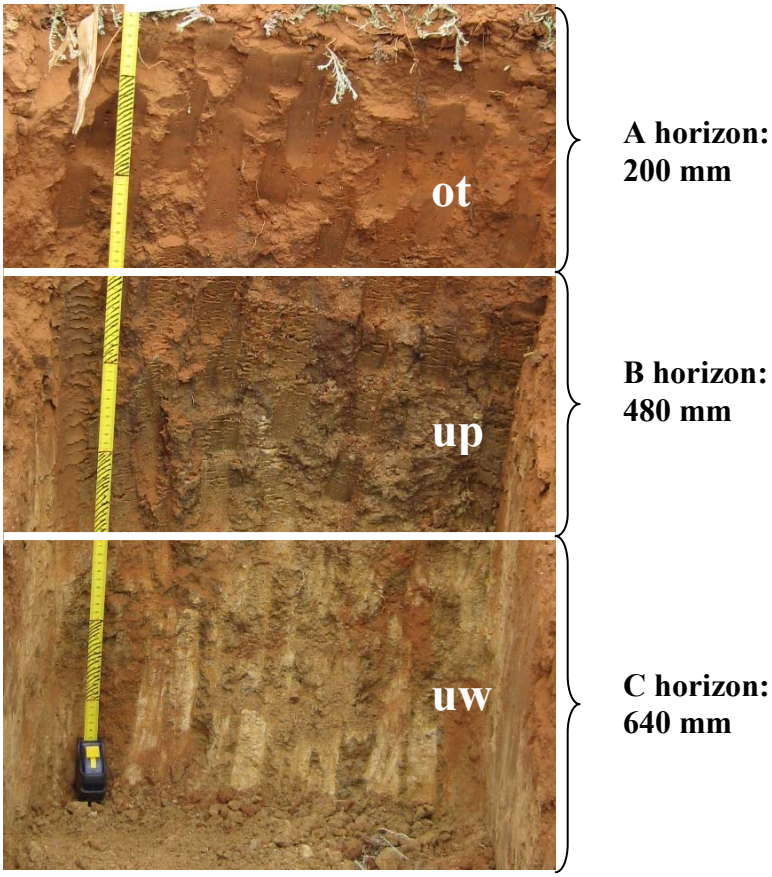

Figure 2.13 Sepane soil form (Profile 13.1).

Bloemdal: The soil is of the Bloemdal Roodeplaat (3200) family. The thickness of the A, B and C horizon varied with 100 mm in the A horizon, 150 mm in the B horizon and 200 mm in the C horizon. The CV values for depth over the 4 selected profiles varied between 22% in the A horizon to 27% in the B horizon and 67% in the C horizon. The A horizon is a sandy clay loam comprising of 17% clay, while the B and C horizon is a sandy clay of 29% and 45% clay respectively. The CV values over the 4 selected profiles vary between 0% in the A horizon and B horizon to 8% in the C horizon. The parent material is slightly weathered colluvial Dolerite over the selected profiles. The structure of the A horizon is massive apedal, with the B horizon having a medium developed blocky structure of medium size (10 mm – 25 mm). The structure of the C horizon is of a well developed medium size prismatic structure (5 mm – 15 mm). An abundance of red, yellow, grey and black mottles occur in the C horizon. The transition between the A horizon, B horizon and C horizons in all cases is smooth. No lime occurred in any of the horizons

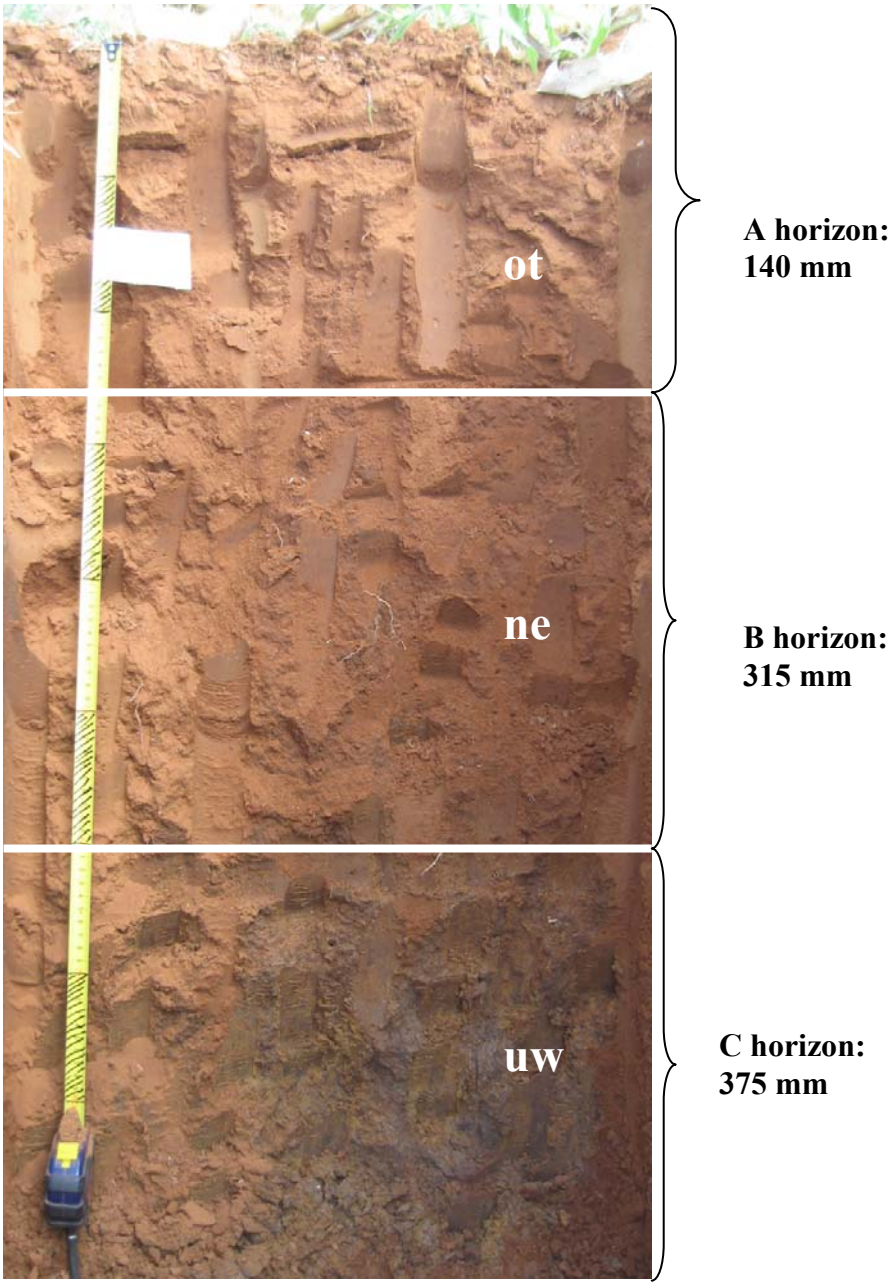

Figure 2.14 Bloemdal soil form (Profile 11.1).

2.3.3 Spatial variation of physical and chemical properties

Spatial representations of physical and chemical properties of the 75 plots are presented in Appendix A - G. Table 2.8 indicates the correlation of the selected chemical and physical properties with one another. All the chemical soil properties except K in the A and B horizon have a strong positive correlation with the clay content for the A, B and C horizons. Potassium like sodium is a very mobile element. Potassium is also redistributed by bio circulation. This may explain the unrelated distribution pattern of potassium.

Table 2.8 Correlation matrix of the soil properties for the A, B and C horizons (n =75)

A horizon	**pH_{H2O}**	**pH_{KCl}**	**Ca**	**K**	**Mg**	**Na**	**Sand**	**Silt**	**Clay**
pH_{H2O}	**1**	0.65	0.42	0.22	0.39	0.38	-0.29	0.17	**0.61**
pH_{KCl}	0.65	**1**	0.48	0.27	0.43	0.39	-0.44	0.34	**0.68**
Ca	0.42	0.48	**1**	-0.13	0.56	0.61	-0.56	0.45	**0.68**
K	0.22	0.27	-0.13	**1**	0.09	-0.07	0.12	-0.30	**0.18**
Mg	0.39	0.43	0.56	0.09	**1**	0.53	-0.40	0.20	**0.64**
Na	0.38	0.39	0.61	-0.07	0.53	**1**	-0.59	0.26	**0.80**
Sand	-0.29	-0.44	-0.56	0.12	-0.40	-0.59	**1**	-0.76	**-0.58**
Silt	0.17	0.34	0.45	-0.30	0.20	0.26	-0.76	**1**	**0.25**
Clay	0.61	0.68	0.68	0.18	0.64	0.80	-0.58	0.25	**1**

B horizon	**pH_{H2O}**	**pH_{KCl}**	**Ca**	**K**	**Mg**	**Na**	**Sand**	**Silt**	**Clay**
pH_{H2O}	**1**	0.43	0.60	-0.24	0.60	0.42	-0.54	-0.00	**0.76**
pH_{KCl}	0.43	**1**	0.46	0.33	0.59	0.68	-0.26	-0.20	**0.55**
Ca	0.60	0.46	**1**	-0.02	0.84	0.41	-0.61	-0.00	**0.81**
K	-0.24	0.33	-0.02	**1**	0.05	0.41	0.20	-0.30	**-0**
Mg	0.60	0.59	0.84	0.05	**1**	0.61	-0.63	-0.10	**0.85**
Na	0.42	0.68	0.41	0.41	0.61	**1**	-0.20	-0.20	**0.52**
Sand	-0.54	-0.26	-0.61	0.20	-0.63	-0.20	**1**	-0.50	**-0.7**
Silt	-0.03	-0.24	-0.04	-0.28	-0.05	-0.24	-0.55	**1**	**-0.1**
Clay	0.76	0.55	0.81	-0.04	0.85	0.52	-0.70	-0.10	**1**

C horizon	**pH_{H2O}**	**pH_{KCl}**	**Ca**	**K**	**Mg**	**Na**	**Sand**	**Silt**	**Clay**
pH_{H2O}	**1.00**	0.70	0.47	0.12	0.31	-0.09	-0.45	0.05	**0.52**
pH_{KCl}	0.70	**1.00**	0.55	0.05	0.18	-0.26	-0.45	0.04	**0.56**
Ca	0.47	0.55	**1.00**	0.41	0.55	0.21	-0.74	0.21	**0.77**
K	0.12	0.05	0.41	**1.00**	0.80	0.52	-0.54	0.10	**0.56**
Mg	0.31	0.18	0.55	0.80	**1.00**	0.51	-0.58	0.00	**0.69**
Na	-0.09	-0.26	0.21	0.52	0.51	**1.00**	-0.31	-0.04	**0.37**
Sand	-0.45	-0.45	-0.74	-0.54	-0.58	-0.31	**1.00**	-0.49	**-0.86**
Silt	0.05	0.04	0.21	0.10	0.00	-0.04	-0.49	**1.00**	**0.05**
Clay	0.52	0.56	0.77	0.56	0.69	0.37	-0.86	0.05	**1.00**

The statistical coefficient of the linear regression between each of the chemical properties and clay content (%) of the homogeneous area are presented in Table 2.9. The clay content

(%) has a strong influence on the chemical properties, regardless of the soil form and horizon.

Table 2.9 Statistical variation of the soil properties

A horizon	Parameter	a	b	R^2	Mean	CV
	$pH_{(H20)}$	2.076x	5.2919	0.37	5.80	0.08
	pH_{KCl}	2.5439x	5.5323	0.46	4.64	0.09
	Ca ($cmol_c.kg^{-1}$)	0.1098x	13.06	0.46	38.93	0.24
	K($cmol_c.kg^{-1}$)	0.0674x	16.645	0.03	10.22	0.39
	Mg($cmol_c.kg^{-1}$)	0.1348x	14.575	0.42	20.46	0.35
	Na($cmol_c.kg^{-1}$)	1.5626x	13.15	0.63	2.68	0.28
B horizon	**Parameter**	**a**	**b**	**R^2**	**Mean**	**CV**
	$pH_{(H20)}$	3.298x	8.3393	0.58	5.97	0.11
	pH_{KCl}	3.273x	11.392	0.30	5.08	0.10
	Ca($cmol_c.kg^{-1}$)	0.1834x	19.548	0.65	46.23	0.28
	K($cmol_c.kg^{-1}$)	-0.0203x	28.208	0.00	8.92	0.62
	Mg($cmol_c.kg^{-1}$)	0.2838x	21.3	0.72	23.71	0.37
	Na($cmol_c.kg^{-1}$)	2.0935x	22.864	0.27	2.47	0.30
C horizon	**Parameter**	**a**	**b**	**R^2**	**Mean**	**CV**
	$pH_{(hH20)}$	3.3271x	23.949	0.27	6.66	0.08
	pH_{KCl}	2.9965x	30.456	0.31	5.23	0.13
	Ca($cmol_c.kg^{-1}$)	0.1468x	36.971	0.59	62.31	0.30
	K($cmol_c.kg^{-1}$)	0.4472x	40.862	0.32	11.76	0.38
	Mg($cmol_c.kg^{-1}$)	0.1407x	39.289	0.47	48.54	0.35
	Na($cmol_c.kg^{-1}$)	1.0867x	42.931	0.13	2.93	0.41

Investigating the soil map (Figure 2.11), together with the clay distribution maps (Figure 2.15), the clay content of the B horizon has a resemblance to the soil map of the experimental site. The clay content increases in an eastern direction of the experimental site. This correlates with the soil forms, as the Sepane (pedocutanic B horizon) occur in the lower lying areas (Eastern direction). The Tukulu and Bloemdal soil form (neocutanic B, and red apedal B horizons) occur higher up the slope in the northern part of the experimental site.

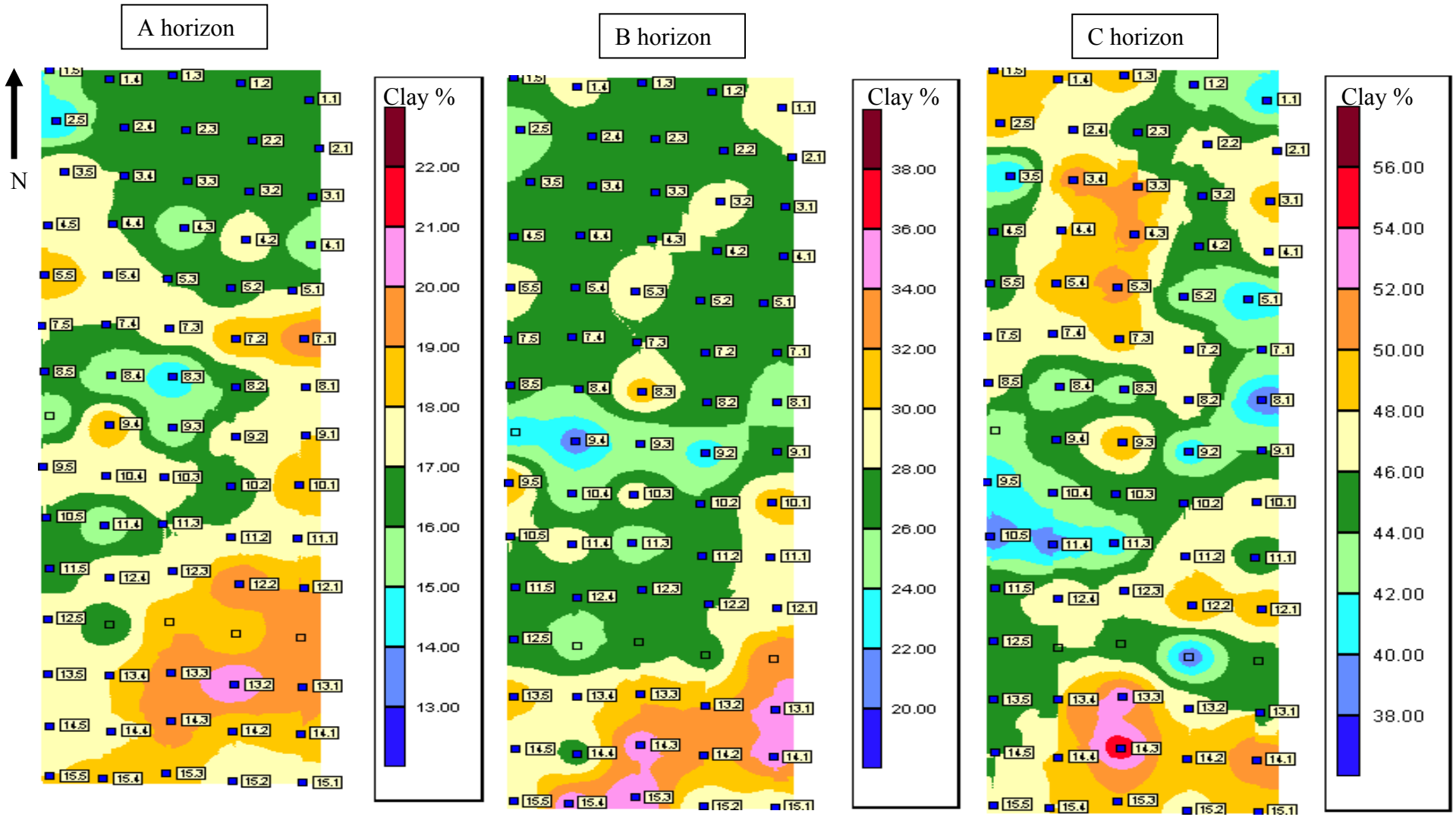

Figure 2.15 Distribution of the clay content for the A, B and C horizon.

Due to cultivation practices (ploughing) over the last 30 years on this experimental site the distribution of the clay content in the A horizon may not have any resemblance with the soil forms. The C horizon has a high degree of variation due to varying parent materials (Dolerite, Mudstone and Schales), and does not have any resemblance with specific soil forms occurring in the experimental site.

Scales were given to different categories of B horizon clay contents namely: 20 – 25%, 25 – 28%, 26 - 28%, 29 - 32% and 29 – 35%. The results in Figure 2.16 show that the different scales given to the clay content of the B horizon for the 75 plots have a close resemblance with the soil forms. The R^2 = 66%, is an indication that the clay content of the B horizon is a good parameter identifying the various soil forms occurring at this experimental site. In boundary areas the clay contents resemble that of the two soil forms it makes part of.

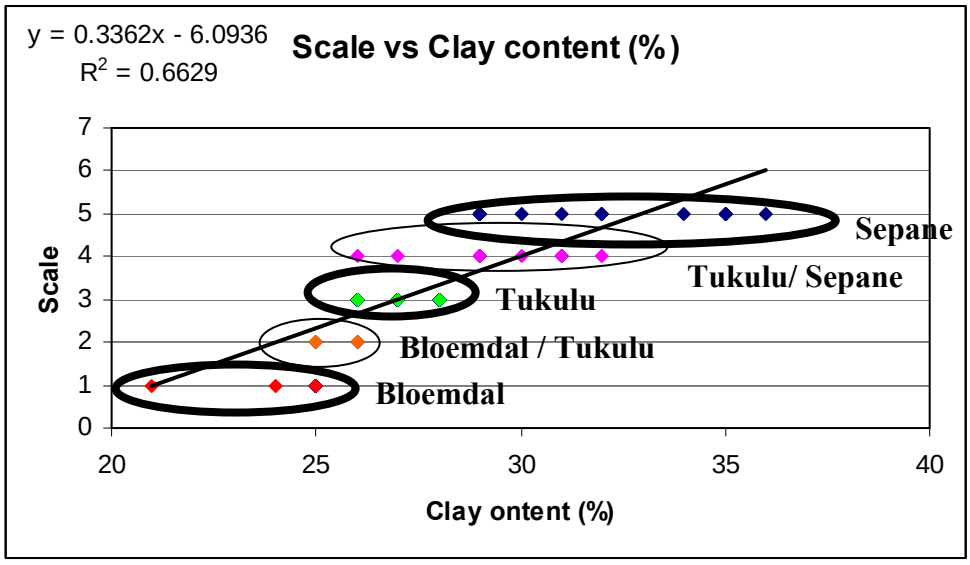

Figure 2.16 Distribution of clay over the soil forms (n=75).

2.3.4 Spatial Variation within map units

Due to the strong correlation between the clay content and some of the chemical properties as well as the soil forms, the clay content will serve as indicator to describe the spatial variation within map units and between map units.

Selected observations from each of the soil forms to evaluate within map unit variation are shown in Figure 2.17.

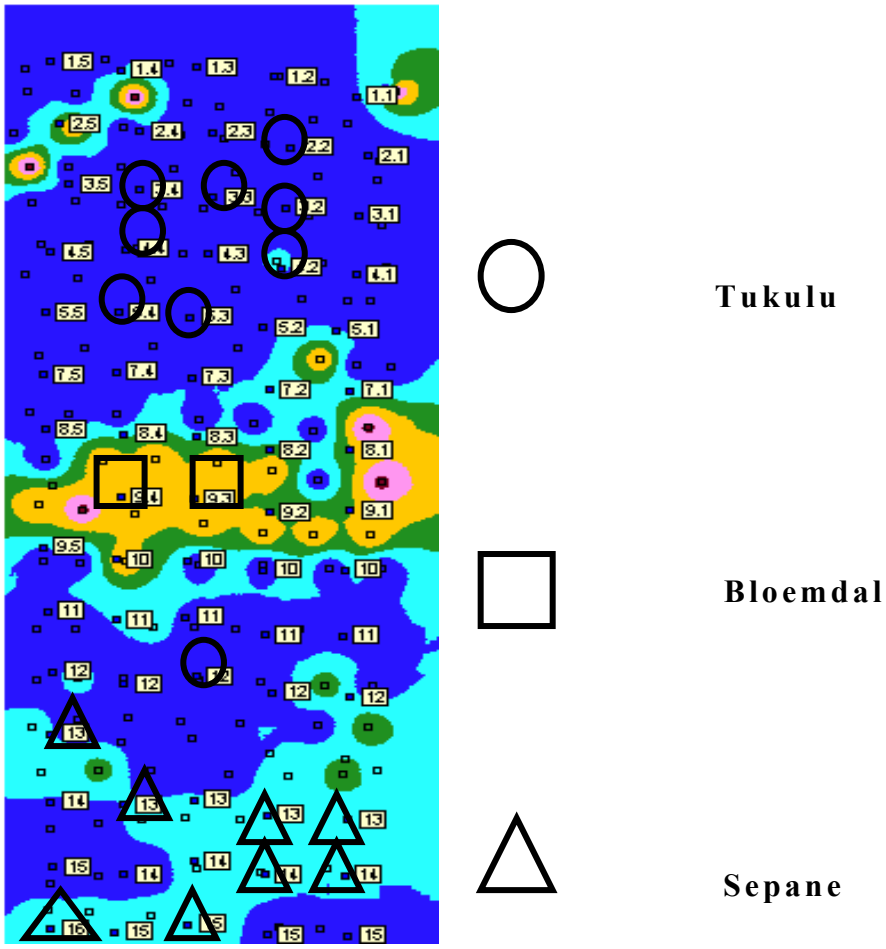

Figure 2.17 Map indicating the areas which was selected to be within the map units of the Tukulu, Sepane and Bloemdal soil forms.

Tukulu: The CV of the clay content was less in the A (4%) and B (4%) horizons than in the C horizon (16%) (Figure 2.18). The range between the 25% - 75% quartile varied from 0 in the A horizon, to 1 in the B horizon and 6.25 in the C horizon. Inverse Distance Weighting (IDW) accurately predicted the clay content in all horizons (Figure 2.19) (A horizon = 99.78%, B horizon = 99.88% & C horizon = 99.41%).

Sepane: The CV of the clay content was higher in the C horizon (14%) than in the A horizon (7%) and B horizon (4%) of the Sepane soil form (Figure 2.18). The range between the 25% - 75% quartile was constant throughout the profile at 1.75. The accuracy of the predicted value generated using IDW (Figure 2.19), had a small variation from the A horizon (97.9%) downwards to the B horizon (96.73%) & C horizon (97.98%).

Bloemdal: The CV was a bit higher in the A horizon (17%) while there was a small variation in the B horizon (9%) and C horizon (6%) (Figure 2.18). There was a small range between the 25% - 75% quartile throughout the profile (1.025). The degree to which the analyzed values were predicted using IDW (Figure 2.19), resembled the statistical variation of the horizons (A horizon = 99.93%, B horizon 97.81% & C horizon 97.64%).

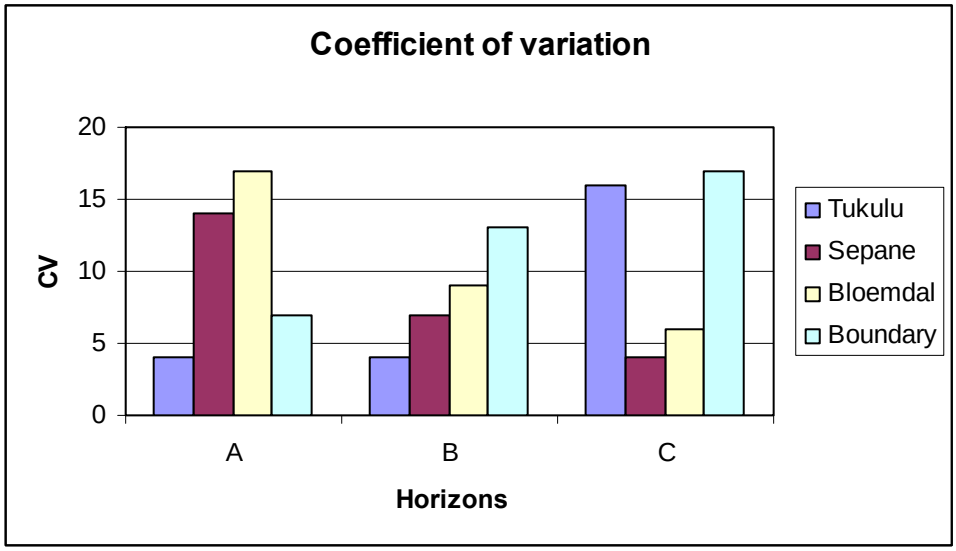

Figure 2.18 Coefficient of variation within map units and between map units.

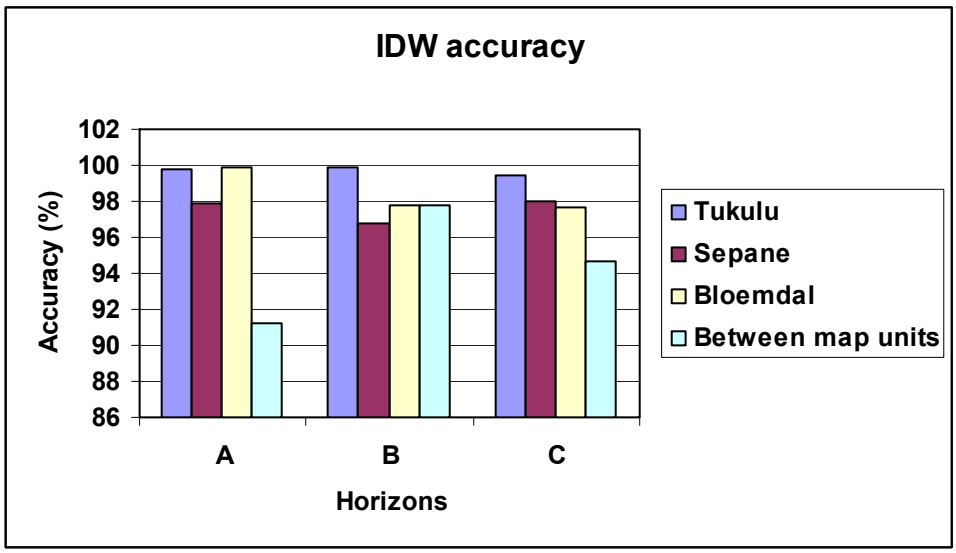

Figure 2.19 Accuracy of IDW predictions within map units and between map units.

From the study done by Cox *et al.* (2003) it is stated that the spatial variability of textural fractions will be more stable on topographic landscapes that tend to be more level, while it will tend to vary more spatially with a topographic landscape that varies in elevation, aspect and slope. The statistical variation of the clay content within the profiles for the Tukulu, Sepane and Bloemdal soil forms were some what lower than the study by Cox *et al.* (2003) in which CV values of 28% over the profile were

reported. This confusing that the topography of the area is quite level, resulting in a lower spatial variation in clay contents. In the case of the Tukulu and Sepane soil forms the statistical variation increased downwards in the profile, while the Bloemdal soil form had a higher variation in the A horizon decreasing to the C horizon, which may be due tillage practices and the process of luviation.

2.3.5 Spatial variation between map units

The area selected between the Tukulu and the Sepane soil forms are shown in Figure 2.20.

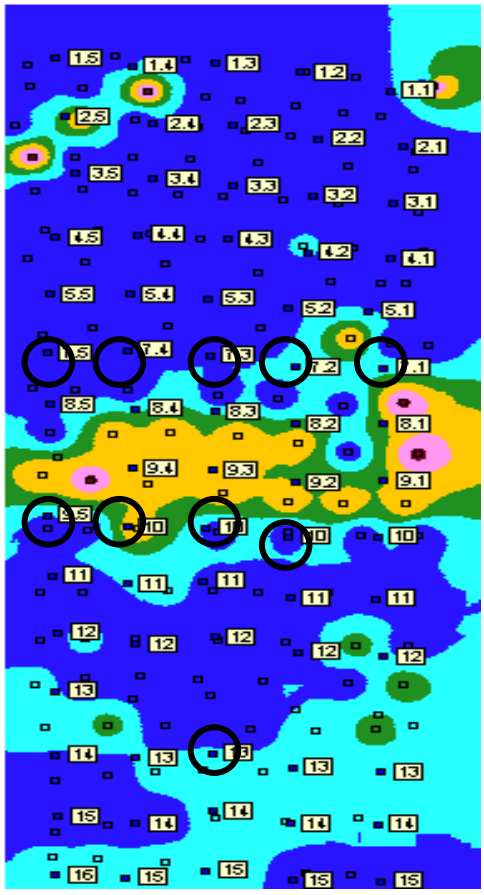

Figure 2.20 Map indicating the areas that has been selected to characterize the variation between map units.

There was a higher CV in clay content between map units than within map units (Figure 2.18). Regardless of the fact, IDW still fairly accurately predicted the lab analyzed values. The CV values varied from 7% in the A horizon, 13% in the B horizon to 17% in the C horizon, which although it was between map units was still lower than CV values reported by Cox *et al*. (2003) (CV of Clay = 28% over the profile). The range between the 25% - 75% quartile varied from 1.75 in the A horizon, 2.5 in the B horizon to 8.5 in the C horizon and the degree of accuracy to which the analyzed values were predicted varied from 91.19% in the A horizon, 97.47% in the B horizon to 94.63% in the C horizon (Figure 2.19).

2.4 Conclusion

From this study it was found that the distribution of soils is influenced by the soil forming factors, *viz.* climate (rainfall, temperature and aridity index), parent material (Dolerite, Beaufort Sandstone and Schale), topography, biology and time. There were three major soil forms found at the experimental site, *viz.* Tukulu, Sepane and Bloemdal. The Tukulu covered 75% of the total area, the Sepane 15% and the Bloemdal 10%.

A correlation matrix of the physical and chemical properties of the three soils indicated that most soil physical and chemical properties have a strong correlation with the silt + clay content. Thus the silt + clay content were used to describe the spatial variation of soil properties in and between map units. There was a higher degree of statistical and spatial variation between map units than within map units. Regardless of the high statistical and spatial variation IDW still accurately predicted the lab analyzed values. This resulted in the more accurate representation of boundaries between map units than previous distinct boundaries. This concludes that maps are in fact a simple representation of a

complex system, but is inevitable for one to understand the evolution of soils and its natural behaviour.

CHAPTER 3

Relationship between soil physical properties and the root density of maize under Infield Rainwater Harvesting.

3.1 Introduction

Roots is a key factor in improving agronomical productivity of crop production systems, because they are responsible for absorbing water and nutrients from the soil and the translocation thereof to the shoots (Klepper, 1990; Bennie, 1996 and Van Antwerpen, 1988). Past studies on root development under South African conditions focussed in the field of irrigation (Bennie & Burger, 1979; Van Antwerpen, 1988 and Bennie *et al*., 1988) and dry land tillage practices (Bennie *et al*., 1988; Snyman, 1987 and Van der Merwe, 1993). These tillage practices include minimum tillage, stubble mulch and no-till, which were mainly applied on sandy to sandy loam soils, with a massive apedal structure. Recent advances in tillage suggested that the Infield Rainwater Harvesting (IRWH) technique is suitable for clay and duplex soils in semi arid zones of South Africa (Hensley *et al*., 2000 and Botha *et al*., 2003). Up to date none of the biophysical studies in IRWH has focussed on root development. This is seen as a serious concern as the system claims that it improves the rainwater productivity (Botha, 2006).

The objectives of this study were therefore to: (i) review literature on the influence of soil physical properties and root development, (ii) investigate the interactions between soil physical properties and (iii) determine how the root density relates to certain soil physical properties under the IRWH system.

3.2 Literature Review

3.2.1 Introduction

This review is structured to provide firstly information on the types of root systems and secondly on specific soil physical properties such as texture, structure, bulk density and soil water content that influences root development. Root growth is influenced greatly by soil factors including the soil structure, strength (compressibility), water content, temperature, porosity, gaseous diffusivity, pH, toxicity, and fertility. The main requirements that has to be met for optimum elongation is as follows: (i) an adequate delivery rate of carbohydrates to the root tip, (ii) soil space for the roots to move into, (iii) adequate supply of inorganic ions for root uptake, (iv) adequate water content during the growing season and (v) a sufficient supply of chemical energy (Bennie *et al.*, 1988). Most of the soils properties influence more than one of the above mentioned requirements, as seen in Table 3.1. Some of the soil properties change rapidly while some of the properties do not change over time. For example, soil structure, pH and porosity may not change much during the growing season of crops, but water content and temperature may change on an hourly basis.

3.2.2 Root systems

Unless various soil factors have an influence, the pattern of root development primarily depends on the plant species. Root systems are of three basic types (Figure 3.1) (i) Fibrous or adventive (ii) taprooted and (iii) modified taproot systems (Klepper, 1990). Adventive systems are mainly related to monocotyledon crops, while dicotyledon crops are associated with taproot and modified taproot systems.

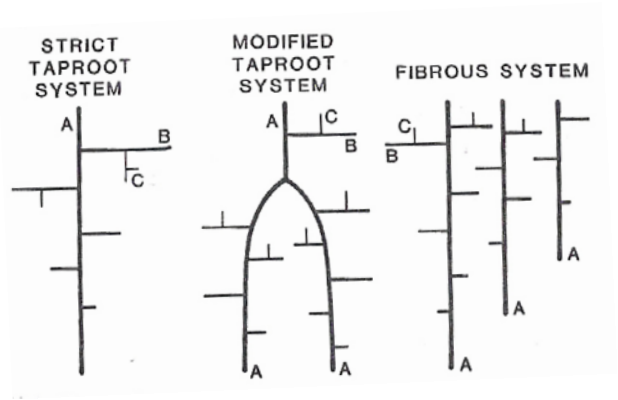

Figure 3.1 Diagram showing the three basic root systems (Klepper, 1990).

Monocotyledons: According to Klepper (1990) monocotyledon crops generally produce roots from stem nodes. These nodes consist of seminal roots that arise from in the embryo and crown roots. In wheat the seminal root system consist of a primary root and up to five roots associated with the two nodes in the seed (Figure 3.1). The foliar nodes in the crown give rise to a crown root system. The early seminal rooting system is not persistent if it subjected to pathogen attack or if it is damaged by frost heaving. Early in the root development, the growth rates of the main axes are slowed and branch roots begin to grow. Generally the axes extend at a rate of 1 cm day^{-1}. Van Antwerpen (1988) measured vertical root depths that varied between 1 m and 2 m in a range of soils at the Vaalharts, Ramha and Sandvet Irrigation Schemes.

Dicotyledons: Dicotyledon taproot systems develop from the radicle and its branches Klepper, 1990 (Figure 3.1). Adventitive roots may also be produced from the stems. Usually it consists of a strong tap root that grows vertically and is supported by strong lateral roots. In some studies it was found that in soybean that the lateral root system grew horizontal for a few centimetres and then grew vertical for a considerable depth. It was also found that

dicots produce fewer roots than the monocots, for example maize, do.

Table 3.1 Primary influences of soil properties on soil requirements for optimal root elongation (Logsdon *et al.*, 1987).

-= absent
X = present

Soil property	**Requirements**			
	Ions	**Pore Space**	**Water**	**Chemical energy**
Structure	-	x	x	-
Porosity	-	x	x	-
Water content	-	x	x	-
Strength	-	x	-	-
Gaseous diffusivity	x	-	x	x
Temperature	x	-	x	x
pH	x	-	-	-
Fertility	x	-	-	-

Even homogenous soil horizons are full of cracks, worm holes and old root channels, which influences root development immensely. Roots tend to grow along a ped surface even if the ped has a low resistance to penetration. At the same time roots grow along the surface of a crack and not in the cracks. These features cause roots to grow around rather than through soil horizons containing cracks and large voids. When roots penetrate the soil, they compress the cylinder of soil immediately around themselves (Hillel, 2004). The compressibility of the soil greatly influences this phenomenon. The compressibility of the soil is usually measured as soil resistance or mechanical impedance with a penetrometer which monitors the force required to press a root shaped probe through the soil. It has been found that the penetrometer pressure (MPa) is an adequate indication of the mechanical impedance of the soil and is correlated with variables such as fresh and dry weight, elongation rates (mm day^{-1}), root length density (cm cm^{-3}) and rooting depth (mm).

3.2.3 Soil texture

Soil texture is a very broad concept and normally refers to the ratio of sand, silt and clay content. However its effect on root growth and development can be further explained by subdividing texture into particle size distribution, specific surface of particles and textural classes (Hillel, 2004). Textural properties influence the mechanical impedance of the soil. Mechanical impedance refers to the resistance offered by the soil matrix against deformation by a growing root. Thus, permitting root elongation only in accordance with the extent to which the root pressure exceeds the mechanical impedance of the soil. For roots to elongate downward in the profile it has to exceed the binding forces between soil particles and the friction when moving soil particles. These forces are soil-to-water adhesion and water-to-water cohesion forces and interparticle cementation. These forces are dependant on the water content, contact area and distance among the individual particles, which is in turn all dependant on for example soil texture, soil structure, bulk density and soil water content (Bennie, 1995).

These above mentioned properties have the following affect on root elongation (Logsdon *et al.*, 1987):

i. Cementing agents can increase the strength of the pore channels making it difficult for the roots to overcome the required pressure to move particles out of the way while roots elongate.
ii. The high critical soil strength values associated with the coarse sandy soils has a affect on elongating roots.
iii. Organic carbon content and water content also modifies the critical soil strength decreasing root elongation.

Bennie & Burger (1988) found that the critical soil strength, defined as the probe pressure at which root elongation stopped, was a function of clay (%) and ranged in cotton seedlings from

7 MPa in coarse textured soils to 2.5 MPa in clay soils. It was also indicated that the penetrometer pressure increases with an increase in the silt + clay content up to 20% for soils with the same degree of compaction and water content (Figure 3.2).

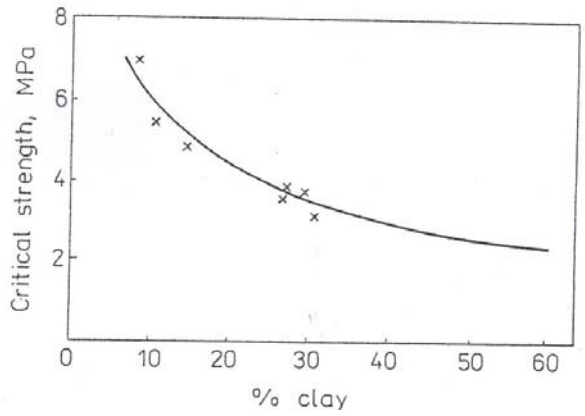

Figure 3.2 Relationship between soil strength and percent of clay (Bennie & Burger, 1988).

To demonstrate the effect of texture on root development under South African conditions, the results from three soils with maize as the test crop, Van Antwerpen (1988), were selected and presented in Table 3.2. All the soils are from types occurred in the Vaalharts Irrigation Scheme, where water and nutrients are not impeding factors. The soils forms were a Hutton from the Ritchie family with a mean silt + clay content of 14.2% over the profile, a Clovelly from the Setlagole Family with a mean silt + clay content of 16.9% and an Oakleaf of the Stella Family with an mean silt + clay content of 31.7%.

Table 3.2 Root density data in relation to three soil forms with different physical properties (Data modified from Van Antwerpen, 1988 and Bennie, 1996)

Author	Location	Soil form	Family	Depth (mm)	Sand fractions (%)	Silt + Clay (%)	Texture class	Bulk density ($kg.m^{-3}$)	Total root length ($mm\ mm^{-2}$)	Root density ($cm\ cm^{-3}$)
R. van Antwerpen (1988)	Vaalharts - M78 (Irrigation)	Hu	1110 - Ritchie	0-300	88.05	10.19	Loamy sand	1651	8.826	1.786
				300-600	84.99	15.32	Loamy sand	1728		0.456
				600-900	82.98	17.2	Loamy sand	1591		0.183
R. van Antwerpen (1988)	Vaalharts - M79 (Irrigation)	Cv	3100 - Setlagole	0-300	85.44	15.35	Loamy sand	1603	4.343	0.485
				300-600	82.8	17.19	Sand	1604		0.434
				600-900	81.75	18.22	Sand	1574		0.201
R. van Antwerpen (1988)	Vaalharts - M83 (Irrigation)	Oa	3100 - Stella	0-300	64	35.37	Sandy loam	1596	6.39	0.489
				300-600	68.28	30.34	Sandy loam	1524		0.478
				600-900	68.49	29.65	Sandy loam	1518		0.218
Bennie (1996)	Hoopstad (Dry Land)	Cv	3100 - Setlagole	0-300	94.6	5	Loamy sand	-	1.776	0.226
				300-600	82.78	16	Sand	-		0.105
				600-900	83.98	16	Sand	-		0.115
Bennie (1996)	Tweespruit (Dry Land)	We	2000- Mareetsane	0-300	85.12	16	sandy loam	-	1.449	0.225
				300-600	74.68	26	sandy loam clay	-		0.158
				600-900	40.42	58	sandy clay	-		0.101

Despite the large differences in clay content (Table 3.2), there was no distinct difference in root density between these three soil forms for each diagnostic horizon, except for the A horizon, which varied between 1.79 cm cm^{-3} for the Hutton, 0.49 cm cm^{-3} for the Clovelly and 0.49 cm cm^{-3} for the Oakleaf. Van Antwerpen (1988) could also find no relationship between root density and the clay + silt content for any of the crops he studied.

Root density results from Van Antwerpen (1988) were complemented by the study done by Callot *et al*. (1982) on soybean grown in loamy and clay soils. They found that there was no clear difference in root density over the profile between this specific loamy and clay soil except for the A horizon (Table 3.3). One factor that should be considered is the fact that the root development of different field crops acts differently on different texture classes.

Root data from Callot *et al*. (1982) demonstrated that coarser textured soils influence the growth of tertiary roots more than finer textured soils. Fine textured soils on the other hand had a larger influence on seminal and secondary roots. Coarser textured soils have a lower fertility, lower unsaturated hydraulic conductivity, and a lower water storage capacity.

Roots of various plants have the tendency to have a higher concentration of roots in a moderate loose-textured soil than in a heavy textured soil.

Table 3.3 Root characteristics of wheat during tillering in three soils of various textures selected from Callot *et al*. (1982)

	Textural fractions		
Root parameters	**Clayey**	**Silty**	**Sandy**
Seminal roots			
Mean length (mm)	42	127	129
Total length (mm)	340	1021	1290
Secondary roots			
Mean length (mm)	10.2	12.8	17
Total length (mm)	960	7200	16000
Tertiary roots			
Mean length (mm)	1.74	1.9	1.49
Total length (mm)	1220	2100	477

3.2.4 Soil structure

Soil structure exerts important influences on plant growth via root growth and development. Soil structure in general refers to the size, shape and arrangement of the basic structural units or peds. The Soil Survey Staff (1993) provided guidelines to describe soil structure based on the peds type, class and grade. Types are further divided into sub grades according to the shape and arrangement of peds and includes subgroups such as platy, prismatic, columnar, blocky, sub angular blocky, granular and crumb. Class refers to the size of structural units or peds. For each of the sub group types there are five class sizes. For example, granular peds (relatively non porous peds) are divided into < 1 mm (very fine), 1 – 2 mm (fine), 2 – 5 mm (medium), 5 – 10 mm (coarse) and > 10 mm (very coarse). Crumb (porous peds) are only divided into three size classes, viz. very fine (< 1 mm), fine (1 – 2 mm) and medium (2 – 5 mm). Grade on the other hand refers to the norms to describe the structural stability of the peds and is therefore divided into four sub groups, *viz*. structure less, weak, moderate and strong.

These norms are very helpful in identifying and describing soil structure qualitatively, but do not really provide information on the effect thereof on plant production. Therefore, scientists often use aggregate sizes and stability as a simple indicator to quantify soil structure (Six *et al*., 2000). Aggregates are secondary particles formed through the combination of mineral particles with organic and inorganic substances. Bromich & Lal (2005) stated that aggregates originate from complex and dynamic processes that depends on the interaction of many factors including the environment, soil management, plant influences and soil properties such as mineral composition, texture, soil organic carbon, pedogenic processes, microbial activities, exchangeable ions, nutrients reserves and moisture availability. Aggregates are often grouped into sizes: micro aggregates (<250 µm) and macro aggregates (> 250 µm). Tisdale & Oades (1982) also states that their groups are often further divided by size.

However, favourable soil structure and high aggregate stability are important to improve root growth. Dexter (1978) described the influence of aggregate size on root development. Accordingly roots grow downward in a profile until it reaches an aggregate. It could then moves around the aggregate, through the aggregate or displaces the aggregate as seen in (Figure 3.3). Narrow roots are more easily deflected and large aggregates are less likely to be displaced by roots.

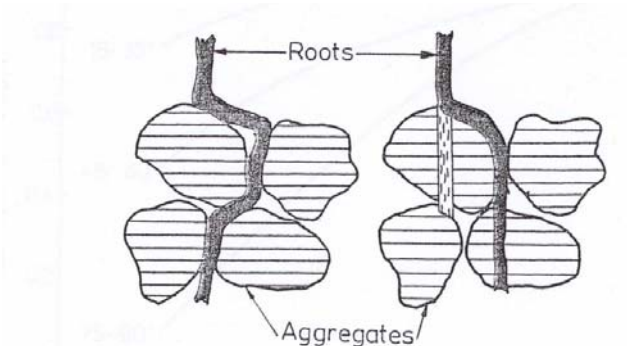

Figure 3.3 Representation of possible paths of a root axis through a bed of aggregates (Dexter, 1978).

Logsdon *et al*. (1987) stated in their study that large aggregates did not have even a slight pressure exerted on them when roots were moving around them. The root diameter increased as aggregate size increased, but root length in most cases stayed the same. Smaller aggregates had little influence on root growth as it was readily displaced. This scenario readily occurs in profiles with varying structural interfaces especially in tilled lands or in areas where compaction is a problem. Compaction in untilled subsoil layers may have cracks and biopores which influences root development. Where cracks are to narrow for roots to move through, the roots tend to buckle behind the root tip to build up sufficient support to push root tips forward (Bennie, 1995).

Most work on the penetrability of roots in soils is done on weak, massive or single grain structured soils. There is definitely less work done on medium to well structured soils. Penetrometry seems not to be the most suitable way of studying the penetrability of roots through peds or macro aggregates in soils with clay contents higher than 20% (Hillel, 2004). Larger aggregates may have large pores or weak planes to accommodate root growth, which cannot be detected by the penetrometer. With smaller aggregates there is less mechanical impedance than with larger aggregates. Preferential root growth may also be caused by natural structured cracks and biopores permitting root development with minimum restrictions. Thus, there is preferential root penetration into zones of weakness. The effect of size of the aggregate is much larger than the strength of the aggregate on root development.

Dexter (1978) found that large axial root growth pressure must be exerted by roots to penetrate the large aggregates. They concluded that an increase in aggregate diameter causes a decrease in total root length, but an increase in root hair length. The main axes of seminal and modal roots were longer in the coarser aggregate system. The diameter of the main axes roots was also greater in the larger aggregate fractions. Since the penetrometer method only calculates soil strength, a thorough qualitative

study should be done to gain a better understanding of how the roots act under mechanical impedance.

Amato & Ritchie (2002) determined the effect of aggregate size on the root development of maize (Table 3.4). They used a sandy clay loam soil (SCL) (clay content = 37.1%) and packed soil columns with different aggregate sizes. Three treatments were employed, *viz.* a column with only the SCL soil, a column with one large aggregate (LA) imbedded in the SCL soil (SCL + LA) and a third column with smaller aggregate sizes (SCL + SA). These aggregates were placed within the 50 – 75 cm depth interval. All the aggregates were sampled from a clay loam soil. One maize plant was planted on each of the columns to observe the distribution of the roots under these two conditions.

Table 3.4 Mean root length density and the standard deviation in each soil layer (Amato & Ritchie, 2002)

Soil layer or peds	**Root length (cm.cm^{-3})**		
	SCL **Mean (std)**	**SCL + LA** **Mean (std)**	**SCL+ SA** **Mean (std)**
0 - 25 cm	1.56 (0.4)	1.2 (0.96)	1.15 (0.85)
25 - 50 cm	1.28 (0.29)	1.02 (0.87)	1.1 (0.8)
50 - 75 cm	1.04 (0.28)	0.75 (0.56)	0.67 (0.43)
75 - 100 cm	0.68 (0.27)	0.39 (0.22)	0.42 (0.29)

(Treatment SCL = Sandy- clay loam soil, SCL+LA = sandy-clay loam soil + Large Aggregate, SCL + SA = sandy-clay loam soil + small aggregates)

The results showed that there was a significant decrease in the root length in the 50 – 75 cm zone with an increase in the size of aggregates. A large proportion of the roots measured were in fact located on the surface of the peds. Growth was limited in the treatments and the only roots found beyond the outer 2 cm of the peds where in biopores or in secondary cracks. Beneath the 50 - 75 cm layer, which contained the peds, the root development was also severely decreased.

Both the Hutton and Clovelly soil forms selected from the study in the Vaalharts irrigation scheme Van Antwerpen (1988) (Table 3.2) is regarded

as apedal due to the low clay content of the B horizons. The Oakleaf soil form also presented in Table 3.2 was identified as a neocutanic B horizon, with a clay content of about 30%. The occurrence of biopores and cracks within the neocutanic B horizon probably enhanced the root growth to comparable levels. In the case of Bennie (1996) (Table 3.2), there is a small increase in root density from the yellow brown apedal B horizon of the Hoopstad area to the soft prismatic horizon of the Tweespruit area. This may also be attributed to the cracks and biopores resulting from aggregates occurring in the soft prismatic horizon as illustrated in Figure 3.3 and Figure 3.4. Water could have also influenced the root density in the soft prismatic horizon as it is prone to fluctuating water levels.

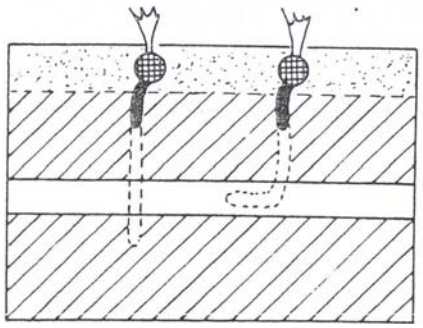

Figure 3.4 Possible behaviors of seminal roots penetrating two clods separated with a crack (Whiteley & Dexter, 1984).

Despite the clear guidelines for describing soil structure in terms of type, class and grade, it seems that this criterion is seldom used to study the effect on root development. This is probably due to the complicated nature to describe root development from structured soils with penetrometer on the one hand, and the difficulty to quantify such a phenomenon. However, from the literature it is clear that aggregate sizes play a prominent role. Thus, when comparing large with small aggregate it is clear that large aggregates result in lower root growth, an increase in root diameter and an occurrence of greater deflection.

3.2.4 Bulk density

Bulk density is the mass of dry soil per unit bulk volume and is an indication of the degree of compaction of the soil. In soils with a high bulk density roots may have difficulty penetrating, while in soils with a low bulk density the contact between the root and the soil may be so low that transport of water and nutrients may be restricted. Figure 3.5 illustrates that soil strength increases with an increase in bulk density at a constant water content. Plants respond to variation in bulk density by growing the fastest at an intermediate density.

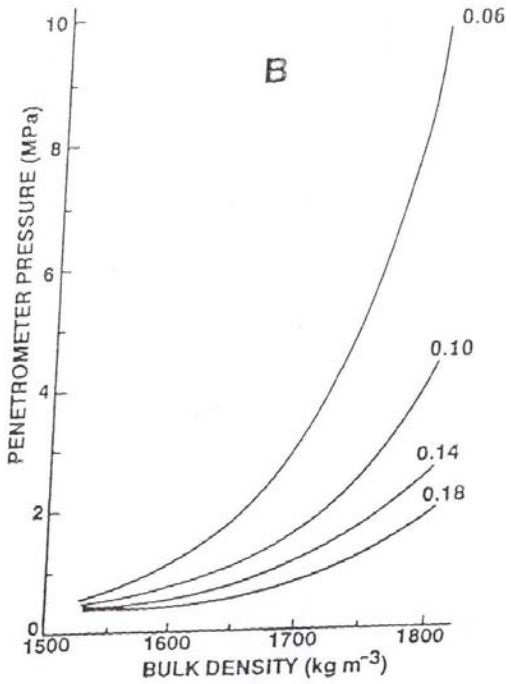

Figure 3.5 Change in penetrometer pressure with bulk density at various water contents (Hillel, 2004).

Stirzaker *et al.* (1996) examined the influence of bulk density and biopores on soil structure and plant growth and found that root development was the greatest at the lowest bulk densities and decreased sharply as the bulk density increased. They also found that the effect of the bulk density was more pronounced when they allowed the minimum soil water content to slowly decrease at one end. Under wet conditions root development decreased with a decrease in water content as the soil

became drier and harder. Under dry conditions there was no clear trend in the rooting pattern. They also found that an increase in bulk density altered the volumetric water content of the soil, the movement of water in response to gradients in water content, the root - soil contact and the mechanical impedance to root growth. An increase in bulk density severely decreases root development.

3.2.5 Soil water content

Root growth is directly affected by the soil water content as it acts as a lubricant to reduce friction amongst soil particles. In drier soil the soil strength increases, causing the root length to decreases to a point where root elongation is almost zero. Figure 3.6 illustrates the relationship between the relative root length for 70 day old maize, cotton, wheat and groundnuts and penetrometer resistance. The high coefficient of determination (R^2 = 0.80) showed that the penetrometer reflects accurately on the mechanical impedance experienced by the crops for the soil used. The slope of the curve indicated a sharp decline in root growth with an increase in the penetrometer resistance from 0 MPa to 2 MPa. At 2 MPa the root length was affected by about 65% (Figure 3.6). Taylor *et al.* (1996) also found an almost linear decrease in root penetration (%) of cotton with an increase in penetrometer resistance from 0 MPa to 2 MPa (Figure 3.7). It seems that root penetration is poor beyond the 2 Mpa threshold value. Figure 3.8 illustrates that there is a definite increase in soil strength with a decrease in water content, which will have a negative affect on root development. The amount of water available to the plants depends widely on the texture, organic matter, soil temperature, soil strength; and soil aeration. Thus the rate of movement of water from the soil to the plants depends on the hydraulic conductivity of the soil and the water potential gradient.

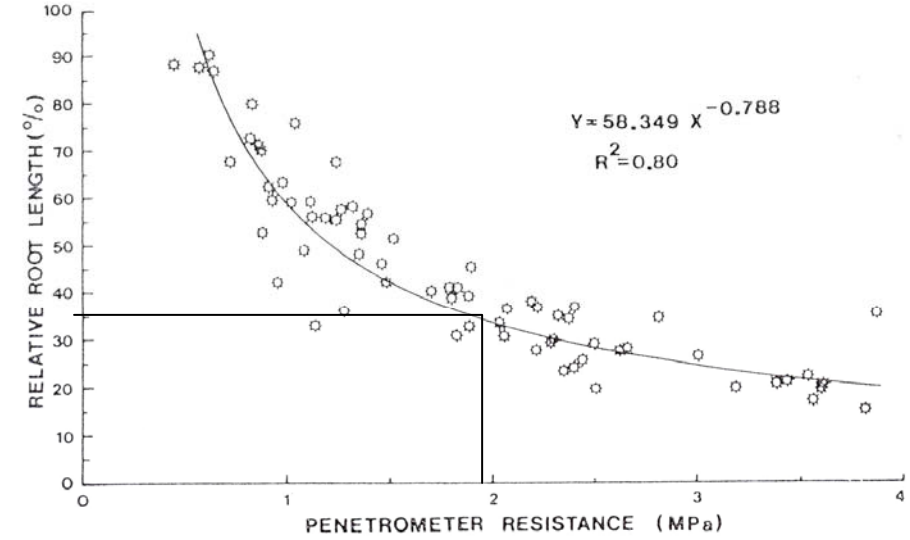

Figure 3.6 Relationship between the relative root length of 70-day-old maize, cotton, wheat, and groundnut plants and penetrometer resistance (Bennie, 1995).

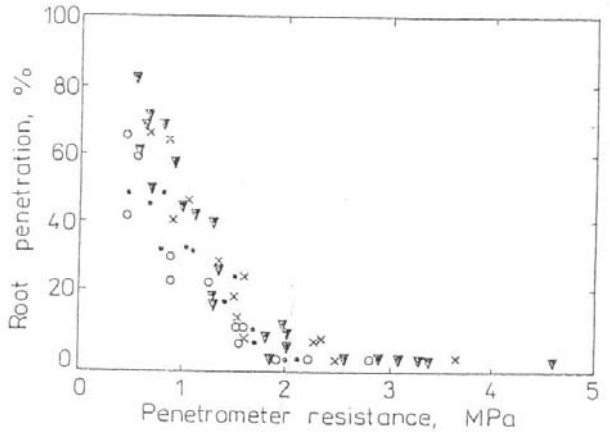

Figure 3.7 Relation between cotton root penetration and penetrometer resistance (Taylor *et al.*, 1996).

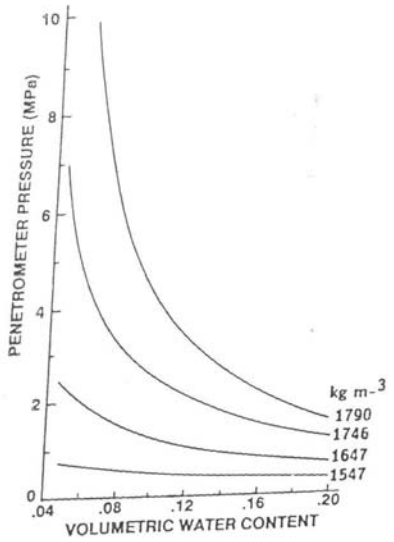

Figure 3.8 Change in penetrometer pressure with water content at different bulk densities (Bennie, 1995).

To characterize the effect of irrigation application amounts on the root development of maize, optimum water and nitrogen treatments from the same field experiment were selected and depicted in Figure 3.9. Accordingly the total root length increased exponentially from 300 mm irrigation to about 450 mm, where it peaked at a total root length of 12.4 km m^{-2}. Further increase in irrigation lowered the total root length gradually to about 8.5 km m^{-2}.

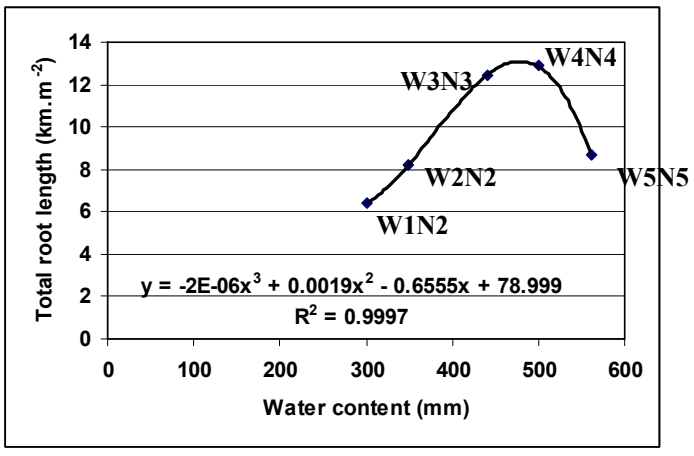

Figure 3.9 Relationship between total root length and various water applications at optimum nitrogen levels (Data processed from Van Rensburg, 1996).

3.3Methodology

The experimental site and field trial, as described in Chapter 1, was used for this study

3.3.1 Treatments

From the 75 plots displayed in Figure 2.21, only 13 plots were selected to study the effect of physical properties on root development within the IRWH system (Figure 2.15). These plots were chosen on the relative performance of above ground biomass at tussling and not at final harvest where severe frost affected the yield. At tussling both the leaves and roots has reached their maximum growth and hence above ground biomass should be a good indicator to select the plots. Biomass weight of the individual plots was expressed relative to the highest value obtained. From these relative yields, 13 plots were randomly selected over the gradient, representing plots from very high to the lowest yield obtained.

3.3.2 Plant Sampling

3.3.2.1 Above ground dry weight

Plants were harvested from an area of 20 m^2, by cutting it as close to the ground as possible. Plants were dried at 65°C until it reached constant weight then weighed. The biomass was expressed in $kg.ha^{-1}$.

3.3.2.2 Root sampling

Soil root samples were taken in triplicate in the basin area as well as on the runoff area at depth intervals of 0 - 300 mm, 300 - 600 mm and 600 - 900 mm, using a 1ℓ core sampler. The roots of each sample were washed over a 0.5 mm mesh and the root length was measured using an infrared line intersection counter (Rowse & Phillips, 1974). Calibration of the infrared line intersection counter was done using 1 m to 5 m cotton thread lengths and root density was expressed as $km\ km^{-2}$.

3.3.3 Soil classification

From the 13 profile that was morphologically described, 5 plots were classified as Tukulu and Sepane respectively, while 3 plots were identified as Bloemdal. Tukulu profiles were found to be in the top and middle part of the land, while the Sepane soil form occurred in the bottom of the land. Bloemdal soils occurred in the middle of the land (Figure 2.21).

3.3.3 Soil physical measurements

For the various physical analysis samples were taken from each diagnostic horizon of the 13 selected plots.

3.3.3.1 Bulk density

Samples were taken in triplicate for each diagnostic horizon using a 1*l* core sampler as indicated in Figures 3.10 a & b. After sampling the soil was oven dried at 104°C for 24 hours (Non - Affiliated Soil Analysis Work Committee, 1990), weighed; and expressed in $kg.m^{-3}$.

Figure 3.10 Illustrating the sampling of the soil for bulk density determination (a) The core is inserted into the soil with a sliding hammer and (b) recovered without disturbing the soil inside the cylinder.

3.3.3.2 Modulus of rupture

The soil samples were first dried in the oven at 105˚C for twenty four hours, before transferred to small rectangular metal frames. The soil briquettes were prepared and the force required to rupture the briquettes was measured as described by the Non-Affiliated Soil Analysis Work Committee (1990) and expressed in bar.

3.3.3.3 Aggregate stability

Soil samples were carefully transferred to a drying room (30 - 35°C). After drying for a week the samples were prepared for the wet sieving procedure described by (Kemper & Rosenau, 1986). A series of five sieves with mesh sizes of 4 mm, 2 mm, 1 mm, 0.5 mm and 0.25 mm was used and the simulator simulated for 10 min per sample frequency of 36 cycles min^{-1}. The water stable aggregates were expressed in percentage of the total weight of the original dried sample.

3.3.3.4 Particle analysis

Seven particle size fractions were determined with the pipette method as described by the Non - Affiliated Soil Analysis Work Committee (1990). The textural fractions were coarse sand (2 mm – 0.5 mm), medium sand (0.5 mm – 0.25 mm), fine sand (0.25 mm – 0.106 mm), very fine sand (0.106 mm – 0.05 mm), coarse silt (0.05 mm – 0.02 mm), fine silt (0.02 mm – 0.002 mm) and clay (less than 0.002 mm).

3.3.4 Statistical analysis

Variation in soil physical properties of the diagnostic horizons was described through calculating the mean, minimum, maximum and coefficient of variation of the observed values. A correlation matrix together with a multiple regression analysis was drawn for the data using NCSS 2000 (Hintze, 2000).

3.4 Results and Discussion

3.4.1 Interaction of soil physical properties

The field was cultivated for more than four decades with conventional tillage methods. These methods include ploughing, disking, harrowing and weeding with tillers which pulverize the soil and doing so moderates the biological, chemical and physical properties of the soil (Hillel, 2004; Beare *et al.*, 1994 and Bronick & Lal, 2004). This section attempts to take stock the physical properties of the soil and interaction between physical properties such as the thickness, silt + clay (Si + Cl) content, organic carbon (OC), modulus of rupture (MOR), aggregate stability (AS) (4, 2, 1, 0.5 and 0.25 mm) and bulk density (Db) of the diagnostic horizon of the 13 plots.

Variation in soil physical properties was expressed in terms of the horizon thickness (depth, mm), Si + Cl (%), OC (%), MOR (bar), AS (5 fractions, %) and Db (kg m^{-3}). Statistical parameters that were used to describe variation are the mean, minimum, maximum and the coefficient of variation. The results of the analysis are summarized in Table 3.5 for the A, B and C horizon of the Bloemdal, Tukulu and Sepane soils, respectively. Results on the individual plots are tabulated in Appendix V. The correlation matrix between soil physical properties for the A, B and C horizon of the Bloemdal, Tukulu and Sepane soils is presented in Table 3.6.

3.4.1.1 A horizon

The A horizon is similar to all the soil forms identified in the field and originates from eolian sands which have mixed naturally with the clays originated from the sandstone, mudstone and dolerite parent material of the area. Soil physical properties developed within the context of natural pedogenic processes and modified by anthropogenic activities. Comparing the means of the different soil revealed that the horizon depth, silt + clay content (Si + Cl), organic carbon content (OC), modulus of rupture (MOR), percentage water stable aggregates (AS) of the larger fractions (4 and 2

mm) increase from the Bloemdal via the Tukulu to the Sepane. Several studies have shown a positive relationship between clay content and organic carbon content (Soane, 1990; Dinel *et al.*, 1997; Dimoyiannis *et al.*, 1998; Schulter and Leinweber, 2000; Chernie *et al.*, 2000), which emphasize which indicated that S+C and OC is the primary mechanism of aggregation of soil particles in its native states.

The results show considerable variation in the soil physical parameters such as AS and OC, irrespective the soil form. Variation (CV) in the modulus of rupture was greater in the Sepane and Tukulu than in the Bloemdal. The rest of the parameters did not vary much within soil forms.

In order to study the interaction of the soil physical properties a correlation matrix analysis was made and the results are summarized in Table 3.7. These results clearly show that soil depth, OC, MOR and Db have a moderately strong positive correlation with an increase in silt + clay of the A horizon. This was expected because these soils contains high activity clays such as montmorrilonite and illite with great surface area, CEC, charge density, dispersivity and expendability that can stimulate interaction between soil physical properties.

Silt + clay content, OC and Db show a strong positive correlation with soil strength as indicated by the MOR correlation statistics. The presence of water can modify soil strength directly as demonstrated by Bennie (1996). He showed that soil strength lowers exponentially with an increase in soil water content. Thus, rain actually helps to reduce the energy required for mouldboard ploughing and other tillage operations. It is often argued that the mouldboard plough is an excellent implement to create “temporal” structure in soils with a massive structure (Fertilizer, 2007) as in the case of the Bd, Tu and Se soils.

Long term effects of conventional tillage on the soil physical properties of these clay soils in semi-arid areas are unknown. Water stable aggregate tests are often used as an indicator to demonstrate the effect of tillage on

soil structure (Six *et al.*, 2000). The correlation matrix results on the water stable aggregates show a strong negative relationship between AS 0.25 and especially S+C (-0.45) and to a lesser extent OC (-0.23). The results suggest that there is a greater tendency for the soils to disperse with an increase in Si + Cl and OC, probably due to the presence of Na in the soils. According to Singer *et al.* (1992) as clay particles swell with the intake of water, they separate from other particles and hence lowering aggregate stability. Under these conditions macro – aggregate (>0.25 mm) disintegrate into smaller or micro – aggregates (<0.25 mm) or can disperse completely. Some of the aggregates might disperse, and rearrange to be flocculated and cemented again. Carbonated C, which exists as primary and secondary minerals in semi – arid soils, is an excellent flocculent and therefore aggregator if present in solution, especially at low soil organic matter concentrations (Boix – Fayos *et al.*, 2001). However, the 10% HCl solution test confirmed that carbonates are absent in both the topsoil- and subsoil, which exclude inorganic C to be an aggregator in these soils. Aggregation can also be mediated by the Fe and Al oxides and sesquioxcides as in the case of oxisols (Oades and Waters, 1991; Dalal and Bridge, 1996). Unfortunately the contribution of these minerals cannot be tested as this was not part of the study, but future analysis of the water stable aggregates should give a better explanation of the stability of the aggregates.

3.4.1.2 B horizon

The B horizon is one of the main factors that distinguish the three soil forms, *viz.* a red apedal (Bloemdal), neocutanic (Tukulu), pedocutanic (Sepane) from each other. The structural change from the Bd via the Tu to the Se is supported by an increase in the mean S+C content, OC, MOR and Db over the soils. There is a clear difference in B horizon depths between the three soil forms with the Tu having the deepest and less variable horizon (CV = 27%). The S+C of the Tu soil form varied between 31% and 34% (CV = 4%) and that of the Se soil form varied between 49% and 55% (CV = 4%), while the Bloemdal varied between 28%

and 34% (CV = 8%). The statistical results show high variability in all aggregate sizes within soil forms.

The correlation statistical results show that texture plays a dominant role in the physical properties of the B horizons. Si + Cl correlates strongly in a positive manner with OC, MOR, AS (0.5 mm) and Db. The strong relationship can be explained by the physical and chemical nature of the type of clay minerals as described in the A horizon. Si + Cl also showed a strong negative relationship with the larger aggregate sizes, which suggest that the clay-bonds between macro-aggregates are not strong and are easily broken in the presence of rainwater. These soils are known for its dispersivity properties due to the presence of sodium.

MOR of the B horizons is positively linked to Si + Cl, OC and Db and shows no strong association with aggregate size fractions. Very interesting to note is the strong positive relationship between the AS 0.5 mm, OC and Db. All the other AS fractions show a moderate to strong negative correlation with Si + Cl, again expose the dispersivity of these soils. Because soil erodibility is linked to soil aggregate stability (Le Bissonnais, 1996; Zotarelli *et al*., 2005), the low percentage of aggregates in the larger fractions (4 and 2 mm) of the Sepane and Tukulu soil confirms the susceptibility of these soils to water erosion.

The aggregate size distribution is dominated by the smaller sizes (0.5 – 0.25 mm) in all soils. Both these soils have larger structural units (medium developed sub angular blocky and strong developed angular blocky, respectively) in its native state. Once the B horizon of these soils are exposed to the impact of rain the peds will easily breakdown which leads to detachment of particles and small aggregates that favours crusting then runoff and transport (Miller and Baharuddin, 1986; Summer, 1992; Barthes *et al*., 1999). Under

rain fed conditions, wet – dry cycles are most common which can be disrupt aggregation in swelling clays (Piccolor *et al*., 1997).

3.4.1.3 C horizon

All the soils have a prismatic structure in the C horizon and therefore confirms the low CV in almost all the soil physical parameters, except some of the AS fractions. The Se has the thickest horizon (mean = 390 mm), the lowest silt + clay content (35%) and the highest Db (1730 kg m^{-3}) of all the soils. The C horizon of the Bd seems to be the thinnest (150 mm) with the highest OC content (0.34%) and MOR (0.57 bar). The variation was generally low in all the soil physical properties, except for the AS fractions. Despite the large structural units present in the native states of the soils, there is a clear absence of water stable aggregates fractions in the 4 and 2 mm classes. Thus, once again the results give proof to the dispersive potential of these soils and emphasize the vulnerability of it to water erosion. Interesting to note that all the AS fractions except 0.5 mm, show a moderately strong positive relationship with silt + clay. The silt + clay content had no relationship with the OC content as it is very low in these soils. The MOR shows no particular association with the other soil physical parameters measured. There was an indication that bulk density is influenced by the presence or absence of silt + clay, OC, MOR and mostly the larger aggregate size fractions.

Table 3.5 Variation in soil physical properties for the Bloemdal, Tukulu and Sepane soil forms

Horizon	Soil form	Statistical Parameter	Horizon depth (mm)	Silt + clay (%)	Organic carbon content (%)	Modulus of rupture (bar)	AS 4 (%)	AS 2 (%)	AS 1 (%)	AS 0.5 (%)	AS 0.25 (%)	Bulk density (kg m^{-3})
A	Bd	Mean	150	20	0.13	0.09	1.28	9.06	24.01	10.19	12.86	1290
		Min	250	25	0.35	0.12	3.23	30.73	32.43	18.33	20.39	1360
		Max	213	21	0.24	0.1	2.13	15.67	28.92	15.41	17.75	1328
		CV	0.22	0.11	0.42	0.13	0.4	0.65	0.12	0.24	0.19	0.02
	Tu	Mean	207	22	0.18	0.15	6.18	12.81	35.14	14.98	16.81	1471
		Min	200	19	0.26	0.06	4.44	4.85	20.34	2.7	6.07	1376
		Max	210	26	0.2	0.25	7.4	25.12	45.32	20.86	30.02	1520
		CV	0.02	0.13	0.19	0.55	0.2	0.67	0.3	0.54	0.66	0.04
	Se	Mean	218	25	0.14	0.23	16.3	14.87	14.71	14.04	7.23	1468
		Min	210	22	0.19	0.1	3.93	8.3	2.43	1.76	2.6	1399
		Max	250	27	0.16	0.37	33.33	22.62	22.1	27	15.44	1532
		CV	0.08	0.08	0.15	0.48	0.81	0.37	0.55	0.76	0.75	0.04
B	Bd	Mean	260	31	0.19	0.17	3.33	13.47	26.06	19.47	23.63	1440
		Min	200	28	0.29	0.15	2.38	12.56	11.77	13.9	6.62	1365
		Max	350	34	0.23	0.2	4.22	14.43	33.23	33.76	30.23	1501
		CV	0.25	0.08	0.19	0.12	0.23	0.06	0.36	0.47	0.46	0.04
	Tu	Mean	425	32	0.16	0.64	4.44	10.53	13.14	14.89	15.72	1665
		Min	250	31	0.22	0.44	1.19	2.83	2.02	4.13	5.45	1605
		Max	500	34	0.2	0.76	8.07	20	21.38	35.88	36.13	1729
		CV	0.27	0.04	0.15	0.22	0.66	0.76	0.61	0.95	0.87	0.04
	Se	Mean	150	51	0.17	0.57	4.42	6.2	19.29	24.53	31.52	1779
		Min	100	49	0.22	0.38	2.62	2.13	10.6	10.9	13.43	1670
		Max	250	55	0.2	0.89	10.4	14	26.19	35.65	50.94	1810
		CV	0.42	0.04	0.12	0.39	0.77	0.84	0.34	0.42	0.46	0.03

Table 3.5 (continue)

Horizon	Soil form	Statistical Parameter	Horizon depth (mm)	Silt + clay (%)	Organic carbon content (%)	Modulus of rupture (bar)	AS 4 (%)	AS 2 (%)	AS 1 (%)	AS 0.5 (%)	AS 0.25 (%)	Bulk density (kg m^{-3})
C	Bd	Mean	150	44	0.09	0.57	2.03	4.07	17.45	28.09	30.48	1606
		Min	50	42	0.17	0.45	1.04	1.45	14.35	11.67	21.11	1580
		Max	250	49	0.13	0.64	2.67	8.32	20.33	34.65	36.54	1643
		CV	0.54	0.07	0.25	0.14	0.34	0.71	0.14	0.37	0.22	0.02
	Tu	Mean	275	47	0.11	0.37	8.19	14.84	17.77	16.36	16.16	1586
		Min	210	43	0.16	0.27	6.2	5.49	11.13	13.25	8.72	1503
		Max	310	54	0.13	0.54	10.57	24.26	27.62	18.46	22.53	1642
		CV	0.16	0.1	0.19	0.33	0.22	0.56	0.39	0.14	0.36	0.04
	Se	Mean	390	35	0.11	0.38	3.16	11.03	22.61	25.88	15.81	1730
		Min	300	30	0.13	0.19	1.45	7.51	10.19	12.85	8.54	1656
		Max	500	41	0.12	0.56	6.45	15.54	39.93	36.05	29.15	1783
		CV	0.22	0.13	0.08	0.39	0.65	0.34	0.57	0.37	0.52	0.03

Table 3.6 Correlation matrix for the Tukulu, Sepane and Bloemdal soil froms

Horizon	Parameter	Depth	Si + Cl	OC	MOR	AS 4	AS 2	AS 1	AS 0.5	AS 0.25	Db
A	**Depth (mm)**	**1**									
	Silt +Clay (Si + Cl, %)	0.33	**1**								
	Organic carbon content (OC %)	0.18	0.42	**1**							
	Modulus of rupture (MOR, bar)	0.09	0.57	0.93	**1**						
	Aggregate Stability 4 mm (AS 4, %)	-0.07	0.05	0.03	0.13	**1**					
	Aggregate Stability 2 mm (AS 2, %)	-0.11	0.02	0.08	0.11	0.18	**1**				
	Aggregate Stability 1 mm (AS 1, %)	-0.06	-0.08	-0.2	-0.39	-0.45	-0.15	**1**			
	Aggregate Stability 0.5 mm (AS 0.5, %)	0.17	0.15	-0.17	-0.08	-0.34	-0.33	-0.01	**1**		
	Aggregate Stability 0.25 mm (AS 0.25, %)	0.05	-0.45	-0.23	-0.33	-0.43	-0.52	0.18	0.4	**1**	
	Bulk density(Db, kg m^{-3})	-0.23	0.61	0.18	0.29	0.31	-0.07	0.05	-0.11	-0.46	**1**
B	**Depth (mm)**	**1**									
	Silt +Clay (Si + Cl, %)	0.16	**1**								
	Organic carbon content (OC %)	0.08	0.23	**1**							
	Modulus of rupture (MOR, bar)	0.4	0.62	0.34	**1**						
	Aggregate Stability 4 mm (AS 4, %)	-0.43	-0.21	0.03	0.12	**1**					
	Aggregate Stability 2 mm (AS 2, %)	0.1	-0.2	-0.23	-0.15	0.2	**1**				
	Aggregate Stability 1 mm (AS 1, %)	-0.07	-0.68	0.19	-0.29	-0.1	-0.1	**1**			
	Aggregate Stability 0.5 mm (AS 0.5, %)	0.4	0.64	0.16	0.13	-0.47	0	-0.67	**1**		
	Aggregate Stability 0.25 mm (AS 0.25, %)	-0.37	-0.03	-0.19	-0.18	-0.17	-0.36	0.15	-0.2	**1**	
	Bulk density(Db, kg m^{-3})	0.43	0.5	0.38	0.49	0.03	-0.15	-0.19	0.38	-0.45	**1**
C	**Depth (mm)**	**1**									
	Silt +Clay (Si + Cl, %)	-0.09	**1**								
	Organic carbon content (OC %)	0.13	-0.08	**1**							
	Modulus of rupture (MOR, bar)	0.11	0.1	0.19	**1**						
	Aggregate Stability 4 mm (AS 4, %)	0.38	0.47	-0.18	-0.05	**1**					
	Aggregate Stability 2 mm (AS 2, %)	0.47	0.32	-0.34	0.07	0.72	**1**				
	Aggregate Stability 1 mm (AS 1, %)	-0.13	0.33	-0.25	-0.24	0.47	0.24	**1**			
	Aggregate Stability 0.5 mm (AS 0.5, %)	-0.14	-0.18	0.24	-0.45	-0.33	-0.67	0.2	**1**		
	Aggregate Stability 0.25 mm (AS 0.25, %)	-0.4	0.18	0.36	-0.01	-0.16	-0.43	0.11	0.52	**1**	
	Bulk density(Db, kg m^{-3})	-0.23	0.44	0.2	0.18	0.25	0.11	-0.01	-0.28	0.16	**1**

3.4.2 Relationship between root development and soil physical properties

Based on the correlation matrix results summarized in Table 3.7, only the soil physical properties that have a collective influence on root development express as the total root length (km m^{-2}) or root length index (RLI), as indicated by an asterisk, were selected to form a soil physical quality index (SPQI). The SPQI was developed by assessing the influence of a soil physical parameter on root development for each master horizon. A relative performance value according to the influence on root development; that varies between 0 and 10, was then assigned to individual plots. The collective performance of each plot was obtained by adding the different points scored for all the soil physical properties. The total score of each plot represents collectively the SPQI. The SPQI was then regressed with the RLI and the results are presented in Figure 3.11 for the A-horizon (a), B-horizon (b) and C-horizon (c).

Table 3.7 Extraction of correlation matrix results for root length index (km m^{-2}) as influenced by the different soil physical properties of the A, B and C horizon in the Bloemdal, Tukulu and Sepane soils

Parameter	Horizon		
	A	B	C
Depth (mm)	-0.2*	0.39*	-0.41*
Silt +Clay (Si + Cl,%)	0.13	-0.21	-0.01
Organic carbon content (OC %)	-0.01	-0.2	-0.36*
Modulus of rupture (MOR, bar)	0.19*	-0.45*	-0.42*
Aggregate Stability 4 mm (AS 4)	0.14	-0.83*	-0.26*
Aggregate Stability 2 mm (AS 2)	-0.02	-0.06	-0.42*
Aggregate Stability 1 mm (AS 1)	-0.53*	0.28*	0.44*
Aggregate Stability 0.5 mm (AS 0.5)	0.1	0.19	0.54*
Aggregate Stability 0.25 mm (AS 0.25)	-0.26*	0.18	-0.09
Bulk density(Db, kg m^{-3})	-0.17	-0.32*	-0.19

(a)

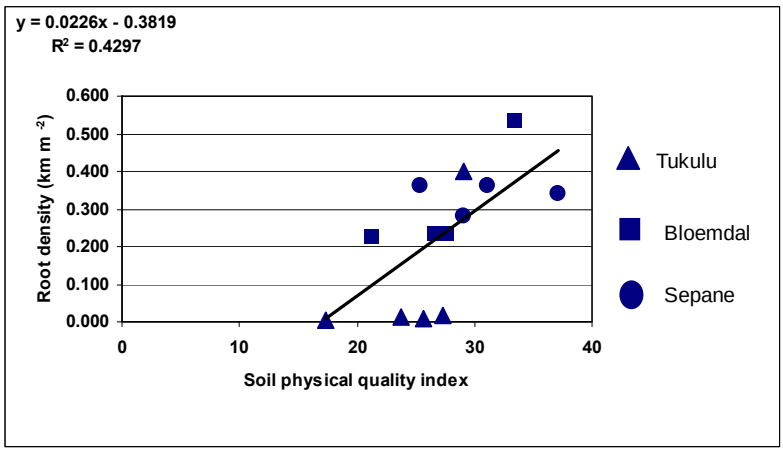

(b)

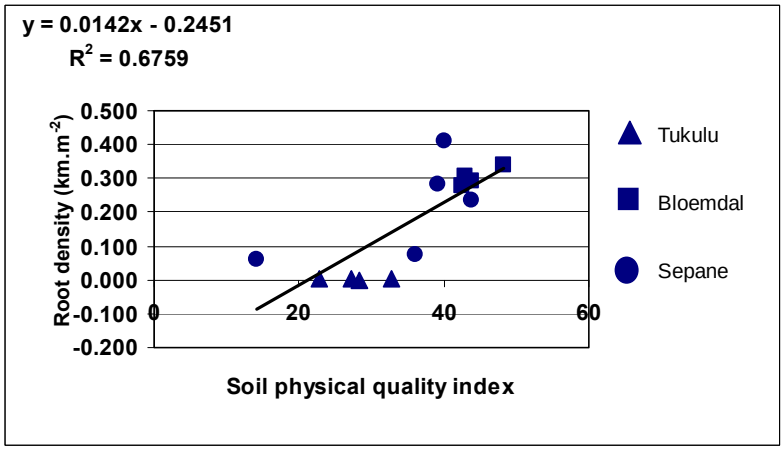

(c)

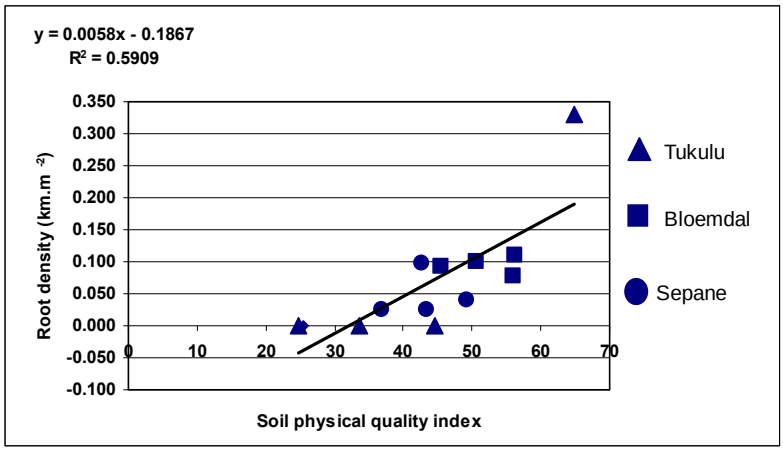

Figure 3.11 Relationship between total root length or root length index (RLI) and the soil physical quality index (SPQI) for the A-horizon (a), B-horizon (b) and C - horizon (c) over the 13 plots investigated, regardless of soil form.

3.4.3 Master horizons

A horizon: As indicated in Table 3.7 (a), horizon depth or thickness, MOR and the 1 and 0.25 mm water stable aggregate fractions were used to calculate the SPQI for the different plots. It should be emphasize that all these parameters correlated negatively with root density indicating that the presence or intensity of these soil properties actually decrease the total root length or root length index. The positive relationship between SPQI and the RLI reflects on the way the plots have been assessed in their performance. It is obvious the plot that has the thickest horizon, lowest MOR and the highest percentage of 1 and 0.25 mm water stable aggregates will have the highest SPQI value and those with the opposite trends will have the lowest value. The regression statistics shows that SPQI related linearly to the RLI, but could only explains 36% of the variation.

B horizon: The water stable aggregate sizes of 4 mm (33%) had a negative correlation on root development as indicated by the RLI (Table 3.7). Amato and Ritchie (2002) also found that the large size aggregates had a negative influence on root density. The aggregate sizes of 1 mm (46%), 0.5 mm (39%) and 0.25 mm (36%) had positive correlations with root density once again complementing the study done by Amato and Ritchie (2002). From the correlation matrix the combination of main parameters which correlated the best with root density and used as part of the SPQI are modulus of rupture, soil depth or horizon thickness, bulk density and the water stable aggregate fractions of 4 mm, 2 mm and 0.25 mm. As seen in Figure 3.11 (b) the R^2 between the main soil physical parameters and RLI is 68%, which indicated that the SPQI relates reasonably accurate to RLI.

C horizon: From Table 3.7 it is clear that the depth of the C horizon had a large negative correlation with RLI (41%). The modulus of rupture had a large negative correlation with root density (42%) and generally followed the trend observed by Taylor *et al.* (1996), a sharp decline in root growth with an increase in soil strength. The aggregate sizes of 4 mm (26 %) and 2 mm (42%) had a large negative effect on root density which corresponded well with the study done by Amato and Ritchie (2002),

where they found that the large aggregate sizes had a large negative influence on root development. The aggregate sizes of 1 mm (43%) and 0.5 mm (54%) had positive correlations with root density once again complementing the study done by Amato and Ritchie (2002). From the correlation matrix the combination of main parameters which correlated the best with root density when drawn into a multiple regression equation, was selected and in the C horizon it was the combination of the thickness of the layer, MOR and the AS fractions of 4 mm, 2 mm, 1mm and 0.25 mm corresponded the best with root density. As seen in Figure 3.11(c) the R^2 of the linear relationship between SPQI and RLI is 48%,

3.4.4 The Profile

The SPQI for each plot's profile were obtained by adding the SPQI value for the different horizons. The SPQI's for the 13 plots were then regressed with the total root length of the profile (RLI) expressed in $km.m^{-2}$. The graph and the statistical results of the linear regression are presented in Figure 3.12. According to the R^2 the SPQI is able to explain 79% of the variation in the RLI.

Further inspection of the data in Figure 3.12 reveals that the soil forms have a prominent role in the SPQI vs RLI relationship. The Tukulu soil form with a Neocutanic B horizon had the lowest corresponding RLI over the profile. This is due to the fact that the strength of the Neocutanic B horizon is so high that it has a negative influence on root elongation. On the other hand, the clay content of the neocutanic B horizon is too low to create planes of weakness that stimulates preferential root paths. The Sepane soil form had the second highest RLI over the profile, which is the result of higher clay contents in the pedocutanic B horizon, causing planes of weakness that serves as preferential root paths downward in the profile. The Bloemdal soil form had the highest corresponding RLI over the profile, which is the result of the red apedal B horizon, which is of lower soil strength than the previous two mentioned, This complements root densities in the A horizon and B horizon as no restriction by soil strength is acting on roots downward in the profile.

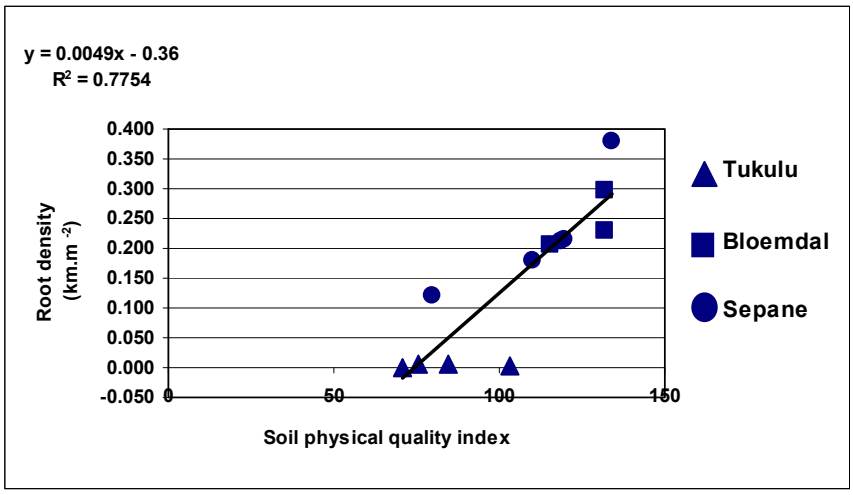

Figure 3.12 Relationship between total root length or root length index (RLI) and the soil physical quality index (SPQI) for the profiles, irrespective soil forms.

3.5 Conclusion

From the review it is clear that soil physical properties have a close inter relationship. Past studies on root development were mainly applied on sandy to sandy loam soils, with a massive apedal structure. Up to date none of the biophysical studies in IRWH has focussed on root development.

Studying the inter relationship between soil physical properties it is clear that the A horizon is generic to all the soil forms identified in the field and originates from eolian sands which is mixed naturally with the clays originated from the sandstone, schale and dolerite parent material of the area. Soil physical properties developed within the context of natural pedogenic processes and onthropogenic activities. Conclusive evidence were obtained on the considerable variation in the physical parameters such as AS and OC, irrespective the soil form. The B horizon is the main factor that distinguishes the three soil forms, *viz*. a red apedal (Bloemdal), neocutanic (Tukulu), pedocutanic (Sepane) from each other. The correlation statistical results show that texture plays a dominant role in the physical properties of the B horizons. The strong inter relationship can be explained by the physical and chemical nature of the type of clay minerals as described in the A horizon. All the soils

have a prismatic structure in the C horizon which in most cases gave a very low degree of inter relationships.

Determining how the RLI relates to soil physical properties, indicated that the A horizon had a variability due to cultivation and the processes of organic breakdown. In the B horizon the Bloemdal had the highest RLI and least influence by soil physical properties on root elongation. This may be due to its lower clay content and massive apedal structure. The Sepane had the second highest root density in the B horizon, although it had a high Si + Cl, strong angular blocky structure etc. The high SI + Cl caused sufficient swell and shrink actions to cause roots to move down cracks and increase the root density downwards in the profile. The Tukulu had the lowest B horizon RLI, which may be due to a Si + Cl that is high enough to have a restricting effect on elongating roots and low enough so that the swelling and shrinking is not sufficient to form cracks. In the C horizon the most limiting factors were the soil strength due to the uniform prismatic horizon throughout the area, together with a high MOR. These two factors caused a low RLI in the C horizon regardless of soil form.

CHAPTER 4

Characterizing the hydrology of the Bloemdal, Tukulu and Sepane soils at Paradys.

4.1 Introduction

Soil hydrology is of crucial importance in countries such as South Africa, where the lack of water limits rain fed crop production (Hutson, 1983). The hydraulic conductivity is a challenging soil property to describe because it can change many orders of magnitude over short distances. Heterogeneity of soil properties within and between soil horizons causes some regions to be more or less favourable to flow. The flow is highly variable with extremes represented by tortuous flow between individual particles and rapid flow through large, continuous macropores.

The spatial variation of the hydraulic conductivity is influenced by much more than topography and soil form and is also strongly affected by the soil structure. To explain this phenomenon, Vanapalli et al. (1999) suggested that when investigating the structure of partially saturated soils, there are two levels to be considered namely: macrostructure and microstructure. Macrostructure governs the soil water characteristic behaviour for the soil particularly at low suction values, while microstructure governs the behaviour of soil water characteristic at relatively high suction values. On the other hand soil texture influences the difference in pore sizes in the soil. In a clayey soil, the pore size distribution is more uniform, and more of the water is adsorbed, so that increasing the matric suction causes a more gradual decrease in wetness. Thus the greater the Si + Cl in general the greater the water retention at any particular suction, and more gradual the slope of the curve (Dexter, 1978). Db also has an effect on the soil water characteristics as an increase in Db means a decrease in total pore space in the soil and a decrease in water movement through the soil (Hillel, 2004). The OC also increases the water holding capacity and conductivity largely as a result

of its influence on soil aggregation and associated pore size distribution. The OC increases the amount of water retained, especially at low suctions, but at higher suctions soil rich in organic carbon releases water rapidly because of large pore spaces (Saxton & Rawls, 2006). Soil properties such as conductivity, porosity and pore size distribution are scale dependant and should be taken into consideration when selecting the sample size. Thus a field estimation of hydraulic character where a larger sample is taken might be more desirable (Hillel, 2004).

Further studies have to be done to identify all the factors affecting the spatial variation of the hydraulic conductivity of different soil forms, before a model to characterize the variation may be established. The objective of this study were therefore to (i) characterize the hydraulic properties of the Bloemdal, Tukulu and Sepane soils, *viz.* volumetric wetness-time relationships, matric suction – time relationships, hydraulic head – depth relationships and the hydraulic conductivity – soil water content relationship for each soil diagnostic horizon within the profile.

4.2 Methodology

4.2.1 Experimental site

The experimental site and field trial as described in Chapter 1 was used for this study. From the 75 plots, plots nr 1.1 (Tukulu), 8.3 (Bloemdal) and 14.2 (Sepane) were selected.

4.2.2 Experimental design

The instantaneous profile method as described by Hillel, 2004 was used. Spades were used to dig a trench of 4 m long, 4 m wide and +/- 1.2 m deep around the modal profile (Figure 4.1).The trench was dug to reach the saprolite at the bottom of the profile. The profile was lined with plastic, while slurry was placed between the profile and the plastic surrounding the profile. The trench was filled up with soil and a ridge was made +/- 600 mm high around the profile, to prevent water from running off when wetting the profile. Five neutron water meter access tubes were inserted 500 mm apart (Figure 4.1) in the middle of the profile using a

hand auger. Three watermarks with automatic loggers were installed 500 mm away from the access tubes at depth intervals of 300 mm, 600 mm and 900 mm (Figure 4.1). Water was added to the profile until the drained upper limit was obtained. The profile was covered with 5 cm thick isolation material to control temperature and plastic to prevent any evaporation and was left to freely drain for a period of 30 days.

4.2.3 Experimental measurements

Water content readings were taken frequently with a Campbell Pacific Neuclear 503 DR hydroprobe during the first three days after which it was taken less often until it was only read once a weak at the end of the trial. The water content was expressed as volumetric water content in mm mm^{-1}consistentent over time in most of the horizons and there seems to be some doubt on the accuracy of the instruments. As an alternative the local retention model developed in the Department of Soil, Crop and Climate Sciences (UFS) (Van Rensburg, 1988) was used to estimate the matric suction head over time from measured soil water content. The model uses silt + clay content (%) as input to make the prediction of water retention.

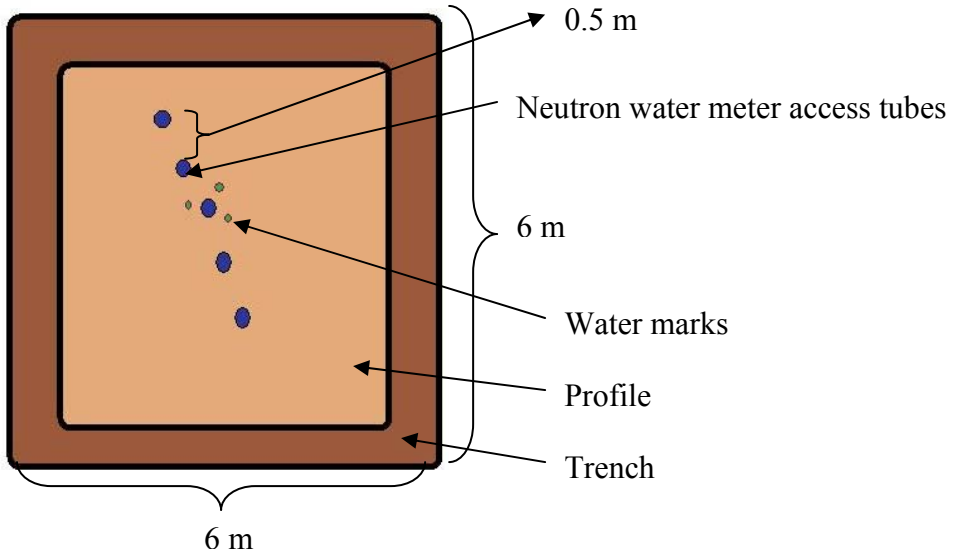

Figure 4.1 Experimental design for the instantaneous profile method.

4.2.4 Calculation of hydraulic conductivity

Firstly the drainage curves were established using the soil water content captured by the CPN. This was expressed as soil water content $mm.mm^{-1}$ vs. days after saturation (DAS). Secondly the locally developed retention model was used to predict matric suction from water content using silt + clay as a input. From these two parameters the soil moisture flux was calculated as follows: (i) For each DAS increment the flux for the specific horizon was estimated using the equation: $dz(\Delta WC/\Delta t$ (cm day^{-1}), where dz is the difference in depth, ΔWC is the difference in water content between 1 and 2 DAS for example and Δt is the difference in DAS. Flux (q) was calculated by adding the A, B and C horizon flux, thus A horizon flux was equal to A horizon flux, B horizon flux was equal to A + B horizon flux and C horizon flux was equal to A + B + C horizon flux.

The Hydraulic head was calculated using the equation: H = Hp + Hg, where Hp is the matric suction from the retention curve and Hg is the thickness of the horizon. The hydraulic head was expressed in cm. ΔH was calculated using the equation: $\Delta H = (H_{\text{B horizon}} - H_{\text{A horizon}})/ z_{\text{(thickness of horizon)}}$. From this K was calculated using the equation $K = q/\Delta H$. K was expressed as cm day^{-1}. The data that was used to calculate K can be found in Appendix X.

4.2.5 Statistical Procedures.

Curve Expert 1.3 (1996) was used to fit the best model to the drainage data, while Microsoft Excel was used to fit the best trend line to the hydraulic head – depth relationship data and the hydraulic conductivity – soil water content relationship data

4.3 Results and discussion

A summary of selected soil physical properties together with a summarized profile description of the three selected profiles is presented in Table 4.1 and Table 4.2.

Table 4.1 Summary of the physical characteristics for the selected Bloemdal, Tukulu and Sepane soils

Horizon	Plot nr	Soil type	Horizon depth (mm)	Silt + Clay (%)	Organic carbon content (%)	Modulus of rupture (bar)	A.S 4 (%)	A. S 2 (%)	A.S 1 (%)	A.S 0.5 (%)	A.S 0.25 (%)	Bulk density (kg m^{-3})	Total porosity
A	**8.1**	**Bd**	250	17	0.24	0.11	1.67	11.23	30.43	15.46	18.43	1342.56	0.49
A	**1.1**	**Tu**	210	16	0.33	0.14	6.36	8.77	20.34	20.86	24.37	1376.19	0.48
A	**14.2**	**Se**	210	18	0.61	0.37	9.98	14.39	20.09	1.76	2.6	1507.18	0.43
B	**8.1**	**Bd**	150	30	0.33	0.61	2.32	3.09	20.33	34.65	34.23	1589.23	0.40
B	**1.1**	**Tu**	250	25	0.39	0.76	1.19	2.83	2.02	4.13	5.45	1728.9	0.35
B	**14.2**	**Se**	100	32	0.33	0.89	2.62	2.85	18.76	19.82	50.94	1807.65	0.32
C	**8.1**	**Bd**	350	39	0.19	0.18	4.22	13.55	33.23	15.67	30.23	1405.12	0.47
C	**1.1**	**Tu**	310	41	0.22	0.54	7.64	9.54	16.53	18.46	19.09	1502.58	0.43
C	**14.2**	**Se**	500	48	0.23	0.56	1.52	15.34	11.09	28.15	12.16	1701.1	0.36

Table 4.2 Summary of the pedological characteristics for the selected Tukulu, Bloemdal and Sepane soil forms

Plot nr	Soil form	Soil family	Horizons	Horizon name	Depth	Mottles	Cutans	Structure	Consistency	Parent material	Transition
8.1	**Bd**	Roodeplaat 3200	A	Ot	250	None	none	Apedal massive	Loose		Smooth, flat
1.1	**Tu**	Dikeni 1220	A	Ot	210	None	none	Apedal massive	Loose		Clear, flat
14.2	**Se**	Katdoorn 1210	A	Ot	210	None	none	Apedal massive	Loose		Abrupt, flat
8.1	**Bd**	Roodeplaat 3200	B	Yr	350	None	none	Apedal massive	Loose		Smooth, flat
1.1	**Tu**	Dikeni 1220	B	Ne	310	None	yes	Weakly developed medium 10-25 mm) Sub block	Slightly hard		Abrupt, flat
14.2	**Se**	Katdoorn 1210	B	Pd	500	None	yes	Well developed medium size (10-25 mm) blocky	Hard		Abrupt, flat
8.1	**Bd**	Roodeplaat 3200	C	Uw	150	Red, black, yellow, grey	yes	Well developed medium size (5-15mm) prismatic	Hard	Schale	Smooth, flat
1.1	**Tu**	Dikeni 1220	C	Uw	250	Red, black, yellow, grey	yes	Medium developed medium size (5-15 mm) prismatic	Hard	Dolerite/Mudstone	Abrupt, flat
14.2	**Se**	Katdoorn 1210	C	Uw	100	Red, black, yellow, grey	yes	Medium developed medium size (5-15 mm) prismatic	Hard	Dolerite	Abrupt, flat

4.3.1 Volumetric wetness-time relationships

The drainage curves are presented in Figures 4.2 - 4.4 for the different horizons of the Bloemdal, Tukulu and Sepane soils, respectively. Various models as indicated in Table 4.3 were fitted to the data set to characterize the drainage profile for the A, B and C horizons. For the discussion the internal drainage process is divided in to four periods, viz. rapid drainage period (i), moderate drainage period (ii), slow drainage period (iii) and the near constant drainage period (iv). Accordingly period (i) stretches from 0 to 2 days after saturation (DAS), period (ii) 2 - 5 DAS, period (iii) 5 – 18 DAS, followed by period (iv) from 18 DAS to the end of the drainage period.

Table 4.3 Model types and their statistical coefficients fitted to the soil water content - time data of the Bloemdal, Tukulu and Sepane soils

Soil	**Statistical parameters**	**Horizon**		
		A	**B**	**C**
Bloemdal	**Model type**	**MMF Model**	**Exponential Association (3):**	**Quadratic Fit:**
	Equation	y=(a*b+c*x^d)/(b+x^d)	y=a(b-exp(-cx))	y=a+bx+cx^2
	a	a = 0.2904573	a = -0.026604003	a = 0.29110621
	b	b = 3.0470824	b = -9.3429491	b = -0.0010260621
	c	c = 0.13549045	c = 0.44820115	c = 1.0452981e-005
	d	d = 0.35557311		
	r^2	r^2 = 0.98	r^2 = 0.94	r^2 = 0.94
Tukulu		**A**	**B**	**C**
	Model type	Harris Model:	Logistic Model:	Logistic Model:
	Equation	y=1/(a+bx^c)	y=a/(1+b*exp(-cx))	y=a/(1+b*exp(-cx))
	a	a = 3.7203276	a = 0.25759274	a = 0.28965797
	b	b = 0.5054181	b = -0.094410141	b = -0.06794273
	c	c = 0.21111037	c = 0.17303465	c = 0.21924716
	r^2	r^2 = 0.97	r^2 = 0.93	r^2 = 0.95
Sepane		**A**	**B**	**C**
	Model type	Rational Function:	Rational Function:	Rational Function:
	Equation	y=(a+bx)/(1+cx+dx^2)	y=(a+bx)/(1+cx+dx^2)	y=(a+bx)/(1+cx+dx^2)
	a	a = 0.27882798	a = 0.28129822	a = 0.28956249
	b	b = 1.017952	b = 0.039460831	b = 2.7038277
	c	c = 4.2759882	c = 0.153095	c = 10.278194
	d	d = -0.0011019731	d = 3.6489891e-005	d = 0.0060851941
	r^2	r^2 = 0.97	r^2 = 0.93	r^2 = 0.95

Bloemdal: The drainage reflects on the pedological characteristics of the horizons. The A and the B horizon both have a massive apedal structure, but have different textural properties. The silt + clay content of the A horizon (17%) is considerably lower than the B horizon (25%), which explains why the relative position of the A – curve falls below that of the B. As expected the C – curve shows the slowest drainage which can be attributed to the slow permeable nature of the prismatic structure of the C horizon, with a silt + clay content of 39%. Phase (iv) is of particular interest because drainage is accepted to be neglectively slow and represents the drained upper limit of plant available water, *viz.* 0.21mm mm^{-1} for the A horizon, 0.25 mm mm^{-1} for the B horizon and 0.27 mm mm^{-1} for the C horizon (Figure 4.2). The volumetric water content at field saturation (FS) for the A, B and C horizons is 0.26 mm mm^{-1}, 0.28 mm mm^{-1} and 0.32 mm mm^{-1}, respectively. This was generally lower than the total porosity (f_t) calculated from the bulk density values listed in Table 4.1. This explains the fact how difficult it is to completely saturate a profile in the field, despite the care taken to fill up the profile. The difference between FS and f_t is ascribed to entrapped air in the profile.

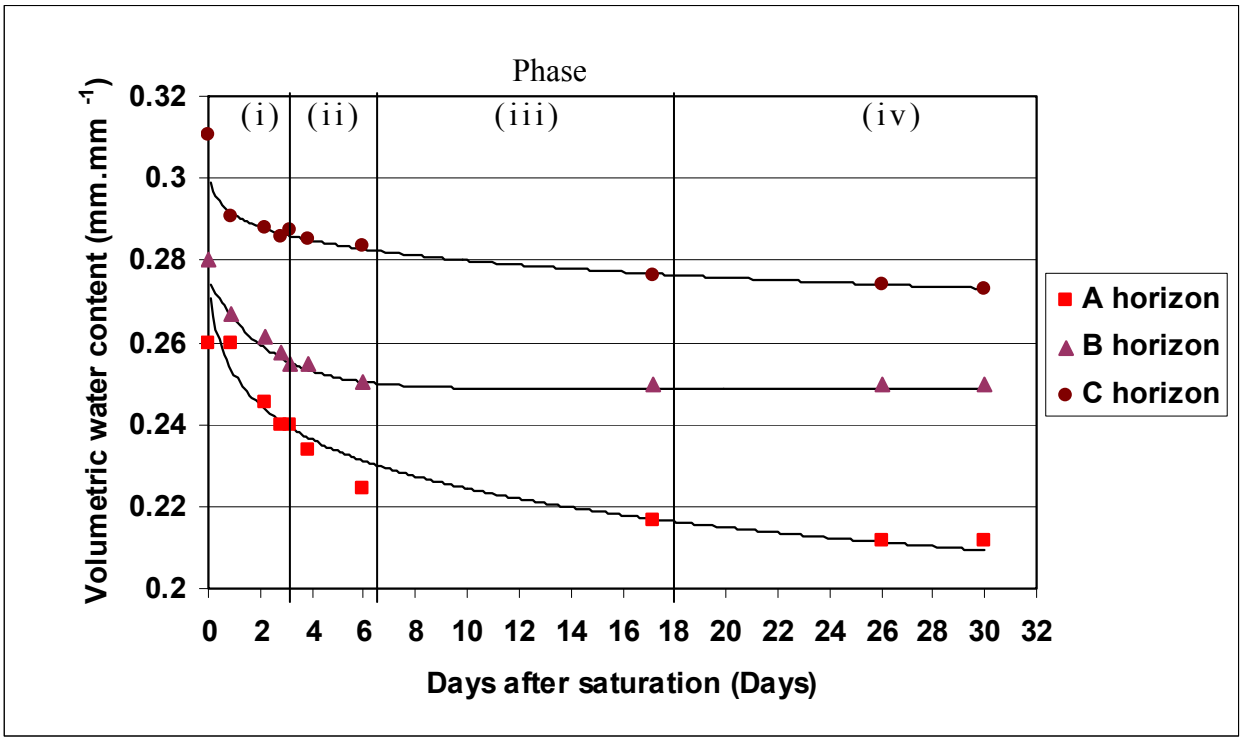

Figure 4.2 Volumetric wetness-time relationship for the A, B and C horizon of the Bloemdal soil form.

Tukulu: The drainage period is also divided into four phases explained earlier, *viz.* 0-2 DAS (phase i), 2 – 6 DAS (phase ii), 6 – 16 DAS (phase iii) and 16 – 30 DAS (phase iv). The relative positions of the curves also reflect on the pedological features of the profile, *viz.* the A at the top, followed by the B and C horizons. This was expected, because of a structural and textural difference between the three horizons. The A horizon has a massive apedal structure; the B horizon has a weakly developed sub angular blocky structure, while the C horizon has a well developed prismatic structure. The silt + clay content of the A horizon is 16% while the silt + clay content of the B and C horizon is 30% and 41%, respectively (Table 4.1). In period (iv) the drained upper limit for the horizons are 0.21 mm mm^{-1} for the A horizon, 0.26 mm mm^{-1} for the B horizon and 0.29 mm $mm^{-1}$for the C horizon, while the FS at the start of phase (i) amounts to 0.25, 0.29 and 0.318 mm mm^{-1}, respectively. FS is considerably lower than that of the theoretical porosity (Table 4.1) as in the case of the Bloemdal.

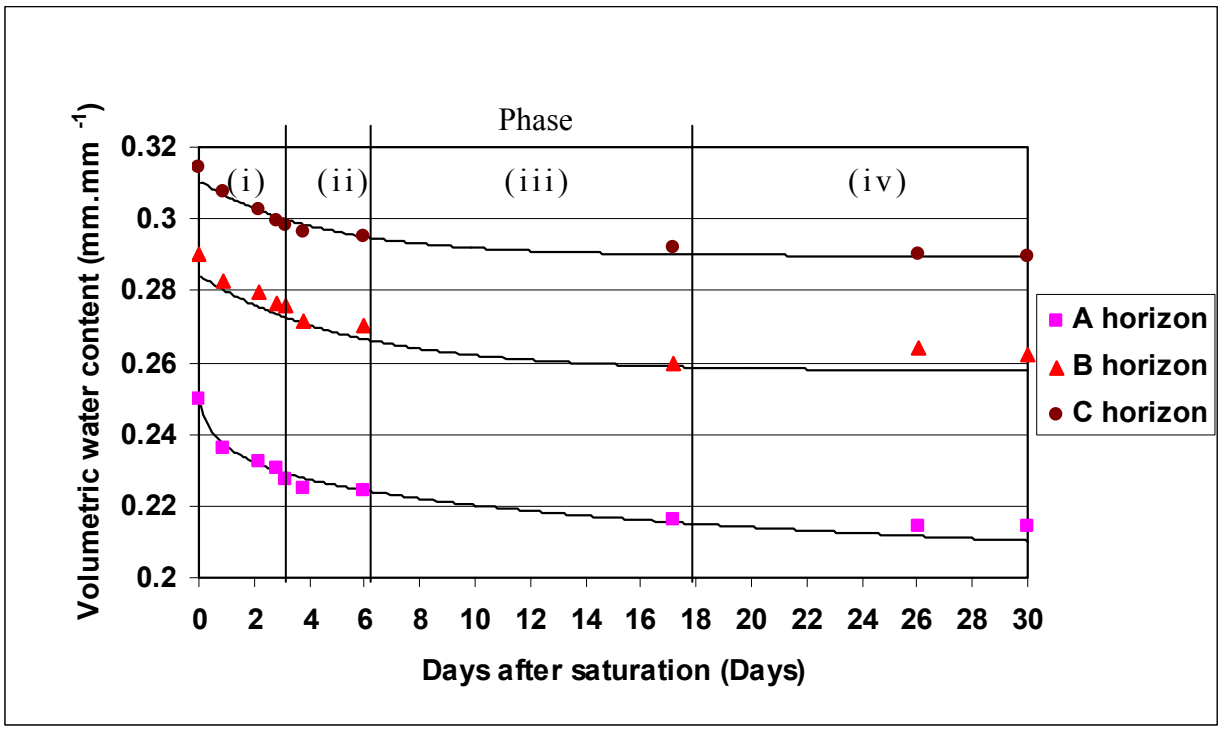

Figure 4.3 Volumetric wetness-time relationship for the A, B and C horizon of the Tukulu soil.

Sepane: Drainage curves of the Sepane's horizons revealed that the wettest regime is associated with the B horizon, which is unexpected when the textural properties (silt + clay = 32%) is considered. The silt + clay content of the C horizon (48%) is considerably higher than the B horizon. Thus, the difference in the water regimes can be attributed towards the pedocutanic structure of the B horizon versus the prismacutanic structure of the C horizon. The shape of the curves reveal further that the B horizon drains gradually slower over phase (i) and (ii), while the C horizon shows a sharp drop in phase (i). The A horizon released water rapidly in phase (i), where after it drained very slowly. In period (iv) the drained upper limit for the horizons are 0.23mm mm^{-1} for the A horizon, 0.26 mm mm^{-1} for the B horizon and 0.25 mm $mm^{-1}$for the C horizon. Again the FS of the horizons are considerably lower than the theoretically calculated total porosity listed in Table 4.1.

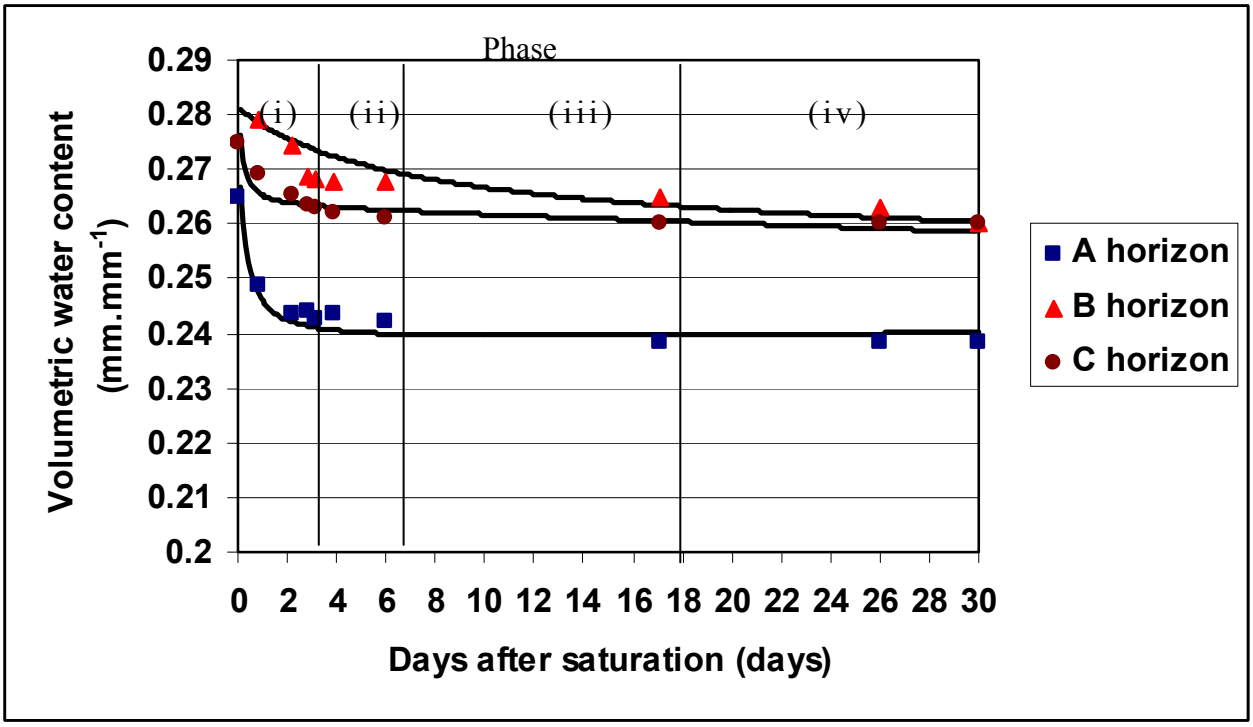

Figure 4.4 Volumetric wetness-time relationship for the A, B and C horizon of the Sepane soil.

4.3.2 Matric suction – time relationships

According to the results only the response curves of a few matric suction response curves were reliable. The rest of the measurements were found to be inaccurate as the watermarks used is sensitive for temperature differences, contact with the soil and only gives accurate readings in the region between 10 kPa and 150 kPa (Vienna, 2008).

In this regard the decision was made rather to predict the matric suction response from a local retention modal using the soil water content from the drainage curves discussed in section 4.2.4. The results are presented in Appendix W for the Bloemdal, Tukulu and Sepane soils and their values were used to calculate the hydraulic head in the next section.

4.3.3 Hydraulic head – depth relationships

The hydraulic head profile curves of the 30 cm, 60 cm and 90 cm depth intervals for the Bloemdal, Tukulu and Sepane soils are presented in Figures 4.5 – 4.7.

Bloemdal: Investigating the hydraulic head profile of the Bloemdal soil revealed water movement or drainage from the A to the C. The only exception was at 30 DAS where there was a negative gradient over 30 to 60 cm depth profiles. In this case it seems if the top soil dried out to such an extent that water started to move upwards from the wetter B to the A.

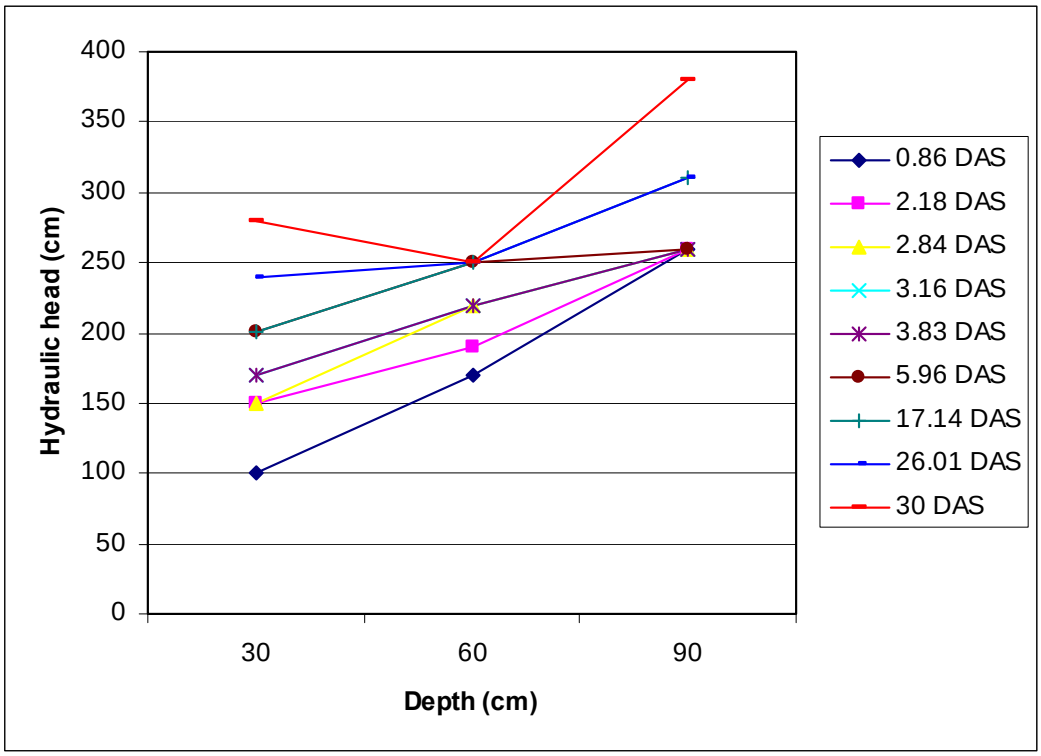

Figure 4.5 Hydraulic head profile at 30 cm, 60 cm and 90 m depths of the Bloemdal over the measuring period in days after saturation (DAS).

Tukulu: The hydraulic head profiles of the Tukulu shows a positive gradient and hence downward flow from the A horizon to the B horizon for the 30 day drainage period. However, the graph also shows a negative slope (upward movement from the C to the B), which do not reflect on the continuous loss of water observed in the drainage curves of the B and C horizon of Figure 4.3. From this it was deducted that the retention model was not able to predict the matrix potential head accurately in the C horizon. This is probably because the model only uses silt + clay content as input and does not concern soil structure which seems to be very important in layers or pseudo duplex soils such as the Tukulu and Sepane soils.

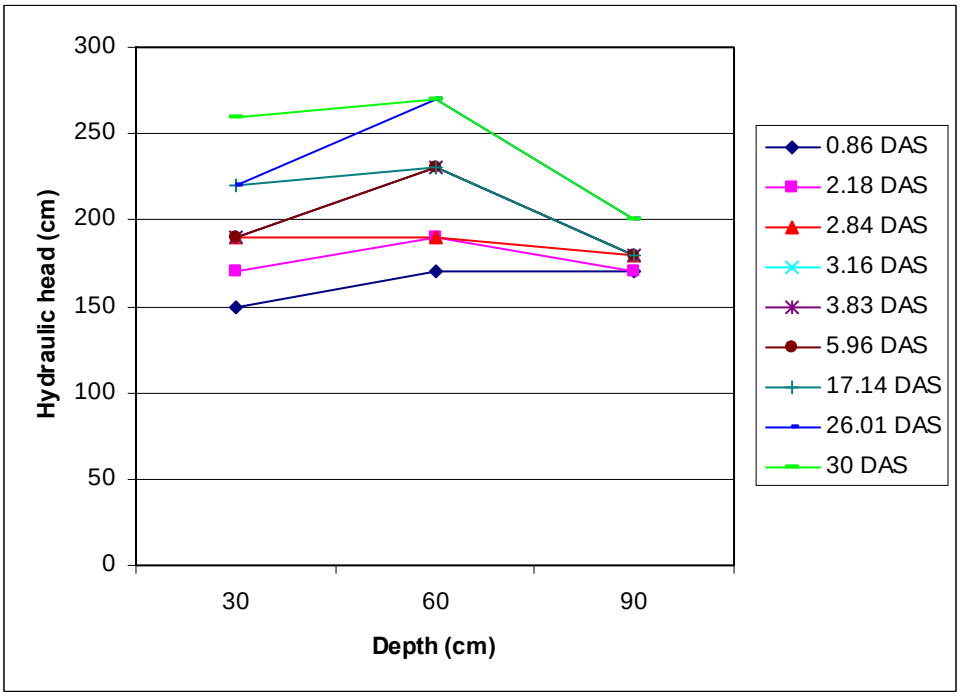

Figure 4.6 Hydraulic head profile at 30 cm, 60 cm and 90 m depths of the Tukulu over the measuring period in days after saturation (DAS).

Sepane: As in the case of the Tukulu, the hydraulic head profile shows that there is a positive slope from the A to the B horizon, followed by a negative slope from the B to the C. Upward movement from the C to the B could probably happens near DUL, but is highly unlikely, because both the horizons shows a loss (although small) of water in all the phases in Figure 4.4. Again the apparent upward flux in Figure 4.7 is probably the result of to low matrix potential suction at the C horizon.

Investigating the hydraulic head profile of the Sepane it is clear that there is a positive gradient from the 30 cm depth increment to the 60 cm depth increment for the 30 day drainage period. Thus there is positive gradient of water flow from the A horizon to the B horizon. There is a negative gradient from the 60 cm depth increment to the 90 cm depth increment indicating that the Pedocutanic B horizon and the prismatic underlying horizon with its strong structure and high clay content cause water to build up on top of the horizons. The water will then move back to a layer (A horizon) with a lower retention causing a negative gradient.

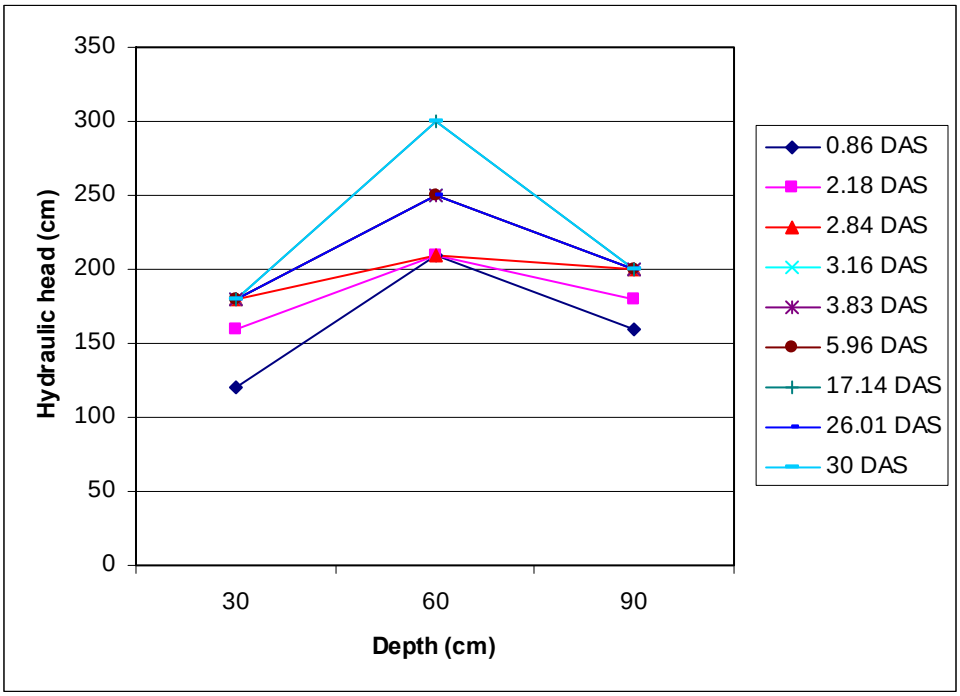

Figure 4.7 Hydraulic head profile at 30 cm, 60 cm and 90 m depths of the Sepane over the measuring period in days after saturation (DAS).

4.3.4 Hydraulic conductivity

The hydraulic conductivity – soil water content relationship curves for the Bloemdal, Tukulu and Sepane soils are presented in Figures 4.8 – 4.10, respectively. A summary of the hydraulic conductivity and related mean volumetric water content for the A, B and C horizon of the soils are presented in Table 4.4.

Table 4.4 Summary of the hydraulic conductivity and related mean volumetric water content for the soils

Horizon									
	A			B			C		
Soil form	**DAS**	**K (cm day^{-1})**	**Mean WC**	**DAS**	**K (cm.day^{-1})**	**Mean WC**	**DAS**	**K (cm.day^{-1})**	**Mean WC**
Bloemdal	**0.86**	0.26	0.27	**0.86**	0.39	0.27	**0.86**	0.31	0.29
	2.18	0.09	0.25	**2.18**	0.22	0.26	**2.18**	0.14	0.29
	2.84	0.03	0.24	**2.84**	0.08	0.26	**2.84**	0.16	0.29
	3.16	0.04	0.24	**3.16**	0.09	0.26	**3.16**	0.14	0.29
	3.83	0.03	0.24	**3.83**	0.08	0.25	**3.83**	0.12	0.29
	5.96	0.02	0.23	**5.96**	0.05	0.25	**5.96**	0.33	0.29
	17.14	0.01	0.22	**17.14**	0.01	0.25	**17.14**	0.02	0.28
	26.01	0.03	0.21	**26.01**	0.03	0.25	**26.01**	0.01	0.27
	30.00	0.01	0.21	**30.00**	0.01	0.25	**30.00**	0.01	0.27
	DAS	**K (cm day^{-1})**	**Mean WC**	**DAS**	**K (cm.day^{-1})**	**Mean WC**	**DAS**	**K (cm.day^{-1})**	**Mean WC**
Tukulu	**0.86**	0.68	0.25	**0.86**	0.90	0.28	**0.86**	0.731	0.31
	2.18	0.10	0.23	**2.18**	0.27	0.28	**2.18**	0.283	0.30
	2.84	0.00	0.23	**2.84**	0.00	0.27	**2.84**	0.215	0.30
	3.16	0.03	0.23	**3.16**	0.09	0.27	**3.16**	0.192	0.30
	3.83	0.02	0.23	**3.83**	0.08	0.27	**3.83**	0.172	0.30
	5.96	0.02	0.23	**5.96**	0.06	0.27	**5.96**	0.130	0.30
	17.14	0.04	0.22	**17.14**	0.10	0.26	**17.14**	0.046	0.29
	26.01	0.02	0.21	**26.01**	0.01	0.26	**26.01**	0.011	0.29
	30.00	0.01	0.21	**30.00**	0.02	0.26	**30.00**	0.001	0.29
	DAS	**K (cm day^{-1})**	**Mean WC**	**DAS**	**K (cm.day^{-1})**	**Mean WC**	**DAS**	**K (cm day^{-1})**	**Mean WC**
Sepane	**0.86**	0.145	0.26	**0.86**	0.22	0.28	**0.86**	1.488	0.28
	2.18	0.009	0.25	**2.18**	0.08	0.28	**2.18**	0.166	0.26
	2.84	0.003	0.25	**2.84**	0.08	0.27	**2.84**	0.092	0.26
	3.16	0.005	0.24	**3.16**	0.03	0.27	**3.16**	0.077	0.26
	3.83	0.004	0.24	**3.83**	0.02	0.27	**3.83**	0.067	0.26
	5.96	0.002	0.24	**5.96**	0.02	0.27	**5.96**	0.050	0.26
	17.14	0.003	0.24	**17.14**	0.001	0.27	**17.14**	0.023	0.26
	26.01	0.003	0.24	**26.01**	0.001	0.26	**26.01**	0.012	0.26
	30.00	0.001	0.24	**30.00**	0.001	0.26	**30.00**	0.010	0.26

Bloemdal: From the relative shape and position of the curves it is clear that each horizon has its own unique K - Θ relationship within the boundaries of the drained upper limit (DUL) and field saturation (FS). The C horizon takes up the furthest right position on the graph which is expected due to the high clay content and prismatic structure of C horizon (39%). This horizon contains smectic clays that can be presumed to swell and shrink. This restricts the soil water conductivity as indicated in the exponential decrease in K from FS 0.31 cm day^{-1} at FS to 0.01 cm $.day^{-1}$ at DUL. The wet water regime between FS (0.29 mm mm^{-1}) and DUL (0.27 mm mm^{-1}) reflect on the signs of wetness as indicated by the abundance of red, black, yellow and grey mottles in this horizon (Table 4.2).

Comparing the K - Θ values of the red apedal B horizon with that of the C shows that the C horizon probably slows down the hydraulic conductivity of the B horizon, due its lower clay content (25%) and massive apedal structure. Another factor that contributed to the low K values of the B horizon is its bulk density of 1728 kg m^{-3}. The K values for the B horizon ranged from 0.39 cm day^{-1} at FS to 0.03 cm day^{-1} at DUL, while the water regime ranged from 0.27 mm mm^{-1} at FS to 0.25 mm mm^{-1} at DUL.

The hydraulic conductivity of the A horizon is unexpectedly low when the texture (silt + clay = 17%), bulk density (1342 kg m^{-3}) and massive apedal structure is considered. This can be attributed towards the influence of the low hydraulic conductivity of the underlying layers. The K values for the A horizon ranged from 0.26 cm day^{-1} at FS to 0.01 cm day^{-1} at DUL, while the water regime ranged from 0.27 mm mm^{-1} at FS to 0.21 mm mm^{-1} at DUL.

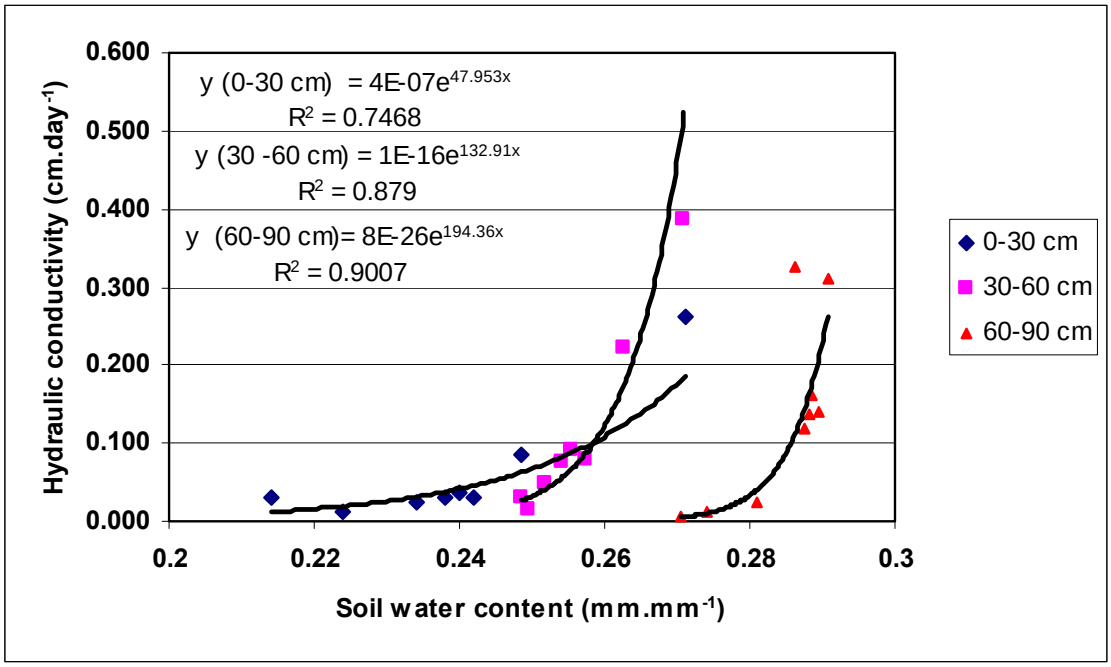

Figure 4.8 Hydraulic conductivity curves for the Bloemdal soil.

Tukulu: Because of the unreliable matric potential head it was not possible to calculate K ($K = q/(\Delta H/\Delta z)$). The water potential model used was not able to accurately predict matric potential from the measured water content, and it was assumed that K = flux (q) for the C horizon.

The relative shape and position of the curves shows that each horizon has it own unique K - Θ relationship which reflects on the different textural and structural properties. The C horizon takes up the furthest right position on the wetness scale. This is expected due to the high clay content (30%) of the prismatic structure. It is clear that the K - Θ relationship of the neocutanic B horizon is also partially controlled by the slow permeability of the underlying C horizon as in the case of the Bloemdal. The C horizon contains smectic clays that swell under wet cycles and shrinks under dry cycles. The weakly developed medium sub angular blocky structure of the B horizon drained at a rate of 0.9 cm day^{-1} at FS. As the pores empty K decreases exponentially and reaches a value of 0.02 cm day^{-1} at DUL.

The hydraulic conductivity of the A horizon is once again unexpectedly low when the texture (silt + clay = 16%), bulk density (1376 kg m^{-3}) and

massive apedal structure is considered. This can be attributed towards the influence of the low hydraulic conductivity of the underlying layers. The K values for the A horizon ranged from 0.68 cm day^{-1} at FS to 0.01 cm day^{-1} at DUL, while the water regime ranged from 0.25 mm mm^{-1} at FS to 0.21 mm mm^{-1} at DUL.

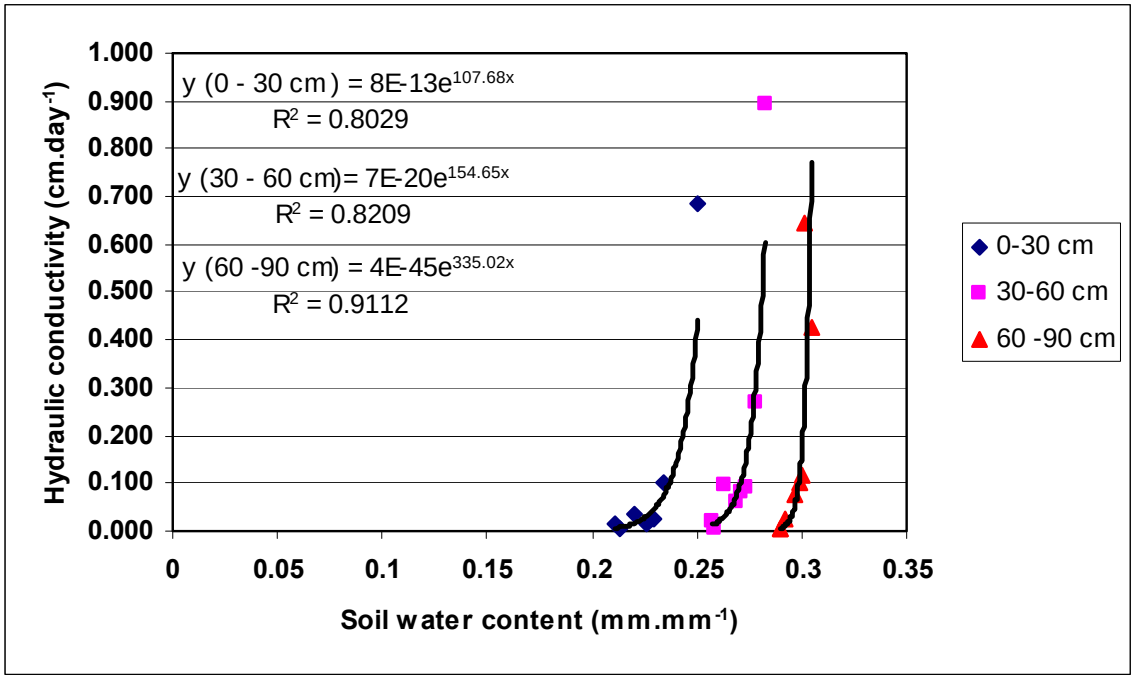

Figure 4.9 Hydraulic conductivity curves for the Tukulu soil.

Sepane: The heterogeneity of the horizons is reflected in the relative shape and position of the K - Θ curves. On the furthest right of the wetness scale is the Pedocutanic B horizon with a well developed medium size blocky structure, followed by the well developed, medium size prismatic structure of the C horizon and the apedal structure of the A horizon on the left. The internal drainage rate is probably controlled by the C horizons at FS, where after it shifts to the B horizon. The water regime of the B horizon varied between FS (0.28 mm mm^{-1}) and DUL (0.26 mm mm^{-1}) reflects on the governing of the B horizon hydraulic conductivity by the C horizon. Examining the shape of the curves it can be deducted that the C horizon has larger pores in the higher wetness range between FS and DUL. Comparing the shape of the A and B horizon it shows that the slow hydraulic conductivity of the B horizon influenced the release of water from the A horizon to the B horizon. The K values for the A horizon ranged from 0.15 cm day^{-1} at FS to 0.001 cm day^{-1} at DUL,

while the water regime ranged from 0.26 mm mm^{-1} at FS to 0.24 mm mm^{-1} at DUL.

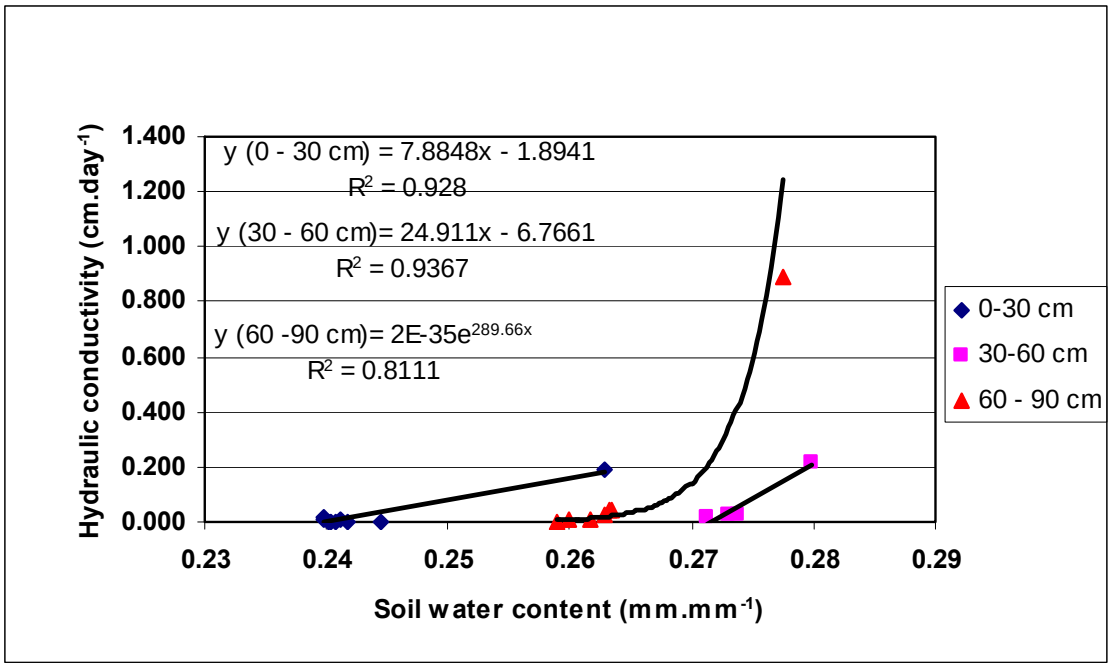

Figure 4.10 Hydraulic conductivity curves for the Sepane soil.

4.4 Conclusion

The general objective of this study was to characterize the hydraulic properties of the Bloemdal, Tukulu and Sepane soils using the internal drainage method.

The volumetric wetness – time relationships of the Bloemdal and Tukulu soil forms were mainly influenced by the compacted and strong prismatic structure of the C horizon. The Sepane on the other hand was mainly influenced by the Pedocutanic B horizon with a moderate clay content, sub angular blocky structure and high bulk density. It was found that the structure of the B horizon was the main constituent influencing the hydraulic head – depth relationship of the Sepane soil. From the K -Θ relationships the same trend was found and was concluded that the hydraulic conductivity of the Bloemdal and Tukulu profiles are mainly influenced by the non diagnostic C horizon, while the hydraulic conductivity of the Sepane profile is mainly influenced by the Pedocutanic B horizon.

CHAPTER 5

Conclusions and Recommendations

The soil properties of Paradys are perceived to vary moderately compared to other areas of South Africa. A greater variation in soil properties between these soil forms than within soil map units implies that soil maps can be used with confidence to predict the behaviour of the land for specific land uses. The soils of the Bloemdal, Tukulu and Sepane forms responded differently to biological (root development) and hydrological (drainage) treatments. The inter relationships between soil properties aid in the simplifying, compilation and interpretation of soil maps.

The systematic variation in Si + Cl between the soil forms implies that it is the main factor controlling the behaviour of these soil forms. The B horizons of the soils dominated biological activity but the C horizons dominated hydrological flow in the apedal Bloemdal and Tukulu soil only. The Pedocutanic B controlled the hydrology of the Sepane. The inability of the neocutanic B to host maize roots favourably confirms field experience. This emphasises the importance of proper classification of soils. The role of the prismatic layer on the hydrology of the apedal soils consider revision as this prismatic layer totally influence the suitability of these soils for certain land use purposes. The inclusion of this layer in naming the soils on series or family levels is of critical importance. Further studies also have to be done on spatial variation of soil properties in and between map unit and on the hydrology of South Africa soil forms.

REFERENCES

AMATO, M and RITCHIE, J.T., 2002. Spatial Distribution of roots and Water Uptake of Maize (Zea Mays L.) as Affected by soil Structure. Journal of Crop Science. 42: 773 – 780

BARTHES, B., ALBRECHT, A., ASSELINE, J., DE NONI, G., ROOSE, E., 1999. Relationship between soil erodibility and topsoil aggregate stability or carbon content ina cultivated mediterranean highland (Aveyron, France). Commun. Soil. Sci. Pant. Anal., 30 (13 and 14), 1929-1938.

BEARE, M. H., HENDRIX, P.F., and COLEMAN, D.C., 1994. Water – stable aggregates and organic matter fractions in conventional and no tillage soils. Soil Sci. Soc. Am. J. 58: 777 – 786.

BENNET, E.M., CARPENTER, S.R. & CLAYTON, M.K., 2004. Soil phosphorus variability: Scale-dependence in an urbanizing agricultural landscape. Landscape Ecology. 20: 389-400.

BENNIE, A.T.P. and BURGER, R. DU T., 1979. Grondverdigting onder besproeiing op die Vaalhartsbesproeiingskema . Vol II. Departement Grondkunde verslag nr. 79/2 U.O.V.S Bloemfontein.

BENNIE, A.T.P., COETZEE, M.J., VAN ANTWERPEN, R., VAN RENSBURG, L.D. and BURGER, R. DU T., 1988. ‘n Waterbalansmodel vir besproeiing gebaseer op profielwatervoorsieningstempo en gewaswaterbehoeftes. Waternavorsingskommissieverslag no. 144/1/88.

BENNIE, A.T.P. and BURGER, R. DU T., 1988. Penetration resistance of fine snady apedal soils as affected by relative bulk density, water content and texture. S. Afr. J. Plant Soil 5.

BENNIE, A.T.P., 1996. Sound water management concepts and their application at farm level. In: Proceedings of the Southern African irrigation symposium, Durban, WRC, Pretoria.

BOIX-FAYOS, C., CALVOS – CASES, A., and IMESON, A.C., 2001. Influence of soil properties on the aggregation of some Mediterranean soils and the use of aggregate size and stability as land degradation indicators. Catena 44: 117 – 125.

BOTHA, F.J.P, BENNIE, A.T.P. and BURGER, R. DU T., 1983. Water use efficiency of irrigated crops as influenced by varying cultivation practices and root configurations. Report to the W.R.C Pretoria.

BOTHA,J.J., 2007. Evaluation of maize and sunflower production in semi arid area using in field rainwater harvesting.

BOTHA, J.J. and VAN RENSBURG, L.D., 2004. Water harvesting to promote food security and employment. Land Care report to the National Department of Agriculture, South Africa

BRONICK, C.J., and LAL, R., 2005. Soil Structure and management: A review. Geoderma 124: 3 -22.

BRULAND, G.L. and RICHARDSON, C.J., 2003. Spatial variability of soil properties in created, restored, and paired natural wetlands. Soil. Sci. Soc. Am. J. 69 : 273-284.

BURT, T.P. and PARK, S.J., 1999. Soil variability revisited. Soil Fert. 56 529- 562.

CALLOT, G., CHAMAYOU, H., MAERTENS, C. and SALSAC, L., 1982. A better understanding of soil – roots interactions. Effects on mineral nutrition. Soil Sci. Soc. Am. J.

CAMBARDELLA, C.A. and KARLEN, D.L., 1999. Spatial analysis of fertility parameters. Precis. Agric. 1: 5-14.

CAMABRDELLA, C.A., MOORMAN, T.B., NOVAK, J.M., PARKIN, T.B., KALEN, D.L., TURCO, R.F. and KONOPKA, A.E., 1994. Field scale variability of soil properties in central Iowa soils. Soil Sci. Soc. Am. J. 58: 1501 – 1511.

CHENU, C., LE BISSONNAIS, Y., and ARROUYAS, D., 2000. Organic matter influence on clay wetability and soil aggregate stability. Soil Sci. Soc. Am J. 64 : 1479 – 1486.

CODY, R.P. and SMITH, J.K., 1997. Applied Statistics and the SAS programming language. Prentice-hall, Englewood cliffs, NJ.

COX, M.S., GERARD, P.D., WARDLAW, M.C. and ABSHIRE, M.J., 2003. Variability of selected soil properties and their relationship with soybean yield. Soil. Sci. Soc. Am. J. 67: 1296 – 1302.

DALAL, R.C., and BRIDGE, B.J., 1996. Aggregation and organic matter storage in sub – humid and semi arid soils. *In*: Carter, M.R., Stewart, B.A. (Eds.), Structure and Organic Matter Storage in Agricultural soils. CRC Press, Boca Raton, FL, pp: 263 – 307.

DE CLERQ, W.P., FEY, M.V., MOOLMAN, J.H., WESSELS, W.P.J., EIGENHUIS, B. and HOFFMAN, J.E., 2001. Experimental irrigation of vineyards with saline water.

DERCON, G., DECKERS, J., GOVERS, G., POESEN, J., SANCHEZ,H., VANEGAS, R., RAMIREZ, M. and LOAIZA, G., 2003. Spatial variability in soil properties on slow-forming terraces in the Andes region of Ecuador. Soil and Tillage Research, 72 : 31-41.

DEXTER, A.R., 1978. A stochastic model for the growth of roots in tilled soil. J. Soil Sci. 29, 102 – 116.

DIMOYIANNIS, D.G., TSADILAS, C.D., and VALMIS, S., 1998. Factors affecting aggregate instability of Greek agricultural soils. Commun. Soil Sci. Plant Anal. 29 : 1239 – 1251.

DINEL, H., RIGHI, D., HARDY, M., and JAMBU, P., 1997. Neutral lipids and structural stability of physical degraded soils. Agrochimica 41 : 97 – 108.

DINNES, D.L., LESCH, S.M., SHOUSE, P.J., SOPPE, R and AYARS, J.E., 2003. Identifying soil properties that influence cotton yield using soil sampling directed by apparent soil electrical conductivity. Agron. J. 95: 352-364.

GOOVAERTS, P., CHIANG, C.N., 1993. Temporal persistane of spatial patterns for mineralizable nitrogen and selected soil properties. Soil. Sci. Soc. Am J. 57: 372 – 381.

GUPTA, R.K., MOSTAGHIMI, S., MCCLELLAN, P.W., BIRCH, J.B. and BRANN, D.E., 1997. Modelling spatial variability of soil chemical parameters for site-specific farming using stochastic methods. Water, air, and soil pollution. 110: 17-34.

HENSLEY, M., BOTHA, JJ., ANDERSON, J.J., VAN STADEN, P.P and DU TOIT, A., 2000. Optimising rainfall use efficiency for developing farmers with limited access to irrigation water. Water Research Commission report 878/1/00, Pretoria, South Africa

HILLEL, D.H., 2004. Environmental soil physics. Academic Press, New York, USA

HINTZE, J., 2000. NCSS help system: Multiple regressions. Kaysville, Utah

KEMPER,W.D and ROSENAU, R.C, 1986. Aggregate stability and size distribution. American Society of Agronomy – Soil science Society of America: Methods of soil analysis, Part 1. Physical and Mineralogical methods.425 – 439.

KLEPPER, B., 1990: Irrigation of Agricultural Crops-Agronomy Monograph no 30. Root Growth and Water Uptake 281 -322.

LE – BISSONAIS, Y., 1996. Aggregate stability and assessment of soil crustability and erodibility: I. Theory and methodology. Eur. J. Soil. Sci. 47: 425 – 437.

LE ROUX, P.A.L., 1996. Die aard, verspreiding en genese van geselekteerde redoksmorfe gronde in Suid Afrika. PHD Thesis. Departement Grondkunde. Fakulteit Landbou aan die Universiteit van die Oranje Vrystaat, Bloemfontein.

LOGSDON, S.D., RENEAU. R.B. Jnr and PARKER, J.C., 1987 Corn seedling root growth as influenced by soil physical properties. Journal of Agronomy. 79: 221 – 224.

LONGLEY, P.A., GOODCHILD, M.F. and MAGUIRE, D.J., 2004. Geographical Information Systems and Science.

LUKAS, E., 1992 WISH ®. Department of Soil Water Studies, Faculty of Natural and Agricultural Science, University of the Free State, Bloemfontein.

MARK, D.M., CSILLAG, F., 1989. The nature of boundaries on 'area-class' maps. Cartographica 26, 65-78.

MIAO, Y., MULLA, D.J. and ROBER, P.C., 2006. Spatial variability of soil properties, corn quality and yield in two Illinois, USA fields: implications for precision corn management. Precision Agric. 7, 5-20.

MILLER, W.P., and BAHARUDDIN, M.K., 1986. Relationship of soil dipersibility to infiltration and erosion of southeastern soils. Soil Sci. 142: 235 – 240.

MVSA FERTILIZER GUIDELINES, 2007. Po Box 75510, Lynwoodrif, 0040, South Africa.

OADES, J.M., and WATERS, A.G. 1991. Aggregate hierarchy in soils. Aust. J Soil Res. 29: 815 – 828.

PETRONE, R. M., PRICE, J. S., CAREY, S. K. and WADDINGTON, J .M., 2003. Statistical characterization of the variability of soil moisture in a cutover peatland. Report to Wiley interscience. Department of Geography and cold regions research centre, Wilfrig Laurier university, 75 University Ave west, Waterloo, Ontario, Canada

PIONKE, H.B., GBUREK, W.J., SHARPLEY, A.N. and ZOLLWEG, J.A., 1997. Hydrologic and chemical controls on phosphorus loss from catchments. CAB international, New York.

PICCOLO, A.,PIETRAMELLARA, G., and MBAGWU, J.S.C., 1997. Use of humic substances as soil conditioners to increase aggregate stability. Geoderma 75 : 267 – 277.

RINGROSE-VOASE, A.J.,1991. Microporphology of soil structure: Description, quantification, application. Aus.Journ.Soil Res. 29: 777 – 813.

ROWSE, H.R. and PHILLIPS, D.A., 1974. Instrument for estimating total length of root in a sample. Journal of applied ecology 11: 309 – 314.

SAXTON, K.E. and RAWLS, W.J., 2006. Soil water characteristic estimates by texture and organic matter for hydrologic solutions. Soil Sci. Soc. Am. J. 70 : 1569 – 1578.

SCHOLES, R.J., DALAL, R. and SINGER, S., 1994. Soil physics and fertility: the effects of water, temperature and texture. Biological management of tropical soil fertility. 117-136.
SCHULTEN, H.R., and LEINWEBER, P., 2000. New insights into organic mineral particles: Composition, properties and models of molecular structure. Biol. Fertil. Soils. 30: 399 – 432.

SHAHANDEH, H., WRIGHT, A.L. and HONS, F.M., 2005. Spatial and temporal variation of soil nitrogen parameters related to soil texture and corn yield. Agronomy Journal. 97: 772 – 782.

SINGER, M.J., SOUTHARD, R.J., WARRINGTON, D.J., and JANITZKY, P., 1992. Stability of synthetic sand clay aggregates after wetting and drying cycles. Soil Sci. Soc. Am. J. 56: 1843 - 1848

SIX, J.K., PAUSTIAN, E.T., and COMBRINK, C. 2000a. Soil structure and organic matter: I. distribution of aggregate – size classes and aggregate – associated carbon. Soil Sci. Am. J. 64: 681 -689.

SNYMAN, K., 1987. The micromorphology of selected diagnostic horizons of the binomial system for soil classification in South Africa. M.Sc. Agric. Dissertation, University of Kwazulu – Natal, Pietermaritzburg.

SOANE, B.D., 1989. The role of organic matter in soil compactibility: A review of some practical aspects. Soil and Tillage Research, 16: 179 – 201.

SOBIERAJ, J.A., ELSENBEER, H. and CAMERON, G., 2003. Scale dependency in spatial patterns of saturated hydraulic conductivity. Department of Civil and Environmental engineering, University of Cincinnati, Cincinnati, OH 45221-0071, USA.

SOIL CLASSIFICATION WORK GROUP., Soil Classification a taxonomic system for South Africa. Department of agricultural development, Pretoria, 1991

STUTTER, M.I., DEEKS, L.K. and BILLET, M.F., 2002. Spatial variability in soil ion exchange chemistry in a granitic upland catchment. Soil. Sci. Soc. Am. J. 68 : 1304 – 1314.

STIRZAKER, R.J, PASSIOURA, J.B and WILMS,Y., 1996. Soil Structure and plant growth: Impact of bulk density and biopores. Journal of Plant and Soil 185: 151 – 162.

SUMMER, M.E., 1992. The electric double layer and clay dispersion. *In* M.E. Summer and B. A. Stewart (ed.) Soil crusting: Chemical and physical processes. Lewis Publ. Chelsea, MI.

TAYLOR, H.M., ROBERTSON, G.M. and PARKER, J.J., 1996. Soil strength- root penetration relations for medium – to coarse- textured soil materials. Journal of Soil Science. 108: 113 – 119.

THE NON-AFFILIATED SOIL ANALYSIS WORK COMMITTEE, 1990. Handbook of standard soil testing methods for advisory purposes. SSSSA, Pretoria

TISDALL, J.M. and OADES, J.M., 1982. Organic matter and water – stable aggregates in soil. J. Soil Sci. 33, 141 – 164.

VAN ANTWERPEN, R., 1988. Die evaluasie van verskillende empiriese modelle vir die voorspelling van wortelgroei: M.Sc. Agric. Verhandeling. U.O.V.S. Bloemfontein.

VANAPALLI, S.K.; FREDLUND, D.G. and PUFAHL, D.E., 1999. The influence of soil structure and stress history on the soil – water characteristics of a compacted till. Geotechnique 49: 143 – 159.

VAN RENSBURG, L.D., 1996. Interaksie tussen stikstof- en wateropname deur koring en mielies. Ph.D. Thesis. U.O.V.S. Bloemfontein.

VENTER, A, 2003. Comparing plant yield and composition with soil properties using classical and geostatisical techniques. S. Afr. J. Plant Soil. In Press. ARC- Institute for Soil, Climate and Water, Private bag X79, 001, Pretoria, South Africa.

VOORTMAN, R.L., BROUWER, J. and ALBERSEN, J.P., 2004. Characterization of spatial soil variability and its effect on Millet yield on Sudano- Sahelian coversands in SW Niger. Geoderma, 121 : 65- 82.

WHITELEY, G.M. and DEXTER, A.R., 1984. Displacement of soil aggregates by elongating roots emerging shoots of crop plants. J. Plant and Soil. 77: 131 – 140.

ZEHETNER, F. and MILLER, W.P., 2006. Soil variation along a climatic gradient in an Andean agro-ecosystem. Geoderma 137, 126 – 134.

ZHU, A.X., QI, F., HARROWER, M. and BURT, J.E., 2006. Fuzzy soil mapping based on prototype category theory. Department of geography, University of Wisconsin, 550 N. Park Street, Madison WI 53706, USA. Geoderma 136 : 774-787.

ZOTARELLI, L., ALVES, S., URQUIAGA, S., TORRES, E., DOS SANTOS, H. P., PAUSTAIN, K., BODDEY, R.M. and SIX, J., 2005. Soil Sci. Soc. Am. J. 69: 482 – 491.

APPENDICES

Appendix A Distribution of the clay content for the A horizon, B horizon and C horizon.

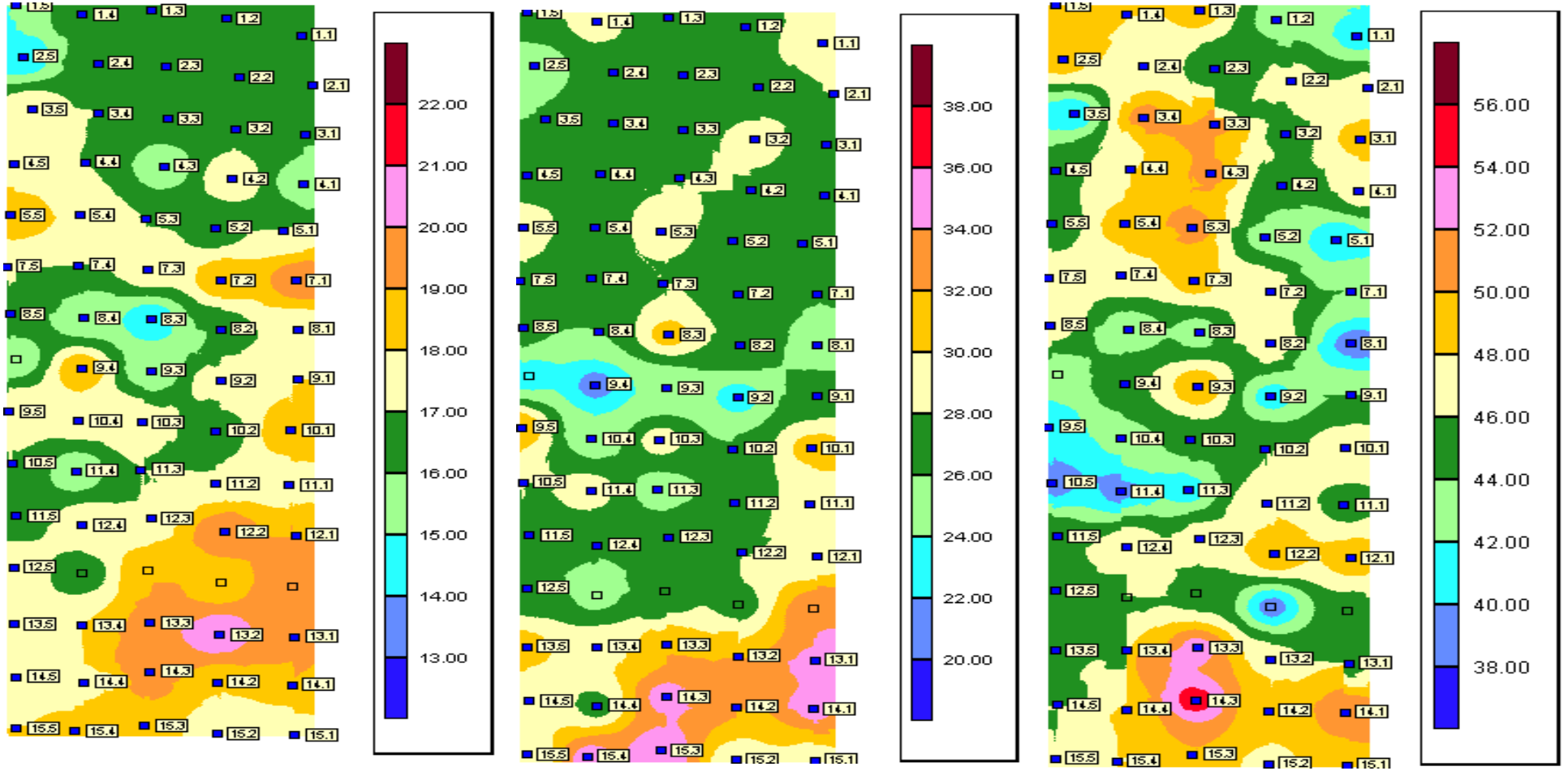

Appendix B Distribution of the pH_{water} for the A horizon, B horizon and C horizon.

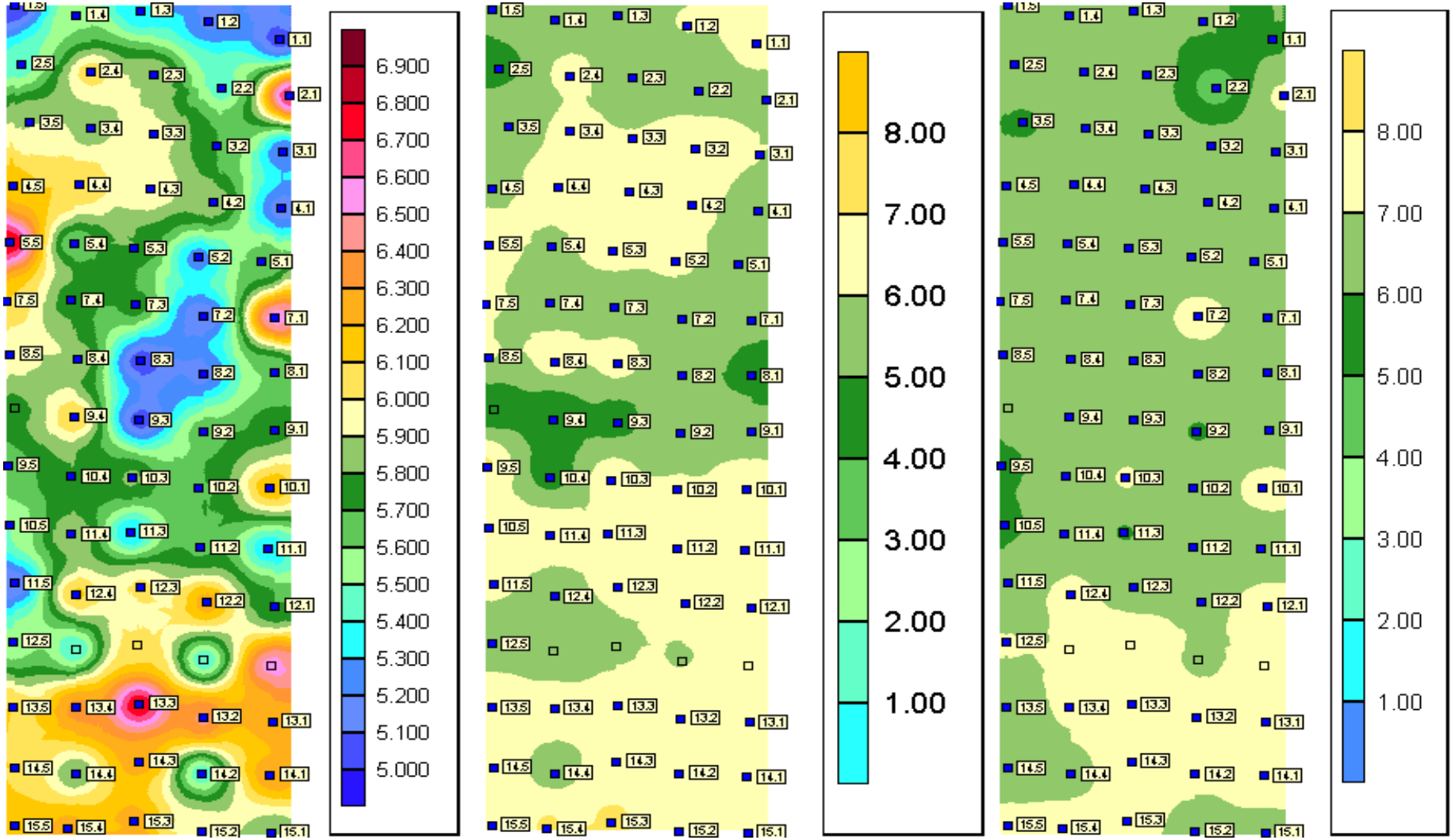

Appendix C Distribution of the pH_{KCl} for the A horizon, B horizon and C horizon.

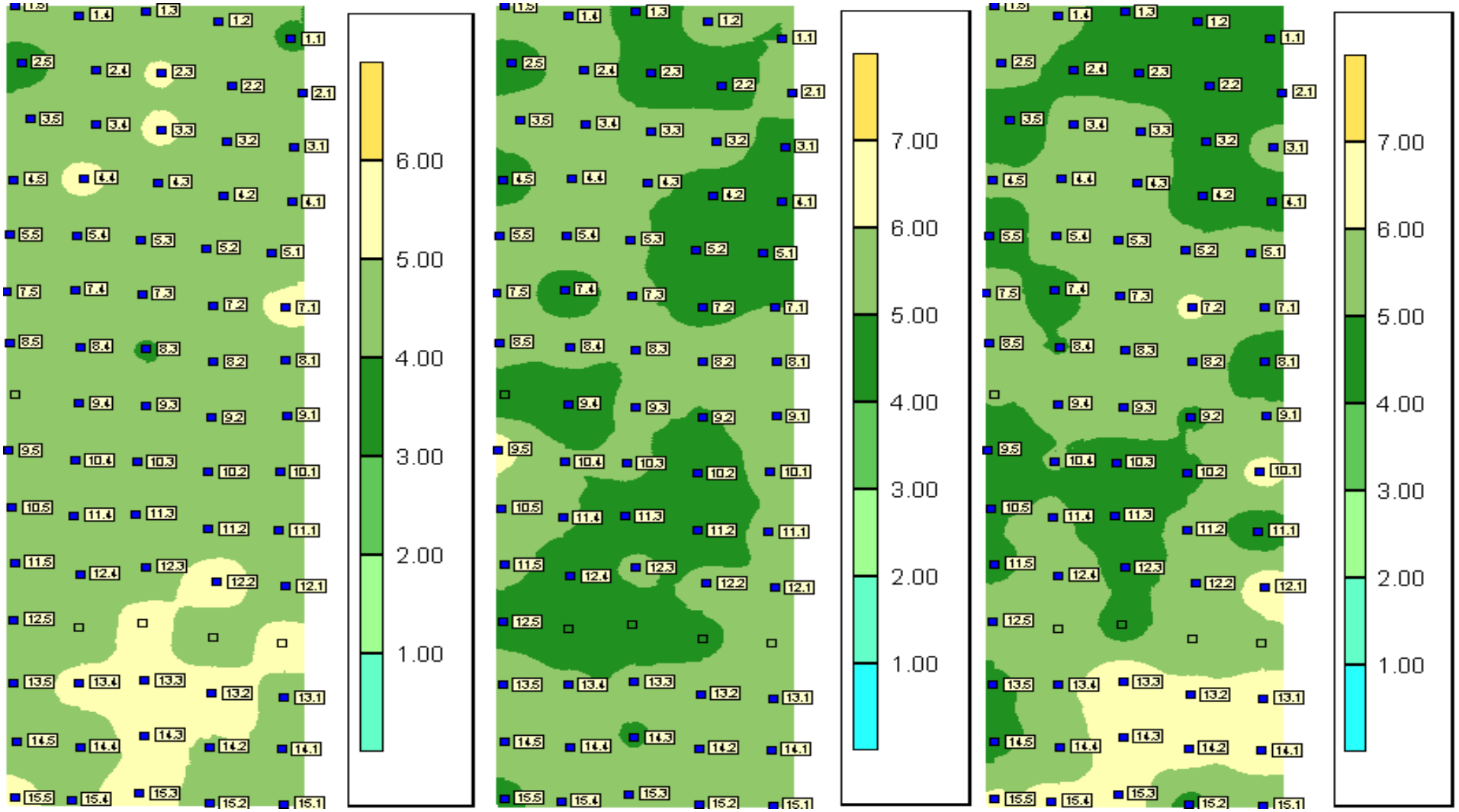

Appendix D Distribution of the Ca ($cmol_c kg^{-1}$) for the A horizon, B horizon and C horizon

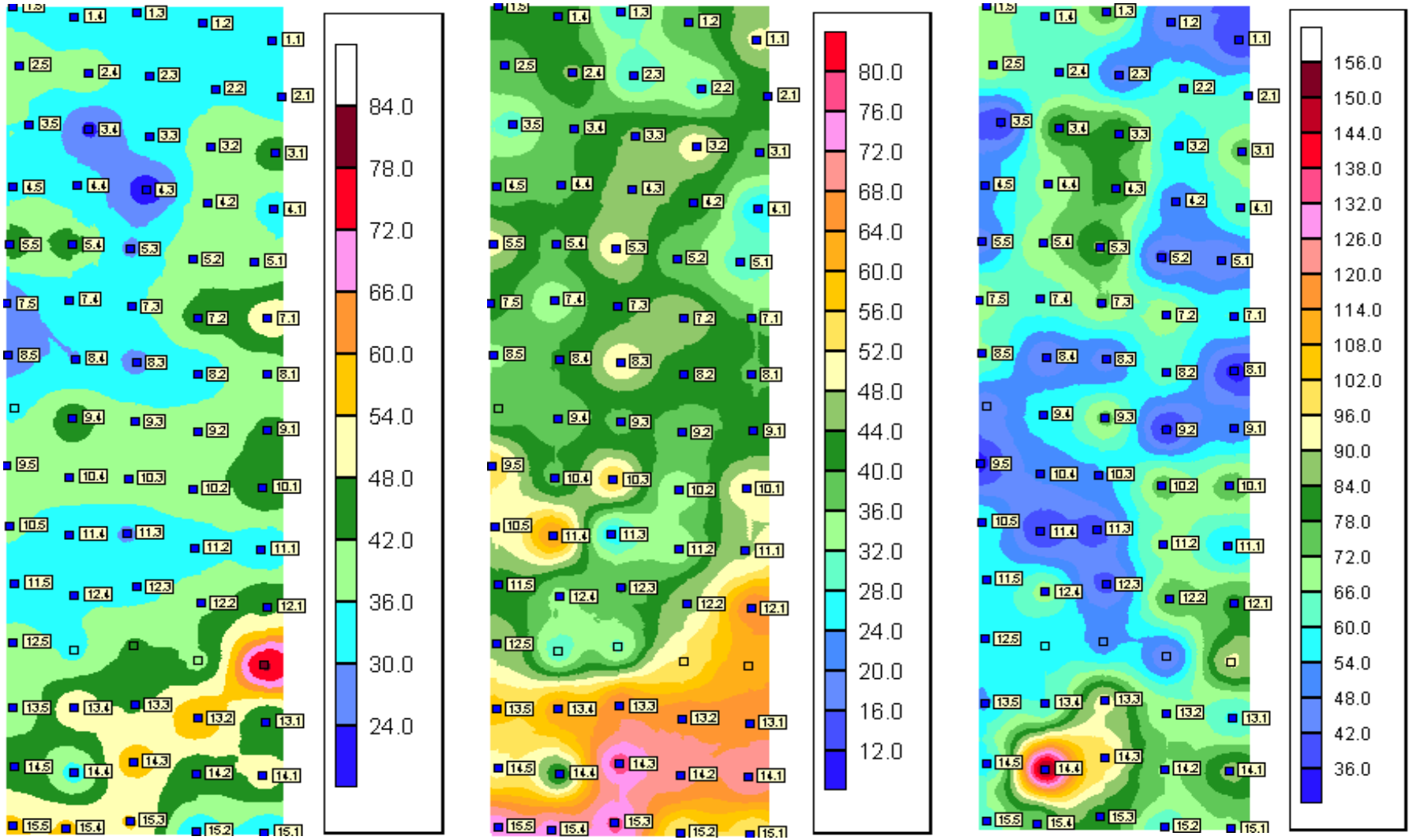

Appendix E Distribution of the K ($cmol_c kg^{-1}$) for the A horizon, B horizon and C horizon

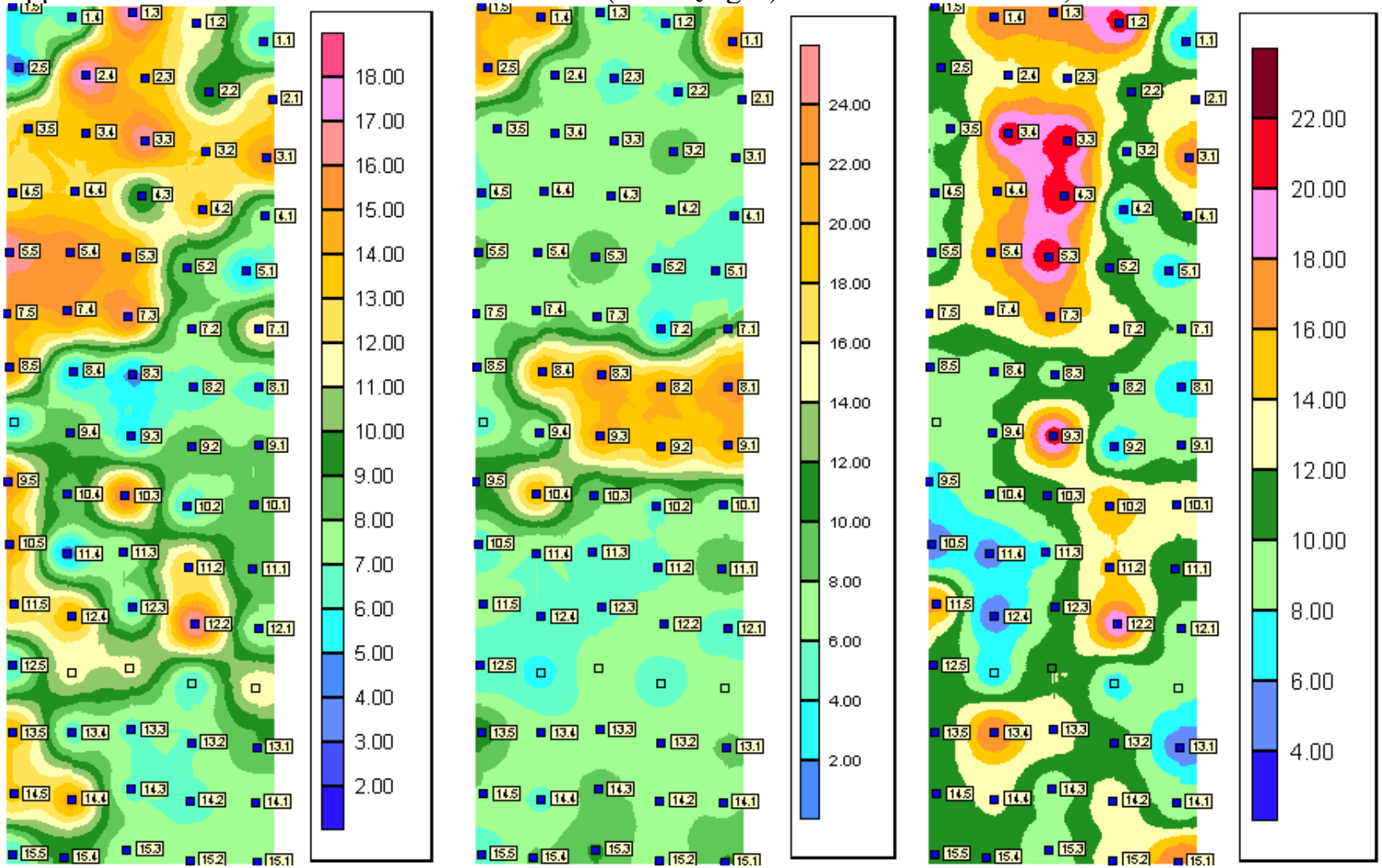

Appendix F Distribution of the Mg ($cmol_c kg^{-1}$) for the A horizon, B horizon and C horizon

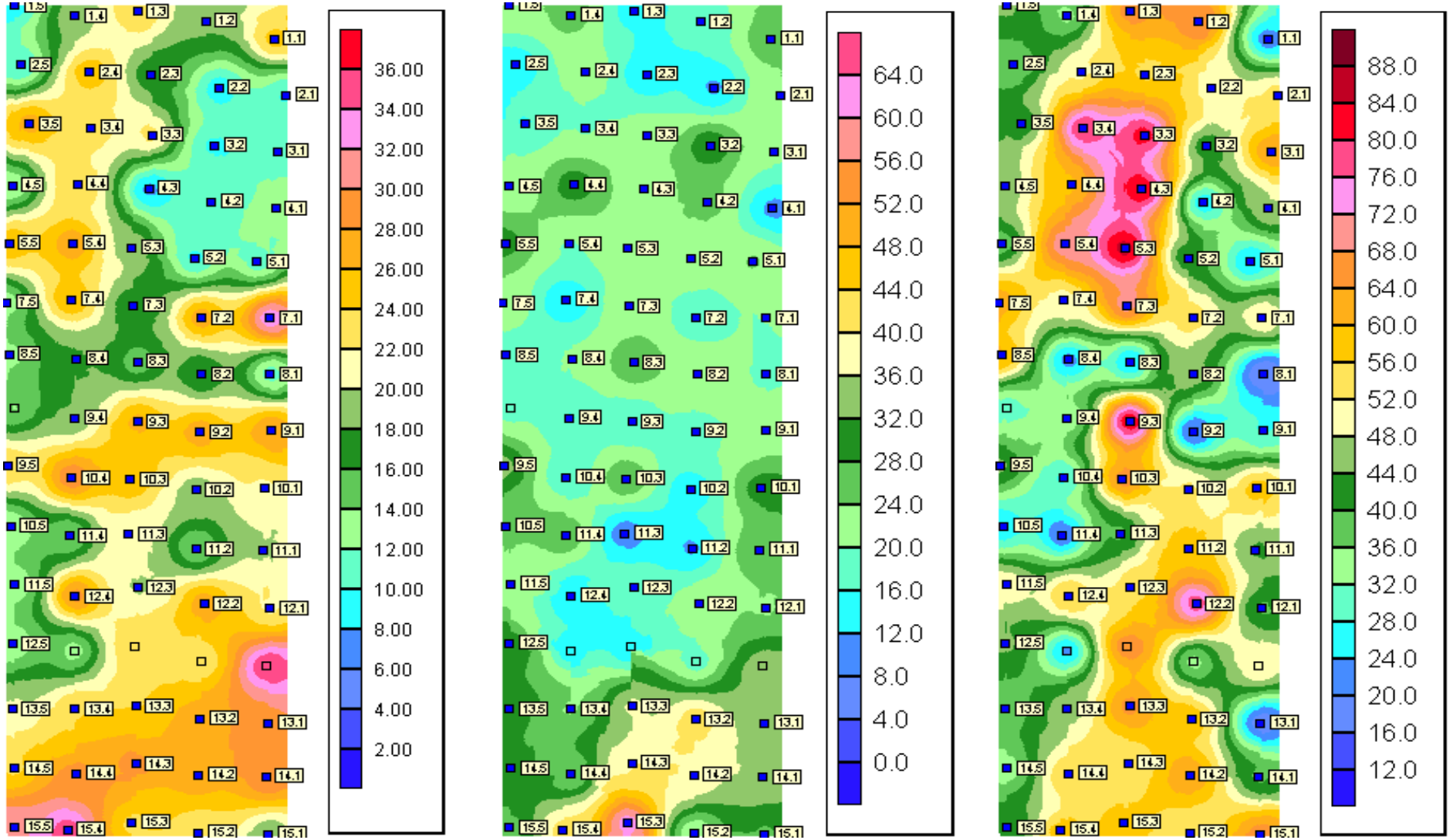

Appendix G Distribution of the Na ($cmol_c kg^{-1}$) for the A horizon, B horizon and C horizon

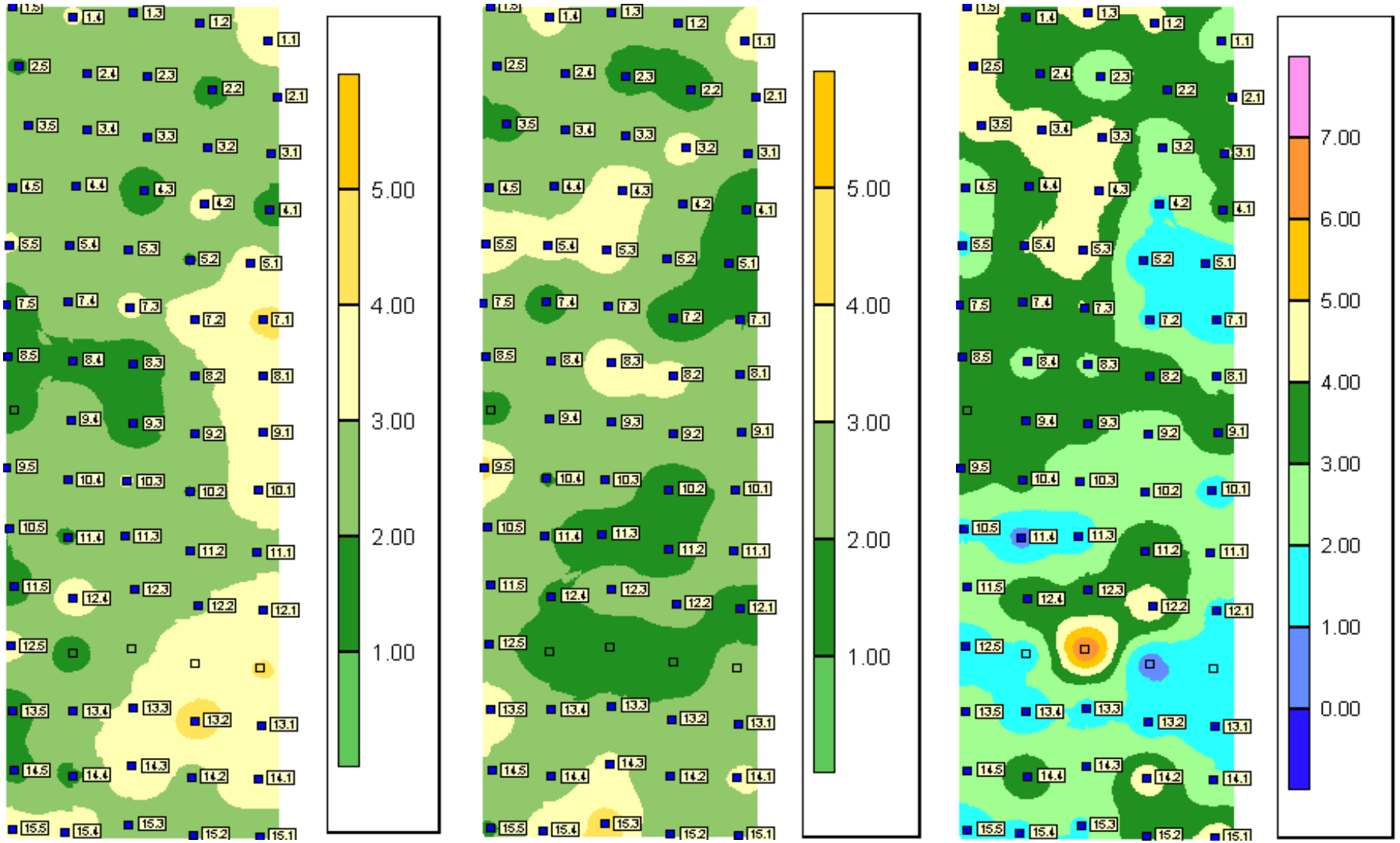

Appendix H Chemical and physical properties of the A horizon of the Tukulu soil form

Plot no	pH_{H2O}	pH_{KCl}	Ca ($cmolc.kg^{-1}$)	K ($cmolc.kg^{-1}$)	Mg ($cmolc.kg^{-1}$)	Na ($cmolc\ kg^{-1}$)	Total Cations	Sand (%)	Silt (%)	Clay (%)
3.5	5.9	4.35	36.00	13.21	26.79	2.91	78.90	74.82	5	18
4.5	6.15	4.65	35.00	12.05	12.30	2.93	62.29	73.34	6	17
5.5	6.8	4.55	45.00	16.79	25.40	3.04	90.24	75.82	3	19
7.5	6.1	4.75	25.78	15.00	13.10	1.52	55.39	77.66	4	17
8.5	5.95	4.65	26.25	14.74	13.49	1.98	56.46	76.34	4	17
9.5	5.63	4.43	40.50	15.33	23.65	2.70	82.18	78.04	2	18
10.5	5.5	4.65	36.73	14.51	12.06	2.00	65.30	77.58	3	17
11.5	5.1	4.53	32.50	13.08	12.54	1.65	59.77	76.00	4	16
13.5	6.1	4.97	37.50	13.69	20.16	1.65	73.00	78.72	4	17
14.5	6.1	4.92	46.10	13.18	23.81	1.83	84.92	76.89	4	17
14.4	5.81	4.67	34.00	14.41	28.57	1.83	78.81	74.50	8	17
B	5.4	4.57	34.80	11.44	13.33	1.57	61.13	77.74	3	16
12.4	6.12	4.73	35.70	14.05	28.57	3.48	81.80	71.52	5	18
7.4	5.74	4.65	32.50	15.26	25.79	2.39	75.94	75.64	4	17
5.4	5.61	4.35	45.00	15.90	27.38	2.93	91.21	76.10	3	18
4.4	6.1	5.25	32.25	12.95	24.01	2.61	71.82	76.51	5	17
3.4	5.85	4.3	23.25	13.59	23.61	2.72	63.17	74.86	3	17
2.4	6.05	4.75	39.88	17.50	25.20	2.61	85.18	76.24	5	17
1.3	5.3	4.2	32.75	17.31	23.81	2.72	76.58	76.24	4	17
2.3	5.9	5.1	31.75	13.46	16.67	2.11	63.99	80.34	2	16
3.3	5.95	5.2	32.75	16.67	22.42	2.39	74.23	75.80	3	17
4.3	6	4.15	21.25	8.97	7.54	1.54	39.31	79.24	4	15
Continue										

5.3	5.8	4.65	29.50	14.94	19.25	2.37	66.05	78.56	2	17
7.3	5.75	4.7	35.63	16.35	16.47	3.15	71.59	74.26	4	18
10.3	5.82	4.72	40.63	15.96	25.79	3.04	85.42	73.82	7	18
11.3	5.29	4.36	29.50	7.05	21.23	2.39	60.17	75.84	3	17
12.3	6.02	4.65	34.13	6.47	19.84	2.39	62.83	78.22	3	17
C	6.05	5.25	42.40	11.28	23.81	2.87	80.36	74.30	5	19
15.2	5.98	4.83	32.25	7.59	22.22	2.35	64.41	74.14	7	17
12.2	6.25	5.56	41.00	17.13	26.98	2.96	88.07	72.94	6	20
11.2	5.68	4.41	31.53	13.09	13.89	2.39	60.89	77.46	2	17
10.2	5.69	4.19	41.25	6.15	19.09	1.98	68.47	70.44	6	16
5.2	5.25	4.2	41.00	8.01	9.72	1.96	60.69	74.66	6	16
4.2	5.89	4.89	41.00	13.46	10.36	3.28	68.10	73.28	6	18
3.2	5.7	4.5	39.88	13.01	9.72	2.39	65.00	78.42	4	17
2.2	5.45	4.05	35.50	9.04	9.13	1.85	55.51	78.80	5	16
1.2	5.18	4.65	34.53	11.55	18.25	2.85	67.18	71.64	4	17
2.1	6.7	4.85	31.25	13.08	9.92	2.61	56.86	76.48	4	17
3.1	5.2	4.6	44.38	15.26	11.51	2.07	73.20	72.77	8	16
4.1	5.15	4.25	34.13	7.44	13.49	1.74	56.79	78.62	6	15
11.1	5.32	4.75	31.88	8.27	19.84	2.39	62.38	75.32	4	17
15.1	5.83	4.7	32.50	7.76	18.65	2.28	61.19	75.06	5	17
Min	**5.10**	**4.05**	**21.25**	**6.15**	**7.54**	**1.52**	**36.47**	**70.44**	**2.00**	**15.00**
Max	**6.80**	**5.56**	**46.10**	**17.50**	**28.57**	**3.48**	**95.65**	**80.34**	**8.00**	**20.00**
Mean	**5.79**	**4.65**	**35.26**	**12.76**	**18.79**	**2.39**	**69.21**	**75.83**	**4.40**	**17.07**
Std Dev	**0.39**	**0.33**	**5.79**	**3.29**	**6.31**	**0.52**	**15.90**	**2.27**	**1.55**	**0.97**

Appendix I Chemical and physical properties of the B horizon for the Tukulu soil form

Plot no	pH_{H2O}	pH_{KCl}	Ca ($cmolc.kg^{-1}$)	K ($cmolc.kg^{-1}$)	Mg ($cmolc.kg^{-1}$)	Na ($cmolc\ kg^{-1}$)	Total Cations	Sand (%)	Silt (%)	Clay (%)
3.5	5.53	5.41	30.53	6.15	15.87	1.74	54.29	69.02	5	26
4.5	5.8	4.55	37.88	5.59	20.63	2.83	66.93	69.76	3	27
5.5	6.38	5.4	49.30	8.46	29.37	3.65	90.78	65.42	4	29
7.5	6.1	5.35	41.38	6.35	23.81	2.65	74.18	66.26	3	28
8.5	6.05	5.45	35.38	6.54	18.06	2.83	62.80	67.84	4	27
9.5	7.05	6.44	55.10	12.05	33.17	4.17	104.50	63.66	2	32
10.5	6.56	5.62	48.10	4.72	24.60	2.78	80.20	65.76	4	28
11.5	6.28	5.31	42.50	6.82	22.22	2.96	74.50	62.92	7	27
13.5	6.91	5.74	57.00	10.82	31.75	3.74	103.31	59.18	9	31
14.5	6.43	5.58	51.10	7.95	29.37	2.96	91.37	61.3	7	29
14.4	5.49	5.49	41.00	5.59	23.81	2.61	73.01	61.94	9	27
B	5.08	4.18	29.40	3.18	12.70	1.39	46.67	63.6	10	25
12.4	5.59	4.27	35.20	5.95	12.70	1.96	55.80	62.76	9	26
7.4	5.32	4.63	32.50	6.35	11.90	1.52	52.27	67.12	4	26
5.4	5.9	5.73	39.13	5.96	19.84	3.15	68.08	67.97	5	27
4.4	6.4	5.5	39.25	6.42	30.16	2.63	78.46	59.2	10	28
3.4	6.16	5.07	39.88	6.47	19.84	2.83	69.02	65.68	4	27
2.4	6.25	5.25	44.63	6.21	22.62	2.83	76.28	63.92	5	28
1.3	5.14	4.61	28.63	5.71	14.48	2.07	50.88	67.12	2	26
2.3	5.43	4.63	28.13	5.45	12.70	1.74	48.01	66.76	5	26
Continue										
3.3	6	5.1	44.50	6.47	21.83	2.61	75.41	61.76	10	27
4.3	6.45	5.08	46.13	6.54	21.23	3.41	77.31	63.58	5	28

5.3	6.55	5.18	50.38	9.87	22.42	3.59	86.25	67.46	3	29
7.3	5.19	5.14	42.88	6.41	23.02	2.50	74.80	66.73	3	28
10.3	6.55	5.32	55.25	8.08	27.78	2.93	94.04	63.4	7	29
11.3	6.07	4.13	25.88	4.87	9.92	1.30	41.97	64.1	8	25
12.3	6.3	5.19	40.13	5.83	19.84	2.48	68.28	68.16	4	27
C	5.88	4.68	31.40	7.03	12.70	1.52	52.65	68.01	4	26
15.2	6.29	5.11	52.30	6.87	20.63	2.17	81.98	63.48	5	28
12.2	6.13	5.17	47.00	6.77	22.70	2.43	78.90	65.61	4	28
11.2	6.15	4.14	33.40	5.54	11.59	1.48	52.00	63.54	7	26
10.2	6.06	4.08	33.00	5.49	13.81	1.30	53.60	68.82	5	26
5.2	6.16	4.2	36.63	5.77	21.63	2.50	66.52	65.84	4	27
4.2	6.1	4.7	42.25	6.41	25.40	2.35	76.40	67.62	4	28
3.2	6.6	5.4	50.50	9.49	31.15	3.30	94.44	64.84	4	29
2.2	5.52	4.8	30.70	5.59	11.43	1.48	49.20	60.6	9	26
1.2	6.05	5.15	39.90	5.74	18.10	2.09	65.83	68.82	4	27
2.1	5.9	5.16	42.50	6.41	24.01	2.39	75.31	65.5	4	28
3.1	6	4.8	38.75	6.22	20.24	2.07	67.27	65	4	27
4.1	5.7	4.35	25.25	5.77	11.11	1.09	43.22	61.88	8	26
11.1	6.37	5.18	47.75	9.94	27.78	2.93	88.40	62.94	5	29
15.1	6.59	5.24	53.13	10.06	27.78	2.93	93.90	62.36	4	29
Min	**5.08**	**4.08**	**25.25**	**3.18**	**9.92**	**1.09**	**39.44**	**59.18**	**2.00**	**25.00**
Max	**7.05**	**6.44**	**57.00**	**12.05**	**33.17**	**4.17**	**106.40**	**69.76**	**10.00**	**32.00**
Mean	**6.06**	**5.04**	**40.85**	**6.76**	**20.85**	**2.47**	**70.93**	**64.93**	**5.38**	**27.45**
Std Dev	**0.46**	**0.52**	**8.58**	**1.76**	**6.44**	**0.74**	**17.51**	**2.71**	**2.29**	**1.47**

Appendix J Chemical and physical properties of the C horizon for the Tukulu soil form

Plot no	pH_{H2O}	pH_{KCl}	Ca ($cmolc.kg^{-1}$)	K ($cmolc.kg^{-1}$)	Mg ($cmolc.kg^{-1}$)	Na ($cmolc\ kg^{-1}$)	Total cations	Sand (%)	Silt (%)	Clay (%)
3.5	5.85	4.14	35.20	9.38	41.27	4.26	90.12	52.92	6	40
4.5	6.57	5.11	52.40	8.67	46.03	2.17	109.27	51.7	3	45
5.5	6.17	4.42	45.70	8.10	38.10	1.83	93.72	48.36	5	44
7.5	6.59	5.33	69.40	14.10	61.90	3.83	149.23	47.86	4	48
8.5	6.56	5.13	67.10	8.82	60.32	3.83	140.06	49.58	2	48
9.5	5.87	4.11	34.80	7.54	44.44	3.74	90.52	53.2	5	40
10.5	5.77	4.96	59.00	4.82	25.40	1.91	91.13	57.76	3	39
11.5	6.23	4.69	57.30	16.51	50.79	2.87	127.48	43.8	8	46
13.5	6.74	4.53	53.50	10.41	38.10	2.26	104.27	45	9	45
14.5	6.54	4.53	57.15	10.28	34.13	2.39	103.95	45.38	9	45
14.4	6.58	5.18	150.50	12.46	55.56	3.83	222.34	38.86	11	48
B	7.05	5.62	54.80	6.62	23.49	1.65	86.56	41.16	12	45
12.4	7.27	5.96	68.30	4.51	56.35	3.83	132.99	44.34	6	48
7.4	6.48	4.79	61.75	12.69	50.20	3.59	128.23	46.86	5	47
5.4	6.64	5.27	71.88	15.90	70.63	4.02	162.43	47.9	6	49
4.4	6.53	5.13	67.25	14.87	59.52	3.85	145.49	45.54	5	48
3.4	6.85	5.46	82.50	20.77	79.37	4.35	186.98	41.84	5	51
2.4	6.48	4.74	60.75	13.27	51.59	3.26	128.87	46.62	4	47
1.3	6.56	4.25	74.75	17.44	65.48	4.24	161.90	44.11	5	49
2.3	6.47	4.49	46.50	13.27	55.56	2.07	117.39	51.36	4	44
3.3	6.88	5.48	84.00	21.54	81.35	4.67	191.56	38.35	7	51
4.3	6.84	5.49	81.75	21.67	83.65	4.67	191.74	41.48	4	51
5.3	6.83	5.46	84.88	21.41	85.32	4.57	196.17	43.31	2	51
7.3	6.64	5.22	72.63	16.35	69.44	4.02	162.44	41.56	6	49
10.3	7.09	4.57	53.50	10.83	65.48	2.39	132.20	48.7	4	45
Continue										
11.3	5.95	4.2	38.88	7.82	39.68	1.52	87.90	52.16	4	41
12.3	6.45	4.72	39.60	10.10	53.97	3.13	106.80	44.76	5	47
C	7.9	4.57	51.60	12.00	66.67	6.70	136.96	51.36	3	45
15.2	6.47	4.75	61.40	12.62	52.38	3.39	129.79	47.06	4	47

12.2	6.78	5.39	76.90	19.44	77.78	4.52	178.64	43.36	4	50
11.2	6.53	5.18	67.90	14.21	58.73	3.83	144.66	46.37	5	48
10.2	6.27	4.88	74.50	15.95	52.38	2.61	145.44	48.2	4	46
5.2	6.08	5.14	40.80	10.97	41.27	1.30	94.35	53.1	3	43
4.2	6.59	4.42	48.60	6.97	25.71	1.91	83.20	49.82	4	44
3.2	6.22	4.58	53.80	9.33	41.75	2.17	107.05	49.28	3	45
2.2	4.43	4.75	61.40	11.18	50.79	3.39	126.76	46.85	5	47
1.2	6.05	4.34	42.90	20.51	68.25	4.09	135.75	50.5	5	43
2.1	7.18	4.71	61.63	13.59	53.57	4.02	132.81	47.42	3	47
3.1	6.94	5.24	74.00	17.44	63.49	4.02	158.95	44.68	4	49
4.1	6.45	4.77	64.88	12.05	47.62	3.15	127.70	49.32	2	47
11.1	6.24	4.53	54.00	10.19	43.65	2.83	110.67	48.3	4	45
15.1	6.67	5.29	71.63	17.88	65.48	4.24	159.22	46.54	3	49
Min	**4.43**	**4.11**	**34.80**	**4.51**	**23.49**	**1.30**	**64.11**	**38.35**	**67.66**	**39.00**
Max	**7.90**	**5.96**	**150.50**	**21.67**	**85.32**	**6.70**	**264.18**	**57.76**	**171.44**	**51.00**
Mean	**6.51**	**4.89**	**62.66**	**12.96**	**54.68**	**3.36**	**133.66**	**47.06**	**118.06**	**46.33**
Std Dev	**0.52**	**0.45**	**19.37**	**4.66**	**15.46**	**1.11**	**40.61**	**4.12**	**25.35**	**3.01**

Appendix K Chemical and physical properties of the A horizon for the Sepane soil form

Plot no	pH_{H2O}	pH_{KCl}	Ca (cmolc.kg^{-1})	K (cmolc.kg^{-1})	Mg (cmolc.kg^{-1})	Na (cmolc kg^{-1})	Total Cations	Sand (%)	Silt (%)	Clay (%)
12.5	5.53	4.55	36.90	5.95	12.70	3.22	58.76	78.84	3	18
15.5	6.15	5.06	54.60	6.21	31.75	3.30	95.86	72.53	7	18
15.4	6.24	4.95	54.80	9.13	34.92	3.57	102.41	70.06	8	19
13.4	6.33	5.11	51.90	6.56	23.81	2.96	85.23	71.45	9	18
11.4	5.9	4.58	30.53	4.63	13.89	1.96	51.00	79.82	5	15
13.3	6.79	5.18	47.70	6.72	23.97	3.04	81.43	71.43	8	20
14.3	6.25	5.1	57.00	6.77	28.57	3.83	96.17	70.3	10	20
15.3	6.25	5.25	54.40	7.28	23.65	2.70	88.03	70.56	8	19
14.2	5.43	4.95	44.10	6.67	26.98	2.78	80.53	71.44	8	18
13.2	6.42	5.55	59.03	6.93	27.02	4.37	97.35	65.44	10	21
D	5.41	4.31	40.70	6.00	22.22	3.57	72.49	75.56	3	18
7.2	5.1	4.4	44.13	7.45	26.98	3.70	82.25	74.52	5	19
5.1	5.65	4.25	37.25	5.06	11.11	3.26	56.69	74.1	4	17
7.1	6.55	5.35	51.38	11.86	33.13	4.13	100.50	74.12	4	20
10.1	6.17	4.72	46.00	8.21	21.87	3.80	79.87	75.82	2	19
12.1	5.7	4.43	47.38	6.99	21.83	3.80	79.99	70.72	7	19
E	6.54	5.25	78.75	11.79	35.71	4.02	130.28	74.38	5	20
13.1	6.25	4.85	42.50	8.97	29.40	3.72	84.60	70.5	8	19
14.1	6.27	4.95	50.00	7.05	29.76	3.91	90.73	70.83	7	19
Min	**5.10**	**4.25**	**30.53**	**4.63**	**11.11**	**1.96**	**48.22**	**65.44**	**2.00**	**15.00**
Max	**6.79**	**5.55**	**78.75**	**11.86**	**35.71**	**4.37**	**130.69**	**79.82**	**10.00**	**21.00**
Mean	**6.05**	**4.88**	**48.90**	**7.38**	**25.23**	**3.45**	**84.96**	**72.76**	**6.37**	**18.74**
Std Dev	**0.46**	**0.38**	**10.43**	**1.92**	**7.03**	**0.59**	**19.97**	**3.36**	**2.43**	**1.33**

Appendix L Chemical and physical properties for the B horizon of the Sepane soil form

Plot no	pH_{H2O}	pH_{KCl}	Ca (cmolc.kg^{-1})	K (cmolc.kg^{-1})	Mg c(molc.kg^{-1})	Na (cmolc kg^{-1})	Total Cations	Sand (%)	Silt (%)	Clay (%)
12.5	5.17	4.61	47.40	4.05	31.75	2.00	85.20	62.56	10	26
15.5	6.13	4.72	74.00	4.41	26.98	1.96	107.35	62.26	9	28
15.4	7.09	5.6	73.70	8.10	41.27	3.26	126.33	59.61	5	35
13.4	6.33	5.11	61.90	6.23	23.81	2.09	94.03	58.45	9	29
11.4	6.53	5.1	64.30	5.95	26.98	2.00	99.23	64.7	4	29
13.3	6.32	5.11	67.90	6.36	36.51	2.09	112.85	64.1	4	32
14.3	6.22	4.91	77.50	8.82	40.00	3.13	129.45	55.72	7	35
15.3	7.15	5.9	76.70	10.15	61.90	4.43	153.19	54.6	6	36
14.2	6.6	5.77	69.40	6.92	39.68	2.35	118.35	60.52	5	32
13.2	6.6	5.26	67.60	6.92	41.90	2.26	118.69	59.42	4	32
D	5.95	4.85	52.10	5.23	18.57	1.09	76.99	61.94	8	27
7.2	5.6	4.75	47.63	2.56	16.87	1.20	68.25	61.93	8	26
5.1	5.9	4.6	30.63	4.10	24.21	1.63	60.56	62.44	8	28
10.1	6.78	5.26	51.25	5.83	29.76	2.07	88.91	57.82	7	31
12.1	6.5	5.05	66.88	4.87	23.81	1.52	97.08	66.4	2	28
E	6.27	5.57	62.88	7.05	34.13	2.26	106.31	62.7	2	34
13.1	6.84	5.31	67.13	8.14	33.73	2.83	111.82	57.57	6	35
14.1	6.85	5.34	71.75	7.82	35.71	3.04	118.33	58.05	5	35
Min	**5.17**	**4.60**	**30.63**	**2.56**	**16.87**	**1.09**	**60.56**	**54.60**	**2.00**	**26.00**
Max	**7.15**	**5.90**	**77.50**	**10.15**	**61.90**	**4.43**	**153.19**	**66.40**	**10.00**	**36.00**
Mean	**6.38**	**5.16**	**62.81**	**6.31**	**32.64**	**2.29**	**104.05**	**60.60**	**6.06**	**31.00**
Std Dev	**0.51**	**0.38**	**12.40**	**1.92**	**10.56**	**0.81**	**23.00**	**3.17**	**2.36**	**3.45**

Appendix M Chemical and physical properties for the C horizon of the Sepane soil form

Plot no	pH_{H2O}	pH_{KCl}	Ca (cmolc.kg^{-1})	K (cmolc.kg^{-1})	Mg c(molc.kg^{-1})	Na (cmolc kg^{-1})	Total Cations	Sand (%)	Silt (%)	Clay (%)
12.5	7.03	5.96	57.60	11.69	44.44	1.48	115.22	45.78	7	45
15.5	7.18	6.05	62.80	11.23	40.63	1.57	116.23	46.63	7	46
15.4	7.33	6.27	72.40	11.59	57.14	1.83	142.96	42.64	8	48
13.4	7.08	5.96	59.70	18.05	46.03	1.43	125.22	46.22	8	45
11.4	6.83	5.16	36.63	5.38	21.03	0.76	63.80	57.32	3	39
13.3	7.66	6.66	91.80	13.49	65.08	1.83	172.19	42.75	4	53
14.3	7.76	6.72	98.80	8.67	52.38	2.09	161.93	40.65	4	55
15.3	7.58	6.45	81.80	8.21	57.14	1.91	149.06	43.58	5	50
14.2	7.06	6.28	71.60	13.33	63.49	4.52	152.95	45.92	5	48
13.2	7.29	6.19	67.70	11.08	58.73	1.65	139.16	46.86	4	47
D	6.88	5.35	43.10	7.28	34.92	0.61	85.91	55.44	4	39
7.2	7.36	6.17	70.30	13.49	53.97	1.87	139.62	47.94	4	48
5.1	6.55	5.29	42.00	6.92	23.81	1.09	73.82	55.78	3	40
7.1	6.93	5.35	60.25	10.00	51.59	1.33	123.16	51.66	3	44
10.1	7.38	6.23	74.75	13.53	57.54	1.76	147.58	45.14	4	48
12.1	7.45	6.37	79.00	8.85	39.68	1.85	129.38	46.68	2	49
E	7.09	5.88	91.00	8.33	51.59	1.41	152.33	48.12	5	45
13.1	7.09	6.16	59.25	4.94	17.86	1.20	83.24	49.02	4	45
14.1	7.65	6.56	85.50	8.59	39.68	2.02	135.79	42.42	3	52
Min	**6.55**	**5.16**	**36.63**	**4.94**	**17.86**	**0.61**	**60.03**	**40.65**	**2.00**	**39.00**
Max	**7.76**	**6.72**	**98.80**	**18.05**	**65.08**	**4.52**	**186.45**	**57.32**	**8.00**	**55.00**
Mean	**7.22**	**6.06**	**68.74**	**10.24**	**46.14**	**1.69**	**126.82**	**47.40**	**4.58**	**46.63**
Std Dev	**0.32**	**0.48**	**17.53**	**3.36**	**14.39**	**0.82**	**36.10**	**4.81**	**1.69**	**4.47**

Appendix N Chemical and physical properties for the A horizon of the Bloemdal soil form

Plot no	pH_{H2O}	pH_{KCl}	Ca (cmolc.kg^{-1})	K (cmolc.kg^{-1})	Mg c(molc.kg^{-1})	Na (cmolc kg^{-1})	Total Cations	Sand (%)	Silt (%)	Clay (%)
1.5	5	4.85	35.25	5.38	9.33	2.39	52.35	70.64	11	15
2.5	5.45	3.55	39.63	4.62	9.92	1.96	56.12	77.26	4	14
A	5.77	4.18	35.40	5.51	13.97	1.57	56.45	78.76	5	15
10.4	5.8	4.66	41.03	8.33	29.40	2.61	81.37	78.36	4	18
9.4	6.1	4.87	44.88	8.85	18.29	2.98	74.99	75.66	4	19
8.4	5.89	4.16	29.88	5.13	17.86	1.85	54.71	77.48	4	15
1.4	5.59	4.51	30.38	6.28	19.25	3.04	58.95	78.32	4	17
8.3	5.04	3.95	28.88	4.74	15.08	0.98	49.68	79.78	5	14
9.3	5.05	4.01	36.88	5.38	26.39	1.20	69.84	76.66	5	15
9.2	5.65	4.49	40.53	8.99	27.02	2.83	79.36	75.42	3	18
8.2	5.17	4.14	31.13	6.28	15.87	2.83	56.11	77.66	3	16
1.1	5.05	3.9	34.03	6.03	24.64	3.48	68.17	79.88	3	16
8.1	5.6	4.25	39.25	6.41	11.31	3.80	60.77	70.84	8	17
9.1	5.78	4.48	42.50	8.08	27.78	3.26	81.62	69.72	8	18
Min	**5**	**3.55**	**28.88**	**4.62**	**9.33**	**0.98**	**49.68**	**69.72**	**3**	**14**
Max	**6.1**	**4.87**	**44.88**	**8.99**	**29.40**	**3.80**	**81.62**	**79.88**	**11**	**19**
Mean	**5.50**	**4.29**	**36.40**	**6.43**	**19.01**	**2.48**	**64.32**	**76.17**	**5.07**	**16.21**
Std Dev	**0.37**	**0.38**	**5.10**	**1.51**	**6.93**	**0.86**	**11.31**	**3.39**	**2.34**	**1.63**

Appendix O Chemical and physical properties for the B horizon of the Bloemdal soil form

Plot no	pH_{H2O}	pH_{KCl}	Ca (cmolc.kg^{-1})	K (cmolc.kg^{-1})	Mg c(molc.kg^{-1})	Na (cmolc kg^{-1})	Total Cations	Sand (%)	Silt (%)	Clay (%)
1.5	5.16	5.7	41.40	20.67	23.81	2.96	88.83	65.12	5	28
2.5	4.6	4.45	38.38	20.71	13.29	2.07	74.44	69.24	4	24
A	4.22	4.33	37.40	4.87	19.05	1.65	62.97	69.68	4	23
10.4	4.44	5.03	38.75	19.74	16.67	1.96	77.12	66	5	24
9.4	4.05	4.1	36.38	6.67	15.87	2.39	61.31	70.22	6	21
8.4	6.57	5.3	40.25	20.13	20.24	2.50	83.12	69.28	3	26
1.4	5.88	5.98	43.50	21.47	26.19	3.26	94.43	64.09	5	29
8.3	6.47	5.03	51.38	22.69	27.78	3.70	105.54	63.86	5	31
9.3	4.62	5.15	39.25	20.90	17.46	2.83	80.43	68.11	6	24
9.2	5.26	4.95	37.50	19.54	18.41	2.52	77.97	67.9	5	23
8.2	5.08	5.72	41.30	20.56	23.49	3.22	88.57	63.5	5	28
1.1	6.24	5	48.75	21.67	27.38	3.37	101.17	64.5	4	30
8.1	4.8	5.5	39.88	22.50	19.64	2.39	84.41	69.32	3	25
9.1	5.07	5.53	40.88	20.32	21.83	2.61	85.63	68.72	2	27
Min	**4.05**	**4.1**	**36.38**	**4.87**	**13.29**	**1.65**	**61.31**	**63.5**	**2**	**21**
Max	**6.57**	**5.98**	**51.38**	**22.69**	**27.78**	**3.70**	**105.54**	**70.22**	**6**	**31**
Mean	**5.18**	**5.13**	**41.07**	**18.75**	**20.79**	**2.67**	**83.28**	**67.11**	**4.43**	**25.93**
Std Dev	**0.82**	**0.55**	**4.28**	**5.59**	**4.45**	**0.58**	**12.57**	**2.47**	**1.16**	**2.97**

Appendix P Chemical and physical properties for the C horizon of the Bloemdal soil form

Plot no	pH_{H2O}	pH_{KCl}	Ca (cmolc.kg^{-1})	K (cmolc.kg^{-1})	Mg c(molc.kg^{-1})	Na (cmolc kg^{-1})	Total Cations	Sand (%)	Silt (%)	Clay (%)
1.5	6.98	5.53	70.30	10.31	44.44	4.26	129.31	43.6	4	50
2.5	6.72	5.48	69.40	10.15	36.51	4.17	120.24	44.08	4	49
A	6.14	5.04	45.70	8.97	30.16	3.30	88.14	53.96	2	43
10.4	6.15	5.03	48.38	9.49	27.58	3.26	88.70	49.76	6	43
9.4	6.41	5.23	58.50	9.68	32.94	3.70	104.81	50.18	3	46
8.4	6.07	4.99	42.63	8.33	22.82	2.83	76.60	54.84	3	42
1.4	6.67	5.37	61.13	17.50	35.32	3.91	117.86	43.72	7	48
8.3	6.19	5.06	45.50	9.23	23.81	2.96	81.50	51.75	4	43
9.3	6.95	5.59	73.63	20.96	83.33	3.15	181.07	44.74	3	50
9.2	5.94	4.96	35.00	6.46	19.05	2.52	63.03	50.38	6	41
8.2	6.65	5.38	63.00	9.90	46.03	3.91	122.84	45.17	5	48
1.1	5.92	4.42	36.13	6.15	21.83	2.61	66.71	54.76	2	41
8.1	6.32	4.29	34.63	6.03	15.87	2.93	59.46	54.16	4	39
9.1	6.21	5.1	51.75	9.55	27.78	3.48	92.56	52.16	2	44
Min	**5.92**	**4.29**	**34.63**	**6.03**	**15.87**	**2.52**	**59.46**	**43.6**	**2**	**39**
Max	**6.98**	**5.59**	**73.63**	**20.96**	**83.33**	**4.26**	**181.07**	**54.84**	**7**	**50**
Mean	**6.38**	**5.11**	**52.55**	**10.19**	**33.39**	**3.36**	**99.49**	**49.52**	**3.93**	**44.79**
Std Dev	**0.36**	**0.38**	**13.51**	**4.15**	**16.91**	**0.57**	**32.86**	**4.39**	**1.59**	**3.66**

Appendix Q Pedological characteristics of the Tukulu soil form

Number	Soil family	Horizons	Name	Depth	Mottles	Cutans	Structure	Clay (%)	Consistency	Lime	Transition
7.1 Tu (Modal)	1220 Dikeni	A	Ot	210	None	none	Apedal massive	18	Loose	None	Clear, flat
		B	Ne	210	None	yes	Weakly developed medium 10-25 mm) Sub block	28	Slightly hard	None	Abrupt, flat
		C	Uw	450	Red, black, yellow, grey	yes	well developed medium size (5-15 mm) prismatic	49	Hard	None	Abrupt, flat
12.2 Tu	1220 Dikeni	A	Ot	200	None	none	Apedal massive	20	Loose	None	Clear, flat
		B	Ne	300	None	yes	Weakly developed medium 10-25 mm) Sub block	28	Slightly hard	Occurrence	Abrupt, flat
		C	Uw	500	Red, black, yellow, grey	yes	Medium developed medium size (5-15 mm) prismatic	50	Hard	None	Abrupt, flat
5.1 Tu	1220 Dikeni	A	Ot	210	None	none	Apedal massive	17	Loose	None	Clear, flat
		B	Ne	280	None	yes	Weakly developed medium 10-25 mm) Sub block	28	Slightly hard	None	Abrupt, flat
		C	Uw	500	Red, black, yellow, grey	yes	Well developed medium size (5-15 mm) prismatic	40	Hard	None	Abrupt, flat
1.1 Tu	1220 Dikeni	A	Ot	210	None	none	Apedal massive	16	Loose	None	Clear, flat
		B	Ne	310	None	yes	Weakly developed medium 10-25 mm) Sub block	30	Slightly hard	Occurrence	Abrupt, flat
		C	Uw	250	Red, black, yellow, grey	yes	Medium developed medium size (5-15 mm) prismatic	41	Hard	Occurrence	Abrupt, flat
1.5 Tu	1220 Dikeni	A	Ot	210	None	none	Apedal massive	15	Loose	None	Clear, flat
		B	Ne	410	None	yes	Weakly developed medium 10-25 mm) Sub block	28	Slightly hard	None	Abrupt, flat
		C	Uw	200	Red, black, yellow, grey	yes	Medium developed medium size (5-15 mm) prismatic	50	Hard	None	Abrupt, flat

Summary

	Min A	**200**	**Max A**	**210**	**Modal A**	**210**		**Min A**	**15**	**Max A**	**20**	**Modal A**	**18**
	Min B	**200**	**Max B**	**410**	**Modal B**	**210**		**Min B**	**28**	**Max B**	**30**	**Modal B**	**28**
Depth (mm)	**Min C**	**200**	**MaxC**	**500**	**Modal C**	**450**	**Clay Content (%)**	**Min C**	**40**	**MaxC**	**50**	**Modal C**	**48**

Appendix R Pedological characteristics of the Sepane soil form

Number	Soil family	Horizons	Horizon Name	Depth	Mottles	Cutans	Structure	Clay (%)	Consistency	Lime	Transition
13.1Se (Modal)	1210 Katdoorn	A	Ot	250	None	none	Apedal massive	19.00	Loose	None	Abrupt, flat
		B	Pd	300	None	yes	Well developed medium size (10-25 mm) blocky	35.00	Hard	None	Abrupt, flat
		C	Uw	250	Red, black, yellow, grey	yes	Well developed medium size (5-15 mm) prismatic	45.00	Hard	None	Abrupt, flat
15.1Se	1210 Katdoorn	A	Ot	210	None	none	Apedal massive	17.00	Loose	None	Abrupt, flat
		B	Pd	300	None	yes	Medium developed medium size (10-25 mm) blocky	29.00	Hard	None	Abrupt, flat
		C	Uw	150	Red, black, yellow, grey	yes	Medium developed medium size (5-15 mm) prismatic	49.00	Hard	None	Abrupt, flat
15.2Se	1210 Katdoorn	A	Ot	210	None	none	Apedal massive	17.00	Loose	None	Abrupt, flat
		B	Pd	400	None	yes	Medium developed medium size (10-25 mm) blocky	28.00	Hard	None	Abrupt, flat
		C	Uw	100	Red, black, yellow, grey	yes	Well developed medium size (5-15 mm) prismatic	47.00	Hard	None	Abrupt, flat
14.2Se	1210 Katdoorn	A	Ot	210	None	none	Apedal massive	18.00	Loose	None	Abrupt, flat
		B	Pd	500	None	yes	Well developed medium size (10-25 mm) blocky	32.00	Hard	None	Abrupt, flat
		C	Uw	100	Red, black, yellow, grey	yes	Medium developed medium size (5-15 mm) prismatic	48.00	Hard	None	Abrupt, flat
12.1Se	1210 Katdoorn	A	Ot	210	None	none	Apedal massive	19.00	Loose	None	Abrupt, flat
		B	Pd	450	None	yes	Well developed medium size (10-25 mm) blocky	28.00	Hard	None	Abrupt, flat
		C	Uw	150	Red, black, yellow, grey	yes	Medium developed medium size (5-15 mm) prismatic	49.00	Hard	None	Abrupt, flat

Summary

Depth (mm)	**Min A**	**210**	**Max A**	**250**	**Modal A**	**250**	**Clay Content (%)**	**Min A**	**17.00**	**Max A**	**19.00**	**Modal A**	19.00
	Min B	**300**	**Max B**	**500**	**Modal A**	**300**		**Min B**	**28.00**	**Max B**	**35.00**	**Modal A**	**35.00**
	Min C	**100**	**MaxC**	**250**	**Modal A**	**250**		**Min C**	**45.00**	**MaxC**	**49.00**	**Modal A**	**45.00**

Appendix S Pedological characteristics of the Bloemdal soil form

Number	Soil family	Horizons	Horizon Name	Depth	Mottles	Cutans	Structure	Clay (%)	Consistency	Transition
11.1Bd (modal)	3200 Roodeplaat	A	Ot	210	None	none	Apedal massive	17.00	Loose	Smooth, flat
		B	Yr	280	None	none	Apedal massive	29.00	Loose	Smooth, flat
		C	Uw	50	Red, black, yellow, grey	yes	Well developed medium size (5-15mm) prismatic	45.00	Hard	Smooth, flat
10.5Bd	3200 Roodeplaat	A	Ot	245	None	none	Apedal massive	17.00	Loose	Smooth, flat
		B	Yr	210	None	none	Apedal massive	28.00	Loose	Smooth, flat
		C	Uw	250	Red, black, yellow, grey	yes	Medium developed medium size (5-15mm) prismatic	39.00	Hard	Smooth, flat
8.1Bd	3200 Roodeplaat	A	Ot	250	None	none	Apedal massive	17.00	Loose	Smooth, flat
		B	Yr	350	None	none	Apedal massive	25.00	Loose	Smooth, flat
		C	Uw	150	Red, black, yellow, grey	yes	Well developed medium size (5-15mm) prismatic	39.00	Hard	Smooth, flat
11.3Bd	3200 Roodeplaat	A	Ot	150	None	none	Apedal massive	17.00	Loose	Smooth, flat
		B	Yr	200	None	none	Apedal massive	25.00	Loose	Smooth, flat
		C	Uw	150	Red, black, yellow, grey	yes	Medium developed medium size (5-15mm) prismatic	41.00	Hard	Smooth, flat

Summary

Depth (mm)	**Min A**	**150**	**Max A**	**250**	**Modal A**	**150**	**Clay Content (%)**	**Min A**	**17.00**	**Max A**	**17.00**	**Modal A**	17.00
	Min B	**200**	**Max B**	**350**	**Modal B**	**200**		**Min B**	**25.00**	**Max B**	**29.00**	**Modal B**	25.00
	Min C	**50**	**MaxC**	**250**	**Modal C**	**150**		**Min C**	**39.00**	**MaxC**	**45.00**	**Modal C**	41.00

Appendix T Landtype Ca22 data

LAND TYPE / *LANDTIP* ..... : **Ca22**
CLIMATE ZONE *KLIMAATSONE* ..... : 45S
Area / Oppervlakte ..... : 156400 ha
Estimated area unavailable for agriculture
Beraamde oppervlakte onbeskikbaar vir landbou : 5000 ha

Occurrence (maps) and areas *Voorkoms (kaarte) en oppervlakte :*
2826 Winburg (68290 ha) 2926 Bloemfontein (88110 ha)

Inventory by *Inventaris deur :*
J F Eloff
Modal Profiles *Modale profiele :*
P459 P460 P480 P592 P595 P596 P597

Terrain uni *Terreineenheid* ..... :	1	3	4	5
% of land type *% van landtipe* ..... :	22	53	18	7
Area *Oppervlakte (ha)* ..... :	34408	82892	28152	10948
Slope / *Helling (%)* ..... :	0 - 2	2 - 8	1 - 3	0 - 4
Slope length *Hellingslengte (m)* ..... :	100 - 900	500 - 1500	200 - 700	50 - 400
Slope shape *Hellingsvorm* ..... :	Y	Y-Z	Y-Z	Z-X
MB0, MB1 (ha) ..... :	29591	78747	28152	10948
MB2 - MB4 (ha) ..... :	4817	4145	0	0

Soil series or land classes *Grondseries of landklasse*	**Depth** *Diepte* (mm)	MB	:	ha	%	ha	%	ha	%	ha	%	**Total** *Totaal* ha	%	**Clay content %** *Klei-inhoud %* A	E	B21	Hor	**Texture** *Tekstuur* Class / *Klas*	*Diepte-beperkende materiaal*
Soil-rock complex			:																
Grond-rotskompleks:			:																
Rock/Rots		4	:	1032	3	1658	2					2690	1.7						
Glendale Sd21, Milkwood Mw11,			:																
Skilderkrans Sw11	100-250	0	:	344	1	829	1					1173	0.8	15-30		35-55	B	fiSaClLm-Cl	R,vr
Mispah Ms10, Williamson Gs16,			:																
Shorrocks Hu36	100-250	3	:	344	1	829	1					1173	0.8	10-18			A	LmfiSa-SaLm	R,so
Waterval Va11, Craven Va21	100-350	0	:	12043	35	20723	25	7038	25			39804	25.5	12-20		45-55	B	fiSaCl-Cl	vp
Arniston Va31, Lindley Va41,			:																
Chalumna Va32,			:																
Sheppardvale Va42	100-300	0	:	8602	25	19065	23	9009	32	2737	25	39413	25.2	12-25		45-60	B	fiSaCl-Cl	vp
Rietvlei We12, Sibasa We13	200-500	0	:	6193	18	12434	15	3660	13			22287	14.3	10-25		25-40	A	fiSaLm-SaClLm	sp
Milkwood Mw11, Graythorne Mw21,			:																
Gelykvlakte Ar20	300-900	0	:			4974	6	2252	8	3832	35	11057	7.1	40-55			A	fiSaCl-Cl	R
Soetmelk Av36	400-800	0	:	688	2	5802	7	1971	7			8461	5.4	8-15		18-25	B	fiSaLm-SaClLm	sp
Shorrocks Hu36	300-1000	0	:	1720	5	6631	8					8352	5.3	8-15		18-25	B	fiSaLm-SaClLm	R
Sterkspruit Ss26	100-250	0	:			4145	5	3378	12			7523	4.8	20-30		55-70	A	fiSaClLm	pr
Mispah Ms10, Williamson Gs16	100-250	3	:	3441	10	1658	2					5099	3.3	10-18			A	LmfiSa-SaLm	R,so
Bainsvlei Bv36	400-800	0	:			4145	5	845	3			4989	3.2	8-15		18-25	B	fiSaLm-SaClLm	sp

1

Continue

LAND TYPE / *LANDTIP* ..... : **Ca22** Continued *Vervolg*

Soil series or land classes *Grondseries of landklasse*	**Depth** *Diepte* (mm)	MB:	ha	%	ha	%	ha	%	ha	%	**Total** *Totaal* ha	%	**Clay content %** *Klei-inhoud %* A	E	B21	Hor	**Texture** *Tekstuur* Class / *Klas*	*Diepte-beperkende materiaal*
Dundee Du10, Killarney Ka20,		:																
Mutale Oa47	300-1200+	0 :							4379	40	4379	2.8	10-30			A	LmfiSa-SaClLm	gc

Terrain type *Terreintipe :* A2

Terrain form sketch *Terreinvormskets*

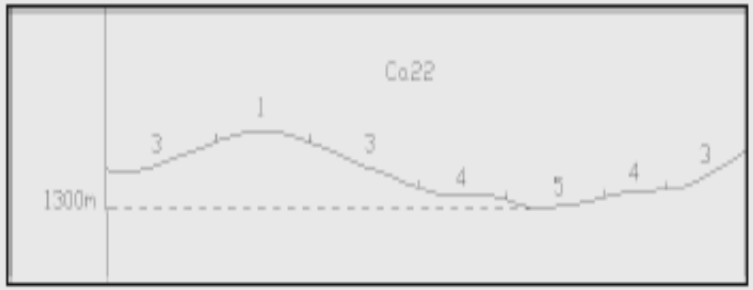

For an explanation of this table consult LAND TYPE INVENTORY (table of contents)

Ter verduideliking van hierdie tabel kyk LANDTIPE - INVENTARIS (inhoudsopgawe)

Geology: Sandstone, shale and mudstone of the Beaufort Group, with dolerite intrusions.

Geologie Sandsteen, skalie en moddersteen van die Groep Beaufort, met dolerietindringings.

Appendix U Interpolation techniques

1 TIN

A triangulated irregular network (TIN) which is defined as a vector data structure is one method used to store and display surface models. A TIN characterizes geographic space using a set of irregularly spaced data points, each of which has x, y and z values (Figure 1). These points are connected by edges to form non overlapping triangles and create a continuous surface that represents the terrain *(*ARC GIS 9.1, 2005*)*

Figure 1 Image illustrating a triangulated irregular network (TIN) surface representation (Clark, 2001)

2 Grid

A grid is a spatial data structure that defines space as an array of cells of equal size that are arranged in rows and columns (Figure 2). In the case of a grid that represents a surface, each cell contains an attribute value that represents a change in Z value. The location of the cell in geographic space is obtained from this position relative to the grids origin. *(*ARC GIS 9*.1, 2005)*

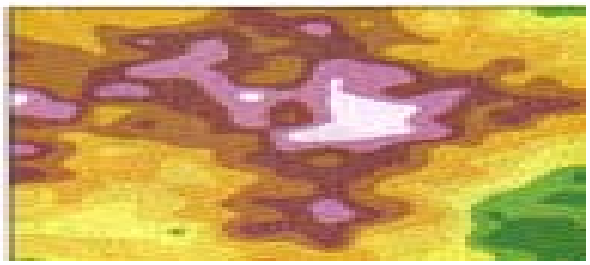

Figure 2 Image illustrating a grid surface representation (Clark, 2001)

From this surfaces that has been established one may then use an interpolation technique that will suite the situation the best. For example: Inverse distance weighing (Interpolation method that uses point data that is close enough to the measured values through its inverse distance.); for which a grid representation will be more affective for the specific interpolation technique as the distance between measured points stay constant. Understanding the different surface representation will assist in the sampling method and density so that it might be adequate for the particular interpolation technique used *(*ARC User, *2004).*

3. Inverse distance weighing (IDW)

Inverse distance weighing is the work horse of spatial interpolation and is thus the method that is most often used by GIS analysts. It employs Tobler's law by estimating unknown measurements as weighted averages over the known measurements at nearby points, giving the greatest weight to the nearest points (Figure 3). There are various ways of defining the weights, but the option most often employed is to compute them as the inverse squares of distance (Equation 1).

$$Wi = 1/d^2i \qquad (1)$$

Wi = Weight of influence of sampled point on unsampled point
d = distance from sampled point to unsampled point
i = constant referring to other factors influencing weight given to sampled data point; for example fixed radius.

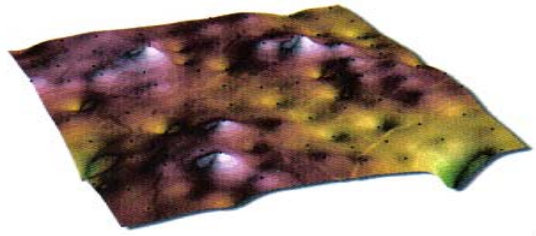

Figure 3 Image illustrating surface representation by Inverse distance weighing (ARC GIS 9.1, 2005)

This means that the weight given to a point drops by a factor of 4 when the distance to the point doubles. In addition, most software gives one the option of ignoring altogether points that is further than a specified distance away, or of limiting the average to a specified number of nearest points, or by averaging over the closest points in each of a number of direction sectors. The inverse distance weighing method achieves the desired objective of creating a smooth surface whose value at any point is more like the values at nearby points than the values at distant points. IDW is described as an exact method of interpolation because its interpolated results honour the data points exactly (Figure 7).

But because IDW is an average it suffers from certain specific characteristics that are generally undesirable. A weighted average that uses weights that are never negative must always return a value that is between the limits of the measures values – no point on the interpolated surface can have an interpolated value that is more than the largest measured value or less than the smallest value measured. Thus IDW may produce counter- intuitive results in areas of peaks and pits, and outside the area covered by the data points. There are many better methods of spatial interpolation that address the problems that were just identified , but the ease of programming of IDW and its conceptual simplicity make it among the most popular. One should just beware, and take care to examine the results of interpolation to ensure that they make good sense (Longley, Goodchild, & Maguire, 2004).

4. Spline Interpolation

Spline Interpolation estimates values using a mathematical function that minimize overall surface curvature (Figure 4). This results in a smooth surface that passes exactly through the input points. Conceptually, it is like bending a sheet of rubber so that it passes through the points while minimizing the total curvature of the surface (Figure 7). It can predict ridges and valleys in the data and is the best method for representing the smoothly varying surfaces of phenomena such as temperature or rainfall. There are variations of spline – regularized and tension. A regularized

spline incorporates the first derivative (slope) and the second derivative (rate of change in slope) into its minimization calculations. Although a tension spline uses only a first and second derivative, it includes more points in the spline calculations, which usually creates smoother surfaces but increases computation time (ARC User, 2004).

Figure 4 Image illustrating surface representation by Spline interpolation (ARC GIS 9.1, 2005)

5. Kriging

"Kriging" is synonymous with "optimal prediction" (Journel & Huijbregts, 1981).

It is a method of interpolation which predicts unknown values from data observed at known locations. This method uses variograms (A two-point statistical function that describes the increasing difference or decreasing continuity, between sample values as separation between them increases) to express the spatial variation; and it minimizes the error of predicted values which are estimated by spatial distribution of the predicted values (Figure 5).

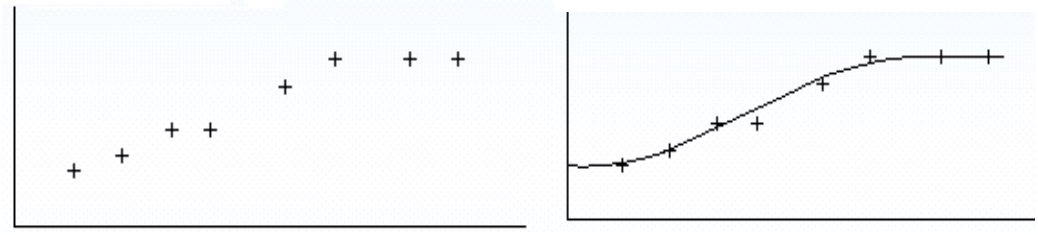

Figure 5 Variograms used in Kriging (Journel & Huijbregts, 1981).

The basic idea is to discover something about the general properties of the surface, as revealed by the measured values, and then to apply these properties in estimating the missing parts of the surface. It is a powerful statistical interpolation method used for diverse applications such as soil science, geology and pollution modelling. Kriging assumes that distance

or direction between sample points reflects a spatial correlation that can be used to explain variation in the surface. It fits a function to a specified number of points or all points within a specified radius to determine the output value for each location (Figure 6). Kriging is most appropriate when a spatially correlated distance or directional bias in the data is known and is often used for applications in soil science and geology. The predicted values are derived from the measure of relationship in samples using sophisticated weighted average technique. It uses a search radius that can be fixed or variable. The generated cell values can exceed value range of samples, and the surface does not pass through samples (Figure 7).

Figure 6 Image illustrating surface representation by Kriging (ARC GIS 9.1, 2005)

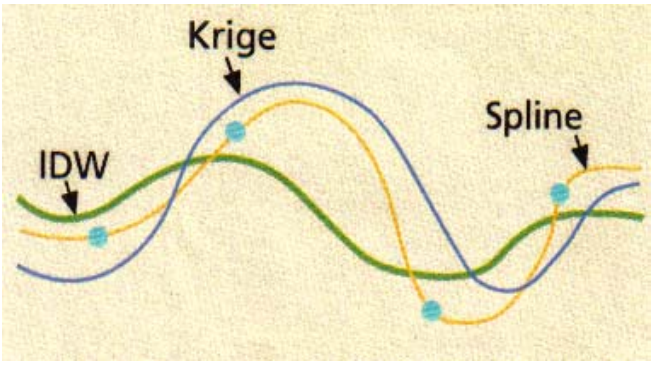

Figure 7 Graph indicating interpolation of values for Inverse distance weighing, Kriging and Spline interpolation techniques (Journel & Huijbregts, 1981).

6. Point interpolation

Similar to IDW, but the point interpolation function allows more control over the sampling neighbourhood. The influence of a particular sample on the interpolated grid cell value depends on whether the sample point is in the cell's neighbourhood and how far from the cell being interpolated it is located. Points outside the neighbourhood have no influence. The weighted value of points inside the neighbourhood is calculated using an inverse distance weighted interpolation or inverse exponential distance interpolation. This method interpolates a raster using point features but allows for different types of neighbourhoods. Neighbourhoods can have shapes such as circles, rectangles, irregular polygons, annuluses, or wedges (Figure 8) (ARC GIS, 2005).

Figure 8 Image illustrating surface representation by point interpolation (ARC GIS 9.1, 2005)

7. Natural neighbourhood

Natural neighbourhood interpolation has many positive features; it can be used for both interpolation and extrapolation. Generally works well with clustered scatter points. Another weighted- average method, the basic equation used in natural neighbourhood interpolation is identical to the one used in IDW interpolation. The method can efficiently handle large input point datasets. When using the Natural Neighbourhood method, local coordinates define the amount of influence any scatter point will have on output cells (Figure 9) (ARC User, 2004).

Figure 9 Image illustrating surface representation by natural neighborhood interpolation (ARC GIS 9.1, 2005)

8. Trend Interpolation

A trend surface describes the general pattern of variation of values for point data across an area. Trend interpolation is easy to understand by considering a plain which is layered through the cloud of point-values in a way that represents the area the best. This interpolation technique is usually used for example in cases where a crop is pH sensitive. Areas above or below the plain is areas not suited for the crop as pH is either to acidic or to alkaline. The surface generated will rarely pass through the original data points since it performs a best fit for the entire surface (Figure 10). The interpolator may generate a surface which has a minimum and maximum value that might exceed the minimum and maximum of the input points. As the area being interpolated becomes more data rich the surface being fitted becomes progressively more complex. A surface rich in data will not always generate the most accurate surface. As such higher intensity surfaces tend to overshoot in areas with less data (as compared to the rest of the study area); these areas are most endangered of bad representation. If there is a trend present in the data, it can be useful to eliminate it by subtracting the trend surface from the data values, perform an interpolation on the remaining residuals, and finally, add the trend again to the resulting surface

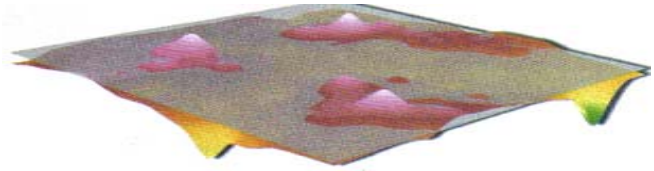

Figure 10 Image illustrating surface representation by Trend interpolation (ARC GIS 9.1, 2005)

Appendix V Variation in soil physical properties

1. Variation in soil physical properties.

A description of the variation in soil physical characteristics of the Tukulu soil form is seen in Table 1

1.1 Tukulu

A horizon:

The depth of the A horizon varied between 200 mm and 210 mm with a mean of 207 mm and a standard deviation of +/- 5. The silt + clay content varied between 19% and 26% with a mean of 23% and a standard deviation of +/- 3. The organic carbon content varied between 30% and 45% with a mean of 35% and a standard deviation of +/- 7%. The modulus of rupture varied between 0.06 bar and 0.25 bar with a mean of 0.15 bar and a standard deviation of +/- 0 bar. The aggregate stability (4 mm) varied between 4% and 7% with a mean of 6% and a standard deviation of +/- 1%. The aggregate stability (2 mm) varied between 5% and 25% with a mean of 13% and a standard deviation of +/- 9%. The aggregate stability (1 mm) varied between 20% and 45% with a mean of 35% and a standard deviation of +/- 11%. The aggregate stability (0.5 mm) varied between 2% and 21% with a mean of 15% and a standard deviation of +/- 8%. The aggregate stability (0.25 mm) varied between 6% and 30% with a mean of 17% and a standard deviation of +/- 11%. The bulk density varied between 1376 $kg.m^{-3}$ and 1520 kg m^{-3} with a mean of 1471 kg m^{-3} and a standard deviation of +/- 63 kg m^{-3}.

B horizon:

The depth of the B horizon varied between 250 mm and 500 mm with a mean of 425 mm and a standard deviation of +/- 113 mm. The silt + clay content varied between 31% and 34% with a mean of 33% and a standard deviation of +/- 1%. The organic carbon content varied between 28% and 39% with a mean of 35% and a standard deviation of +/- 5%. The modulus of rupture varied between 0.44 bar and 0.76 bar with a mean of 0.64 bar and a standard deviation of 0 bar. The aggregate stability (4 mm) varied between 1% and 8% with a mean of 4% and a standard deviation of +/- 3%.

The aggregate stability (2 mm) varied between 3% and 20% with a mean of 11% and a standard deviation of +/- 8%. The aggregate stability (1 mm) varied between 2% and 21% with a mean of 13% and a standard deviation of +/- 8%. The aggregate stability (0.5 mm) varied between 4% and 36% with a mean of 15% and a standard deviation of +/- 14%. The aggregate stability (0.25 mm) varied between 5% and 36% with a mean of 16% and a standard deviation of +/- 14%. The bulk density varied between 1605 kg m^{-3} and 1729 kg m^{-3} with a mean of 1665 kg m^{-3} and a standard deviation of 59 kg m^{-3}.

C horizon:

The depth of the C horizon varied between 210 mm and 310 mm with a mean of 275 mm and a standard deviation of +/- 44 mm. The silt + clay content varied between 43% and 54% with a mean of 48% and a standard deviation of +/- 5%. The organic carbon content varied between 18% and 28% with a mean of 22% and a standard deviation of +/- 4%. The modulus of rupture varied between 0.27 bar and 0.54 bar with a mean of 0.36 bar and a standard deviation of +/- 0 bar. The aggregate stability (4 mm) varied between 6% and 11% with a mean of 8% and a standard deviation of 2%. The aggregate stability (2 mm) varied between 5% and 24% with a mean of 15% and a standard deviation of +/- 8%. The aggregate stability (1 mm) varied between 11% and 28% with a mean of 18% and a standard deviation of +/- 7%. The aggregate stability (0.5 mm) varied between 13% and 18% with a mean of 16% and a standard deviation of +/- 2%. The aggregate stability (0.25 mm) varied between 8% and 22% with a mean of 16% and a standard deviation of +/- 6%. The bulk density varied between 1502kg m^{-3} and 1641 kg m^{-3} with a mean of 1585 kg m^{-3} and a standard deviation of 61 kg m^{-3}.

Table 1 Physical characteristics of the Tukulu soil form

Plot nr	Soil type	Horizon Depth (mm)	Silt + Clay (%)	Organic carbon Content (%)	Modulus of Rupture (bar)	A.S 4 (%)	A. S 2 (%)	A.S 1 (%)	A.S 0.5 (%)	A.S 0.25 (%)	Bulk density (kg m^{-3})	Rootdensity (km m^{-2})	Dry weight (kg.ha-1)
7.1A	**Tu**	210	24	32	0.13	4.44	4.85	33.43	16.63	30.02	1520.12	0.0078479	8567
12.2A	**Tu**	200	26	45	0.25	6.5	25.12	41.46	19.72	6.78	1510.62	0.0153246	4283
5.1A	**Tu**	210	22	30	0.06	7.4	12.48	45.32	2.7	6.07	1478.22	0.0029695	7025
1.1A	**Tu**	210	19	33	0.14	6.36	8.77	20.34	20.86	24.37	1376.19	0.0116658	7110
	Mean	**207.5**	**22.75**	**35**	**0.145**	**6.175**	**12.805**	**35.1375**	**14.9775**	**16.81**	**1471.288**	**0.009452**	**6746.25**
	Min	**200**	**19**	**30**	**0.06**	**4.44**	**4.85**	**20.34**	**2.7**	**6.07**	**1376.19**	**0.002969**	**4283**
	Max	**210**	**26**	**45**	**0.25**	**7.4**	**25.12**	**45.32**	**20.86**	**30.02**	**1520.12**	**0.015325**	**8567**
	StdDev	**4.72**	**2.93**	**6.58**	**0.08**	**1.23**	**8.60**	**10.69**	**8.06**	**11.08**	**63.44**	**0.005171**	**1775.60**
7.1B	**Tu**	450	34	28	0.44	2.98	3.2	14.05	35.88	36.13	1605.34	0.0022271	8567
12.2B	**Tu**	500	32	38	0.69	8.07	16.07	15.11	15.07	15	1610.96	0.0012726	4283
5.1B	**Tu**	500	31	33	0.67	5.53	20	21.38	4.46	6.31	1714.32	0.0001061	7025
1.1B	**Tu**	250	34	39	0.76	1.19	2.83	2.02	4.13	5.45	1728.9	0.0047724	7110
	Mean	**425**	**32.75**	**34.5**	**0.64**	**4.4425**	**10.525**	**13.14**	**14.885**	**15.7225**	**1664.88**	0.0045603	**6746.25**
	Min	**250**	**31**	**28**	**0.44**	**1.19**	**2.83**	**2.02**	**4.13**	**5.45**	**1605.34**	**0.000106**	**4283**
	Max	**500**	**34**	**39**	**0.76**	**8.07**	**20**	**21.38**	**35.88**	**36.13**	**1728.9**	**0.004772**	**8567**
	StdDev	**113.52**	**1.37**	**4.81**	**0.14**	**2.91**	**7.98**	**8.03**	**14.18**	**13.65**	**58.65**	**0.002145**	**1775.60**
7.1C	**Tu**	210	47	28	0.27	8.36	5.49	11.13	16.15	22.53	1630.44	0.0008484	8567
12.2C	**Tu**	300	54	18	0.29	10.57	24.26	15.78	17.59	8.72	1641.86	0.0001061	4283
5.1C	**Tu**	280	46	20	0.37	6.2	20.08	27.62	13.25	14.29	1568.4	0.0000530	7025
1.1C	**Tu**	310	43	22	0.54	7.64	9.54	16.53	18.46	19.09	1502.58	0.0011666	7110
	Mean	**275**	**47.5**	**22**	**0.3675**	**8.1925**	**14.8425**	**17.765**	**16.3625**	**16.1575**	**1585.82**	0.0046663	**6746.25**
	Min	**210**	**43**	**18**	**0.27**	**6.2**	**5.49**	**11.13**	**13.25**	**8.72**	**1502.58**	**0.000053**	**4283**
	Max	**310**	**54**	**28**	**0.54**	**10.57**	**24.26**	**27.62**	**18.46**	**22.53**	**1641.86**	**0.004666**	**8567**
	StdDev	**43.63**	**4.60**	**4.23**	**0.12**	**1.81**	**8.24**	**6.91**	**2.22**	**5.83**	**61.00**	**0.002104**	**1775.60**

1.2 Sepane

A description of the variation in physical characteristics of the Sepane soil form is seen in Table 2.

A horizon:

The depth of the A horizon varied between 210 mm and 250 mm with a mean of 218 mm and a standard deviation of +/- 18 mm. The silt + clay content varied between 22% and 27% with a mean of 25% and a standard deviation of +/- 2%. The organic carbon content varied between 22% and 61% with a mean of 41% and a standard deviation of +/- 17%. The modulus of rupture varied between 0.1 bar and 0.4 bar with a mean of 0.23 bar and a standard deviation of +/- 0.1 bar. The aggregate stability (4 mm) varied between 4% and 33% with a mean of 16% and a standard deviation of +/- 13%. The aggregate stability (2 mm) varied between 8% and 15% with a mean of 15% and a standard deviation of +/- 6%. The aggregate stability (1 mm) varied between 2% and 22% with a mean of 15% and a standard deviation of +/- 8%. The aggregate stability (0.5 mm) varied between 2% and 27% with a mean of 14% and a standard deviation of +/- 11%. The aggregate stability (0.25 mm) varied between 3% and 15% with a mean of 7% and a standard deviation of +/- 5%. The bulk density varied between 1399 kg m^{-3} and 1532 kg m^{-3} with a mean of 1469 kg m^{-3} and a standard deviation of +/- 60 kg m^{-3}.

B horizon:

The depth of the B horizon varied between 100 mm and 250 mm with a mean of 150 mm and a standard deviation of +/- 62 mm. The silt + clay content varied between 49% and 55% with a mean of 52% and a standard deviation of +/- 2%. The organic carbon content varied between 33% and 50% with a mean of 40% and a standard deviation of +/- 7%. The modulus of rupture varied between 0.38 bar and 0.89 bar with a mean of 0.57 bar and a standard deviation of +/- 0.2 bar. The aggregate stability (4 mm) varied between 3% and 10% with a mean of 4% and a standard deviation of +/- 3%. The aggregate stability (2 mm) varied between 2% and 14% with a mean of 6% and a standard deviation of +/- 5%. The aggregate stability (1 mm) varied between 10% and 26% with a mean of 19% and a

standard deviation of +/- 7%. The aggregate stability (0.5 mm) varied between 10% and 36% with a mean of 25% and a standard deviation of +/- 10%. The aggregate stability (0.25 mm) varied between 13% and 51% with a mean of 32% and a standard deviation of +/- 14%. The bulk density varied between 1670 kg m^{-3} and 1810 kg m^{-3} with a mean of 1778 kg m^{-3} and a standard deviation of +/- 62 kg m^{-3}.

C horizon:

The depth of the C horizon varied between 300 mm and 500 mm with a mean of 390 mm and a standard deviation of +/- 86 mm. The silt + clay content varied between 30% and 41% with a mean of 35% and a standard deviation of +/- 5%. The organic carbon content varied between 16% and 30% with a mean of 22% and a standard deviation of +/- 6%. The modulus of rupture varied between 0.19 bar and 0.56 bar with a mean of 0.38 bar and a standard deviation of +/- 0.2 bar. The aggregate stability (4 mm) varied between 1% and 6% with a mean of 3% and a standard deviation of +/- 2%. The aggregate stability (2 mm) varied between 8% and 16% with a mean of 11% and a standard deviation of +/- 4%. The aggregate stability (1 mm) varied between 10% and 40% with a mean of 23% and a standard deviation of +/- 13%. The aggregate stability (0.5 mm) varied between 13% and 36% with a mean of 26% and a standard deviation of +/- 10%. The aggregate stability (0.25 mm) varied between 9% and 29% with a mean of 16% and a standard deviation of +/- 8%. The bulk density varied between 1656kg m^{-3} and 1783 kg m^{-3} with a mean of 1729 kg m^{-3} and a standard deviation of +/- 52 kg m^{-3}.

Table 2 Physical characteristics of the Sepane soil form

Plot nr	Soil type	Horizon depth(mm)	Silt + Clay(%)	Organic Carbon (%)	Modulus of rupture (bar)	A.S 4 (%)	A. S 2 (%)	A.S 1 (%)	A.S 0.5 (%)	A.S 0.25 (%)	Bulk density (kg m^{-3})	Root density (km.m^{2})	Dry weight (kg.ha-1)
13.1A	**Se**	250.00	27.00	54.18	0.30	3.93	8.30	17.63	27.00	15.44	1399.34	0.36	5054.00
15.1A	**Se**	210.00	22.00	43.86	0.25	29.04	22.62	2.43	4.00	9.66	1401.22	0.28	5226.00
15.2A	**Se**	210.00	24.00	22.19	0.10	33.33	12.50	22.10	16.00	5.37	1504.33	0.36	5483.00
14.2A	**Se**	210.00	26.00	60.54	0.37	9.98	14.39	20.09	1.76	2.60	1507.18	0.34	2913.00
12.1A	**Tu/Se**	210.00	26.00	25.11	0.15	5.23	16.54	11.32	21.43	3.05	1532.09	0.40	5568.00
	Mean	**218.00**	**25.00**	**41.18**	**0.23**	**16.30**	**14.87**	**14.71**	**14.04**	**7.23**	**1468.83**	**0.35**	**4848.80**
	Min	**210.00**	**22.00**	**22.19**	**0.10**	**3.93**	**8.30**	**2.43**	**1.76**	**2.60**	**1399.34**	**0.28**	**2913.00**
	Max	**250.00**	**27.00**	**60.54**	**0.37**	**33.33**	**22.62**	**22.10**	**27.00**	**15.44**	**1532.09**	**0.40**	**5568.00**
	StdDev	**18.11**	**2.03**	**16.50**	**0.11**	**13.14**	**5.54**	**8.08**	**10.67**	**5.39**	**59.71**	**0.05**	**1129.52**
13.1B	**Se**	250.00	49.00	45.84	0.69	3.12	2.13	15.48	34.86	29.48	1798.32	0.10	5054.00
15.1B	**Se**	150.00	52.00	49.62	0.52	10.40	14.00	26.19	10.90	28.15	1807.77	0.02	5226.00
15.2B	**Se**	100.00	51.00	33.37	0.38	2.85	9.56	10.60	21.42	35.62	1810.44	0.04	5483.00
14.2B	**Se**	100.00	55.00	33.02	0.89	2.62	2.85	18.76	19.82	50.94	1807.65	0.02	2913.00
12.1B	**Tu/Se**	150.00	51.00	37.32	0.38	3.11	2.45	25.43	35.65	13.43	1670.43	0.33	5568.00
	Mean	**150.00**	**51.60**	**39.84**	**0.57**	**4.42**	**6.20**	**19.29**	**24.53**	**31.52**	**1778.92**	**0.10**	**4848.80**
	Min	**100.00**	**49.00**	**33.02**	**0.38**	**2.62**	**2.13**	**10.60**	**10.90**	**13.43**	**1670.43**	**0.02**	**2913.00**
	Max	**250.00**	**55.00**	**49.62**	**0.89**	**10.40**	**14.00**	**26.19**	**35.65**	**50.94**	**1810.44**	**0.33**	**5568.00**
	StdDev	**62.32**	**2.31**	**7.24**	**0.22**	**3.42**	**5.20**	**6.53**	**10.40**	**14.35**	**61.90**	**0.13**	**1129.52**
13.1C	**Se**	300.00	41.00	30.01	0.47	3.19	8.32	10.19	36.05	29.15	1763.24	0.07	5054.00
15.1C	**Se**	300.00	33.00	21.16	0.39	6.45	7.51	39.93	12.85	8.54	1783.24	0.06	5226.00
15.2C	**Se**	400.00	33.00	19.09	0.19	3.21	15.54	18.85	33.29	12.68	1743.56	0.24	5483.00
14.2C	**Se**	500.00	40.00	22.70	0.56	1.52	15.34	11.09	28.15	12.16	1701.10	0.28	2913.00
12.1C	**Tu/Se**	450.00	30.00	15.53	0.30	1.45	8.45	32.99	19.04	16.54	1656.09	0.41	5568.00
	Mean	**390.00**	**35.40**	**21.70**	**0.38**	**3.16**	**11.03**	**22.61**	**25.88**	**15.81**	**1729.45**	**0.21**	**4848.80**
	Min	**300.00**	**30.00**	**15.53**	**0.19**	**1.45**	**7.51**	**10.19**	**12.85**	**8.54**	**1656.09**	**0.06**	**2913.00**
	Max	**500.00**	**41.00**	**30.01**	**0.56**	**6.45**	**15.54**	**39.93**	**36.05**	**29.15**	**1783.24**	**0.41**	**5568.00**
	StdDev	**86.31**	**4.69**	**5.63**	**0.15**	**2.06**	**3.74**	**12.87**	**9.65**	**8.29**	**51.61**	**0.15**	**1129.52**

1.3 Bloemdal

A description of the physical characteristics of the Bloemdal soil form is seen in Table 3.

A horizon:

The depth of the A horizon varied between 150 mm and 260 mm with a mean of 260 mm and a standard deviation of +/- 50 mm. The silt + clay content varied between 20% and 32% with a mean of 32% and a standard deviation of +/- 5%. The organic carbon content varied between 21% and 33% with a mean of 21% and a standard deviation of +/- 5%. The modulus of rupture varied between 0.09 bar and 0.17 bar with a mean of 0.17 bar and a standard deviation of +/- 0.1 bar. The aggregate stability (4 mm) varied between 1% and 3% with a mean of 3% and a standard deviation of +/- 1%. The aggregate stability (2 mm) varied between 9% and 31% with a mean of 13% and a standard deviation of +/- 10%. The aggregate stability (1 mm) varied between 24% and 32% with a mean of 26% and a standard deviation of +/- 4%. The aggregate stability (0.5 mm) varied between 10% and 19% with a mean of 19% and a standard deviation of +/- 4%. The aggregate stability (0.25 mm) varied between 13% and 24% with a mean of 24% and a standard deviation of +/- 4%. The bulk density varied between 1290 kg m^{-3} and 1440 kg m^{-3} with a mean of 1440 kg m^{-3} and a standard deviation of +/- 63 kg m^{-3}.

B horizon:

The depth of the B horizon varied between 50 mm and 250 mm with a mean of 150 mm and a standard deviation of +/- 82 mm. The silt + clay content varied between 42% and 49% with a mean of 45% and a standard deviation of +/- 3%. The organic carbon content varied between 29% and 38% with a mean of 34% and a standard deviation of +/- 4%. The modulus of rupture varied between 0.45 bar and 0.64 bar with a mean of 0.57 bar and a standard deviation of +/- 0.1 bar. The aggregate stability (4 mm) varied between 1% and 3% with a mean of 2% and a standard deviation of +/- 1%. The aggregate stability (2 mm) varied between 1% and 8% with a mean of 4% and a standard deviation of +/- 3%. The aggregate stability (1 mm) varied between 14% and 20% with a mean of 17% and a standard

deviation of +/- 3%. The aggregate stability (0.5 mm) varied between 12% and 35% with a mean of 28% and a standard deviation of +/- 11%. The aggregate stability (0.25 mm) varied between 21% and 37% with a mean of 30% and a standard deviation of +/- 7%. The bulk density varied between 1580 kg m^{-3} and 1643 kg m^{-3} with a mean of 1605 kg m^{-3} and a standard deviation of +/- 27 kg m^{-3}.

C horizon:

The depth of the C horizon varied between 200 mm and 350 mm with a mean of 260 mm and a standard deviation of +/- 66 mm. The silt + clay content varied between 28% and 34% with a mean of 32% and a standard deviation of +/- 3%. The organic carbon content varied between 19% and 23% with a mean of 21% and a standard deviation of +/- 2%. The modulus of rupture varied between 0.15 bar and 0.20 bar with a mean of 0.17 bar and a standard deviation of +/- 0.1 bar. The aggregate stability (4 mm) varied between 2% and 4% with a mean of 3% and a standard deviation of +/- 1 bar. The aggregate stability (2 mm) varied between 13% and 14% with a mean of 13% and a standard deviation of +/- 1%. The aggregate stability (1 mm) varied between 12% and 33% with a mean of 26% and a standard deviation of +/- 10%. The aggregate stability (0.5 mm) varied between 14% and 34% with a mean of 19% and a standard deviation of +/- 9%. The aggregate stability (0.25 mm) varied between 7% and 30% with a mean of 24% and a standard deviation of +/- 11%. The bulk density varied between 1365kg m^{-3} and 1501 kg m^{-3} with a mean of 1440 kg m^{-3} and a standard deviation of +/- 61 kg m^{-3}.

Table 3 Physical characteristics of the Bloemdal soil form

Plot nr	Soil type	Horizon depth(mm)	Silt + Clay(%)	Organic matter (%)	Modulus of rupture (bar)	A.S 4 (%)	A. S 2 (%)	A.S 1 (%)	A.S 0.5 (%)	A.S 0.25 (%)	Bulk density (kg m^{-3})	Root density (km m^{2})	Dry weight (kg.ha-1)
11.10	**Bd**	210.00	21.00	27.69	0.09	3.24	30.73	24.01	10.19	12.86	1321.43	0.24	4283.00
10.50	**Bd**	245.00	20.00	33.37	0.10	2.34	11.65	32.43	18.33	19.32	1290.34	0.23	5997.00
8.10	**Bd/Tu**	250.00	25.00	23.74	0.11	1.67	11.23	30.43	15.46	18.43	1342.56	0.24	5997.00
11.30	**Bd**	150.00	20.00	26.14	0.12	1.28	9.06	28.80	17.67	20.39	1360.43	0.54	3427.00
	Mean	**260.00**	**31.75**	**20.90**	**0.17**	**3.33**	**13.47**	**26.06**	**19.47**	**23.63**	**1440.15**	**0.30**	**4926.00**
	Min	**150.00**	**20.00**	**20.90**	**0.09**	**1.28**	**9.06**	**24.01**	**10.19**	**12.86**	**1290.34**	**0.23**	**3427.00**
	Max	**260.00**	**31.75**	**33.37**	**0.17**	**3.33**	**30.73**	**32.43**	**19.47**	**23.63**	**1440.15**	**0.54**	**5997.00**
	StdDev	**49.32**	**5.44**	**5.26**	**0.04**	**0.95**	**9.80**	**3.67**	**4.08**	**4.47**	**63.47**	**0.14**	**1177.74**
11.10	**Bd**	50.00	49.00	37.15	0.64	1.04	8.32	16.68	11.67	21.11	1580.14	0.09	4283.00
10.50	**Bd**	250.00	42.00	37.67	0.58	2.67	3.43	14.35	34.54	36.54	1610.45	0.10	5997.00
8.10	**Bd/Tu**	150.00	43.00	33.37	0.61	2.32	3.09	20.33	34.65	34.23	1589.23	0.11	5997.00
11.30	**Bd**	150.00	45.00	28.90	0.45	2.10	1.45	18.43	31.51	30.03	1643.12	0.08	3427.00
	Mean	**150.00**	**44.75**	**34.27**	**0.57**	**2.03**	**4.07**	**17.45**	**28.09**	**30.48**	**1605.74**	**0.10**	**4926.00**
	Min	**50.00**	**42.00**	**28.90**	**0.45**	**1.04**	**1.45**	**14.35**	**11.67**	**21.11**	**1580.14**	**0.08**	**3427.00**
	Max	**250.00**	**49.00**	**37.67**	**0.64**	**2.67**	**8.32**	**20.33**	**34.65**	**36.54**	**1643.12**	**0.11**	**5997.00**
	StdDev	**81.65**	**3.00**	**3.86**	**0.08**	**0.69**	**2.91**	**2.50**	**10.52**	**6.61**	**27.02**	**0.01**	**1177.74**
11.10	**Bd**	280.00	34.00	21.50	0.16	2.38	14.43	11.77	33.76	6.62	1489.12	0.31	4283.00
10.50	**Bd**	210.00	32.00	20.47	0.15	3.56	12.56	28.43	14.55	30.11	1365.04	0.29	5997.00
8.10	**Bd/Tu**	350.00	28.00	18.92	0.18	4.22	13.55	33.23	15.67	30.23	1405.12	0.34	5997.00
11.30	**Bd**	200.00	33.00	22.70	0.20	3.16	13.34	30.83	13.90	27.55	1501.32	0.28	3427.00
	Mean	**260.00**	**31.75**	**20.90**	**0.17**	**3.33**	**13.47**	**26.06**	**19.47**	**23.63**	**1440.15**	**0.30**	**4926.00**
	Min	**200.00**	**28.00**	**18.92**	**0.15**	**2.38**	**12.56**	**11.77**	**13.90**	**6.62**	**1365.04**	**0.28**	**3427.00**
	Max	**350.00**	**34.00**	**22.70**	**0.20**	**4.22**	**14.43**	**33.23**	**33.76**	**30.23**	**1501.32**	**0.34**	**5997.00**
	StdDev	**66.04**	**2.57**	**1.58**	**0.02**	**0.76**	**0.77**	**9.42**	**9.11**	**10.86**	**61.05**	**0.03**	**1177.74**

Appendix W Matric suction response curves

(a)

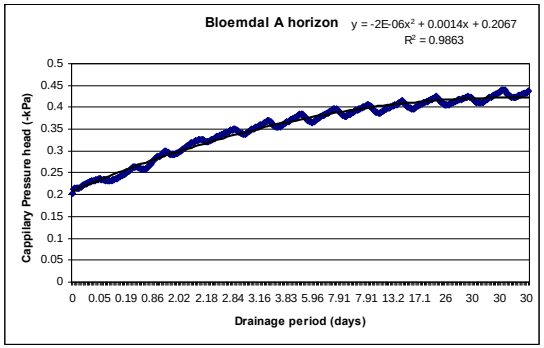

(b)

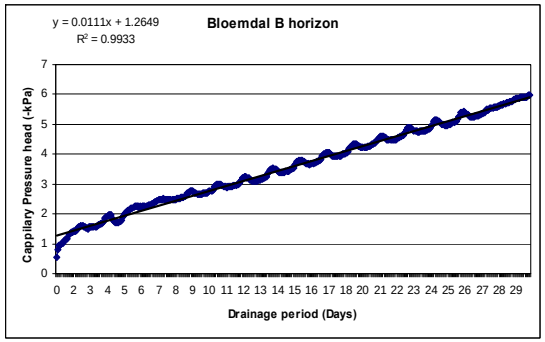

(c)

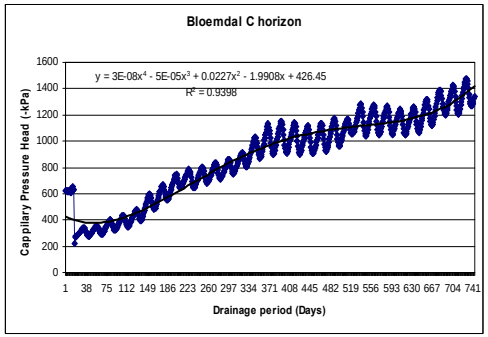

(d)

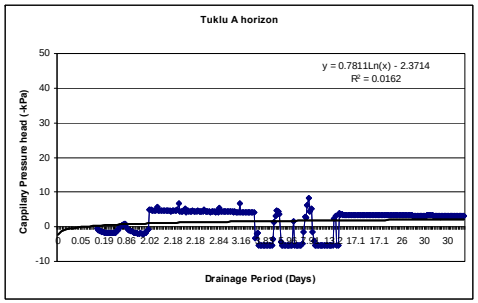

(e)

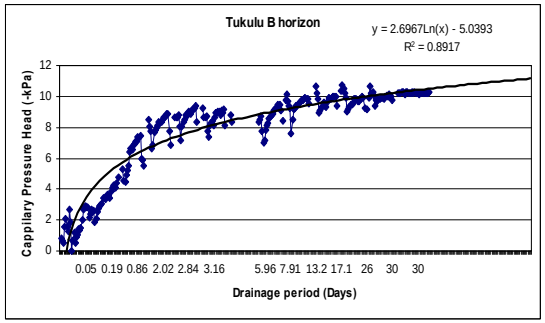

(f)

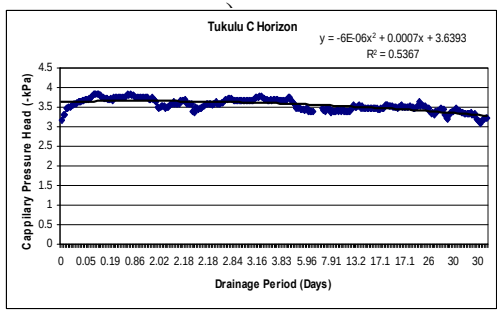

(g)

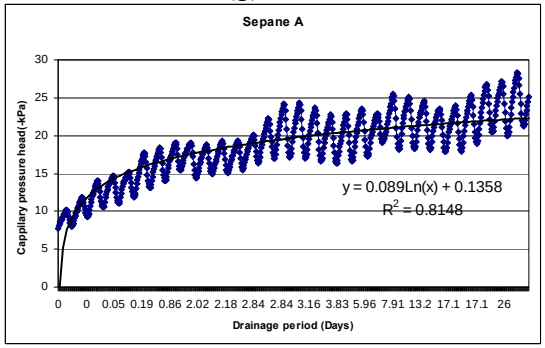

(h)

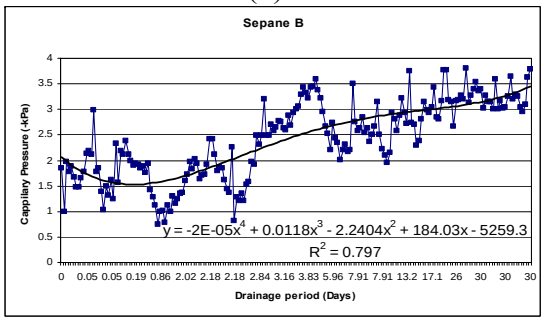

(i)

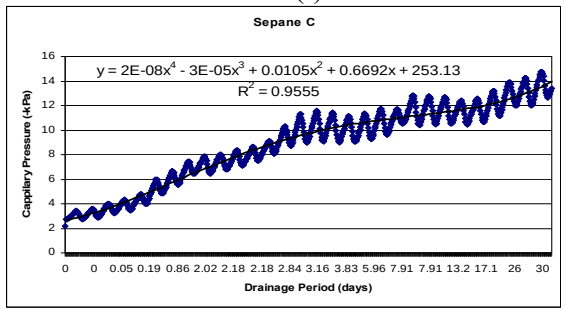

Figure 1 (a – i) Matric suction response curves over the drainage period for the Bloemdal, Tukulu and Sepane soils.

Appendix X Data used in the process for calculating the hydraulic conductivity of the Bloemdal, Tukulu and Sepane soils

Table 1 Data used for the calculation of soil moisture flux (q) of the Bloemdal

DAS	z (cm)	Volumetric WC	ΔWC/Δt (cm day^{-1})	dz X (ΔWC/Δt (cm day^{-1})	q (flux)
0.00	0-15	0.289			
	15-45	0.275			
	45-75	0.291			
0.86	0-15	0.254	0.041	0.608	0.608
	15-45	0.267	0.010	0.297	0.905
	45-75	0.290	0.001	0.031	0.936
2.18	0-15	0.244	0.008	0.114	0.114
	15-45	0.259	0.006	0.184	0.298
	45-75	0.289	0.001	0.030	0.328
2.84	0-15	0.241	0.005	0.071	0.071
	15-45	0.256	0.004	0.117	0.188
	45-75	0.288	0.001	0.029	0.217
3.16	0-15	0.239	0.004	0.061	0.061
	15-45	0.255	0.003	0.093	0.154
	45-75	0.288	0.001	0.029	0.183
3.83	0-15	0.237	0.004	0.053	0.053
	15-45	0.253	0.002	0.075	0.128
	45-75	0.287	0.001	0.029	0.157
5.96	0-15	0.231	0.003	0.040	0.040
	15-45	0.250	0.001	0.041	0.081
	45-75	0.285	0.001	0.028	0.109
17.14	0-15	0.217	0.001	0.019	0.019
	15-45	0.249	0.000	0.005	0.024
	45-75	0.277	0.001	0.024	0.048
26.01	0-15	0.211	0.001	0.010	0.010
	15-45	0.249	0.000	0.000	0.010
	45-75	0.271	0.001	0.017	0.027
30.00	0-15	0.209	0.000	0.007	0.007
	15-45	0.249	0.000	0.000	0.007
	45-75	0.270	0.000	0.013	0.021

Table 2 Data used for the calculation of K for the Bloemdal

z (cm)	DAS	q (cm day^{-1})	Vol WC	Hp (cm)	Hg	H	ΔH/	K (cm day^{-1})	Mean WC
0-15	0.00		0.289						
	0.86	0.608	0.254	70	30	100	2.333333	0.261	0.271124
	2.18	0.114	0.244	120	30	150	1.333333	0.086	0.248663
	2.84	0.071	0.241	120	30	150	2.333333	0.030	0.24207
	3.16	0.061	0.239	140	30	170	1.666667	0.036	0.239858
	3.83	0.053	0.237	140	30	170	1.666667	0.032	0.238026
	5.96	0.040	0.231	170	30	200	1.666667	0.024	0.23402
	17.14	0.019	0.217	170	30	200	1.666667	0.011	0.224097
	26.01	0.010	0.211	210	30	240	0.333333	0.029	0.214123
	30.00	0.007	0.209	250	30	280	-1	-0.007	0.210271
0-45	0.00		0.275						
	0.86	0.905	0.267	110	60	170	2.333333	0.388	0.270909
	2.18	0.298	0.259	130	60	190	1.333333	0.223	0.262614
	2.84	0.188	0.256	160	60	220	2.333333	0.080	0.257292
	3.16	0.154	0.255	160	60	220	1.666667	0.092	0.255512
	3.83	0.128	0.253	160	60	220	1.666667	0.077	0.254177
	5.96	0.081	0.250	190	60	250	1.666667	0.049	0.25187
	17.14	0.024	0.249	190	60	250	1.666667	0.014	0.249486
	26.01	0.010	0.249	190	60	250	0.333333	0.029	0.248566
	30.00	0.007	0.249	190	60	250	-1	-0.007	0.24856
0-75	0.00		0.291						
	0.86	0.936	0.290	170	90	260	3	0.312	0.290669
	2.18	0.328	0.289	170	90	260	2.333333	0.140	0.289575
	2.84	0.217	0.288	170	90	260	1.333333	0.163	0.288598
	3.16	0.183	0.288	170	90	260	1.333333	0.137	0.288122
	3.83	0.157	0.287	170	90	260	1.333333	0.117	0.287649
	5.96	0.109	0.285	170	90	260	0.333333	0.326	0.286346
	17.14	0.048	0.277	220	90	310	2	0.024	0.280976
	26.01	0.027	0.271	220	90	310	2	0.014	0.27404
	30.00	0.021	0.270	290	90	380	4.333333	0.005	0.270611

Table 3 Data used for the calculation of soil moisture flux (q) of the Tukulu

DAS	z(cm)	Volumetric WC	ΔWC/Δt (cm day^{-1})	dz(ΔWC/Δt (cm day^{-1})	q (flux)
0.00	0-15	0.264			
	15-45	0.284			
	45-75	0.311			
0.86	0-15	0.238	0.030	0.456	0.456
	15-45	0.280	0.005	0.141	0.597
	45-75	0.307	0.004	0.134	0.731
2.18	0-15	0.232	0.004	0.066	0.066
	15-45	0.275	0.004	0.113	0.180
	45-75	0.302	0.003	0.103	0.283
2.84	0-15	0.230	0.003	0.041	0.041
	15-45	0.273	0.003	0.093	0.134
	45-75	0.301	0.003	0.081	0.215
3.16	0-15	0.229	0.002	0.035	0.035
	15-45	0.272	0.003	0.084	0.120
	45-75	0.300	0.002	0.072	0.192
3.83	0-15	0.228	0.002	0.031	0.031
	15-45	0.271	0.003	0.077	0.108
	45-75	0.298	0.002	0.064	0.172
5.96	0-15	0.224	0.002	0.024	0.024
	15-45	0.267	0.002	0.059	0.083
	45-75	0.295	0.002	0.047	0.130
17.14	0-15	0.215	0.001	0.012	0.012
	15-45	0.259	0.001	0.021	0.033
	45-75	0.290	0.000	0.013	0.046
26.01	0-15	0.212	0.000	0.007	0.007
	15-45	0.258	0.000	0.003	0.010
	45-75	0.290	0.000	0.001	0.011
30.00	0-15	0.210	0.000	0.005	0.005
	15-45	0.258	0.000	0.001	0.006
	45-75	0.290	0.000	0.000	0.006

Table 4 Data used for the calculation of K for the Tukulu

z (cm)	DAS	q (cm day^{-1})	Vol WC	Hp (cm)	Hg	H	ΔH/	mean WC	K (cm day^{-1})
	0.00		0.264						
0-15	0.86	0.456	0.238	120	30	150	0.666667	0.250602	0.684
	2.18	0.066	0.232	140	30	170	0.666667	0.234612	0.100
	2.84	0.041	0.230	160	30	190	4.74E-15	0.230778	
	3.16	0.035	0.229	160	30	190	1.333333	0.229489	0.027
	3.83	0.031	0.228	160	30	190	1.333333	0.228414	0.023
	5.96	0.024	0.224	160	30	190	1.333333	0.22604	0.018
	17.14	0.012	0.215	190	30	220	0.333333	0.219914	0.036
	26.01	0.007	0.212	190	30	220	1.666667	0.213533	0.004
	30.00	0.005	0.210	230	30	260	0.333333	0.210917	0.015
	0.00		0.284						
0-45	0.86	0.597	0.280	110	60	170	0.666667	0.282426	0.895
	2.18	0.180	0.275	130	60	190	0.666667	0.277915	0.269
	2.84	0.134	0.273	130	60	190	4.74E-15	0.274403	
	3.16	0.120	0.272	170	60	230	1.333333	0.272932	0.090
	3.83	0.108	0.271	170	60	230	1.333333	0.271626	0.081
	5.96	0.083	0.267	170	60	230	1.333333	0.268668	0.062
	17.14	0.033	0.259	170	60	230	0.333333	0.262709	0.098
	26.01	0.010	0.258	210	60	270	1.666667	0.258357	0.006
	30.00	0.006	0.258	210	60	270	0.333333	0.257796	0.018
	0.00		0.311						
0-75	0.86	0.731	0.307	80	90	170	0	0.30885	
	2.18	0.283	0.302	80	90	170	-0.66667	0.304663	-0.424
	2.84	0.215	0.301	90	90	180	-0.33333	0.301507	-0.646
	3.16	0.192	0.300	90	90	180	-1.66667	0.300232	-0.115
	3.83	0.172	0.298	90	90	180	-1.66667	0.29913	-0.103
	5.96	0.130	0.295	90	90	180	-1.66667	0.296749	-0.078
	17.14	0.046	0.290	90	90	180	-1.66667	0.292602	-0.028
	26.01	0.011	0.290	110	90	200	-2.33333	0.289921	-0.005
	30.00	0.006	0.290	110	90	200	-2.33333	0.289705	-0.003

Table 5 Data used for the calculation of soil moisture flux (q) of the Sepane

DAS	z(cm)	Volumetric WC	ΔWC/Δt (cm day^{-1})	dz(ΔWC/Δt (cm day^{-1})	q (flux)
0.00	0-15	0.279			
	15-45	0.281			
	45-75	0.290			
0.86	0-15	0.247	0.037	0.558	0.558
	15-45	0.279	0.003	0.096	0.654
	45-75	0.266	0.028	0.834	1.488
2.18	0-15	0.242	0.004	0.053	0.053
	15-45	0.275	0.002	0.072	0.126
	45-75	0.264	0.001	0.040	0.166
2.84	0-15	0.241	0.001	0.018	0.018
	15-45	0.274	0.002	0.057	0.076
	45-75	0.264	0.001	0.016	0.092
3.16	0-15	0.241	0.001	0.013	0.013
	15-45	0.274	0.002	0.052	0.065
	45-75	0.263	0.000	0.013	0.077
3.83	0-15	0.241	0.001	0.009	0.009
	15-45	0.273	0.002	0.047	0.056
	45-75	0.263	0.000	0.011	0.067
5.96	0-15	0.240	0.000	0.005	0.005
	15-45	0.270	0.001	0.037	0.042
	45-75	0.263	0.000	0.008	0.050
17.14	0-15	0.240	0.000	0.000	0.000
	15-45	0.263	0.001	0.017	0.018
	45-75	0.261	0.000	0.005	0.023
26.01	0-15	0.240	0.000	-0.001	-0.001
	15-45	0.261	0.000	0.008	0.007
	45-75	0.259	0.000	0.005	0.012
30.00	0-15	0.240	0.000	-0.001	-0.001
	15-45	0.260	0.000	0.006	0.005
	45-75	0.259	0.000	0.005	0.010

Table 6 Data used for the calculation of K for the Sepane

z (cm)	DAS	q (cm day^{-1})	Vol WC	Hp (cm)	Hg	H	ΔH/	mean WC	K (cm day^{-1})
	0.00		0.279						
0-15	0.86	0.558	0.247	90	30	120	3	0.262816	0.186
	2.18	0.053	0.242	130	30	160	1.666667	0.244478	0.000
	2.84	0.018	0.241	150	30	180	1	0.241731	0.000
	3.16	0.013	0.241	150	30	180	2.333333	0.241191	0.005
	3.83	0.009	0.241	150	30	180	2.333333	0.240843	0.004
	5.96	0.005	0.240	150	30	180	2.333333	0.240294	0.002
	17.14	0.042	0.240	150	30	180	4	0.239806	0.010
	26.01	0.050	0.240	150	30	180	2.333333	0.239838	0.021
	30.00	0.000	0.240	150	30	180	4	0.24012	0.000
	0.00		0.281						
0-45	0.86	0.654	0.279	150	60	210	3	0.279925	0.218
	2.18	0.126	0.275	150	60	210	1.666667	0.276962	0.075
	2.84	0.076	0.274	150	60	210	1	0.274739	0.076
	3.16	0.065	0.274	190	60	250	2.333333	0.273831	0.028
	3.83	0.056	0.273	190	60	250	2.333333	0.273029	0.024
	5.96	0.042	0.270	190	60	250	2.333333	0.271193	0.018
	17.14	0.018	0.263	240	60	300	4	0.266677	0.004
	26.01	0.007	0.261	190	60	250	2.333333	0.262328	0.003
	30.00	0.005	0.260	240	60	300	4	0.26081	0.001
	0.00		0.290						
0-75	0.86	1.488	0.266	70	90	160	-1.66667	0.277586	-0.893
	2.18	0.166	0.264	90	90	180	-1	0.264753	-0.166
	2.84	0.092	0.264	110	90	200	-0.33333	0.263692	-0.276
	3.16	0.077	0.263	110	90	200	-1.66667	0.263446	-0.046
	3.83	0.067	0.263	110	90	200	-1.66667	0.263258	-0.040
	5.96	0.050	0.263	110	90	200	-1.66667	0.262859	-0.030
	17.14	0.023	0.261	110	90	200	-3.33333	0.261582	-0.007
	26.01	0.012	0.259	110	90	200	-1.66667	0.259886	-0.007
	30.00	0.010	0.259	110	90	200	-3.33333	0.25888	-0.003